risks

MDPI

Article

Formulating MCoVaR to Quantify Joint Transmissions of Systemic Risk across Crypto and Non-Crypto Markets: A Multivariate Copula Approach

Arief Hakim and Khreshna Syuhada *

Faculty of Mathematics and Natural Sciences, Institut Teknologi Bandung, Bandung 40132, Indonesia
* Correspondence: khreshna@office.itb.ac.id

Abstract: Evidence that cryptocurrencies exhibit speculative bubble behavior is well documented. This evidence could trigger global financial instability leading to systemic risk. It is therefore crucial to quantify systemic risk and investigate its transmission mechanism across crypto markets and other global financial markets. We can accomplish this using the so-called multivariate conditional value-at-risk (MCoVaR), which measures the tail risk of a targeted asset from each market conditional on a set of multiple assets being jointly in distress and on a set of the remaining assets being jointly in their median states. In this paper, we aimed to find its analytic formulas by considering multivariate copulas, which allow for the separation of margins and dependence structures in modeling the returns of the aforementioned assets. Compared to multivariate normal and Student's *t* benchmark models and a multivariate Johnson's SU model, the copula-based models with non-normal margins produced a MCoVaR forecast with superior conditional coverage and backtesting performances. Using a corresponding Delta MCoVaR, we found the crypto assets to be potential sources of systemic risk jointly transmitted within the crypto markets and towards the S&P 500, oil, and gold, which was more apparent during the COVID-19 period encompassing the recent 2021 crypto bubble event.

Keywords: cryptocurrency; speculative bubble; conditional value-at-risk; asymmetric loss function; asymmetry; leptokurticity; tail dependence; elliptical copula

Citation: Hakim, Arief, and Khreshna Syuhada. 2023. Formulating MCoVaR to Quantify Joint Transmissions of Systemic Risk across Crypto and Non-Crypto Markets: A Multivariate Copula Approach. *Risks* 11: 35. https://doi.org/10.3390/risks11020035

Academic Editor: Mogens Steffensen

Received: 9 December 2022
Revised: 12 January 2023
Accepted: 2 February 2023
Published: 7 February 2023

1. Introduction

Cryptocurrencies are relatively new digital financial instruments to which financial market participants and policy-makers have paid much attention. They were initially launched as fully decentralized payment systems based on blockchain technology, allowing the transaction process to take place directly from one party to another without the need for any financial institution or governing body (Wang et al. 2019, 2020). Nevertheless, rapid appreciations and extreme fluctuations in their prices and market capitalization have led them to be speculative investment assets instead of currencies (Baur and Dimpfl 2021; Baur et al. 2018) and thus prone to high risk and uncertainty (Almeida et al. 2022). This evidence results from their speculative aspects dominating their ability to work as a medium of exchange, a unit of account, and a store of value, as fiat currencies do (Cheah and Fry 2015). Due to such a speculative nature and lack of a central regulator controlling the crypto markets, drastic increases in crypto-asset prices are frequently followed by dramatic declines, resulting in giant bubbles. The vulnerability of crypto assets to speculative bubbles was statistically significant, as tested by Cheah and Fry (2015), Corbet et al. (2018), Agosto and Cafferata (2020), Haykir and Yagli (2022), and Bazán-Palomino (2022). This phenomenon could trigger the instability of the global financial system leading to systemic financial risk. Managing potential systemic risk transmitted from the crypto markets towards other global financial markets and vice versa is thus of importance for maintaining global financial stability.

Systemic risk can be quantitatively managed using (1) the so-called conditional value-at-risk (CoVaR), which measures the tail risk of a targeted asset conditional on another asset being under distress, and (2) the corresponding ΔCoVaR, which quantifies the systemic risk contribution of the latter to the former. These measures were first proposed by Adrian and Brunnermeier (2016) and originally modeled using Koenker and Bassett's (1978) quantile regression model. More specifically, the quantile regression-based (Δ)CoVaR specifies the conditional quantile of the targeted asset return as a linear combination of (1) the VaR for another asset and (2) a set of covariates by taking no account of any distributional assumption. This framework was adopted by Borri (2019) to measure systemic risk in the crypto markets by involving four global conventional assets as covariates. The author highlighted that the major crypto assets under study (i.e., Bitcoin, Ethereum, Ripple, and Litecoin) were greatly exposed to risk within the crypto markets. In addition, the above CoVaR model was also employed by Xu et al. (2021) and Akhtaruzzaman et al. (2022) to develop systemic risk contagion networks for cryptocurrencies only by considering the same four conventional assets as covariates. The former authors revealed that Ethereum and Bitcoin played roles as the largest systemic risk transmitter and receiver, respectively, while the latter provided evidence of higher transmissions of systemic risk due to the global outbreak of COVID-19.

As an alternative to the quantile regression-based (Δ)CoVaR, Adrian and Brunnermeier (2016) proposed a parametric model approach based on a bivariate normal distribution, as in Girardi and Ergün (2013). This approach was modified by Girardi and Ergün (2013) using a bivariate skewed Student's *t* distribution that is a special case of the bivariate generalized hyperbolic distribution. According to their empirical study on the US financial industries, the CoVaR formulated using the skewed Student's *t* distribution was shown to better satisfy coverage properties, suggesting the importance of accounting for returns' asymmetry and leptokurticity. This is in line with Chu et al. (2015) (and Catania and Grassi 2022), who found more accurate risk measure forecasts for Bitcoin (and other crypto assets) when considering an asymmetric and leptokurtic distribution, namely, a generalized hyperbolic (skewed Student's *t*) distribution. This is also supported by Núñez et al. (2019), who employed another member of the family of generalized hyperbolic distributions for the returns of Bitcoin exchange rates against seven major currencies during different periods when bubbles were detected. Despite their capability to capture asymmetry and leptokurticity, the above distributions may have infinite moments for high orders. To overcome this shortcoming, one may take Johnson's SU distribution into consideration. This distribution was derived by Johnson (1949) and Choi and Nam (2008) from a normal distribution through a simple increasing transformation, making its distributional and moment properties as uncomplicated as those of the normal distribution. In particular, its moments are finite for all orders with explicit expressions. Accordingly, it can be a useful alternative for more accurately formulating risk measure forecasts with analytically tractable expressions, as in Gurrola (2008), Choi et al. (2012), Castillo-Brais et al. (2022), and Hakim et al. (2022). Their superior coverage and backtesting performances for cryptocurrencies and other assets were reported by, e.g., Venkataraman and Rao (2016), Troster et al. (2019), Patra (2021), and Som and Kayal (2022).

Another challenging task in modeling and quantifying systemic risk is to account for the tail dependence between the returns of targeted and conditioning assets. The tail dependence structure shows the tendency of their extreme events to take place simultaneously. This typical feature cannot be described using quantile regression (Bernard and Czado 2015) and some of the above classical models. Thus, one may require more sophisticated tools, namely copulas, to overcome this limitation. Basically, copulas are joint distribution functions of random variables uniformly distributed over a unit interval (McNeil et al. 2015). By relating our random risks with such uniformly distributed random variables through the (inverse) probability integral transform, we can employ copulas to link the marginal and joint distributions of these random risks based on Sklar's (1959) famous theorem. This framework enables us to obtain many choices of greatly flexible risk models, whose margins and dependence structure can be analyzed separately. The dependence information is contained in the chosen copula. For instance, Student's *t* (normal) copula derived from Student's *t* (normal) distribution provides tail (in)dependence. It belongs to the elliptical copula family with radially symmetric dependence. To allow for asymmetric dependence, Demarta and McNeil (2005) proposed a skewed elliptical copula, namely a skewed Student's *t* copula, constructed from a skewed Student's *t* distribution. Chan and Kroese (2010) also did this based on an adjusted skewed normal distribution. Asymmetric dependence may also be accommodated using Archimedean copulas, as extensively studied by McNeil and Nešlehová (2009). Two popular members of the Archimedean copula family are Clayton and Gumbel copulas, which exhibit lower tail dependence and upper tail dependence, respectively.

Elliptical and Archimedean copulas, along with other copula families, have been applied by numerous studies, e.g., Cherubini and Luciano (2001), Embrechts et al. (2003a), Embrechts and Höing (2006), Rosenberg and Schuermann (2006), and Li et al. (2015), for aggregate or portfolio risk quantification. Recently, their bivariate versions were utilized by, e.g., Mainik and Schaanning (2014), Hakwa et al. (2015), Bernard and Czado (2015), Bernardi et al. (2016), and Jaworski (2017), to analytically formulate the (Δ)CoVaR systemic risk measure with generally closed-form expressions. Karimalis and Nomikos's (2018) empirical study on the European banking sectors found that a combination of bivariate copulas exhibiting tail dependence with asymmetric and leptokurtic margins was the best candidate for accurately forecasting CoVaR. This indicates the importance of taking account of asymmetric and leptokurtic margins and their tail dependence and hence complements the findings of previous studies (e.g., Girardi and Ergün 2013; Hakim et al. 2022). Similar approaches were adopted by Yu et al. (2021) and Rehman et al. (2022) to forecast the (Δ)CoVaR for Bitcoin, gold, and currencies.

In practice, multiple assets may simultaneously experience financial distress at the same time. To obtain a complete picture of systemic risk transmissions in a basket of financial assets that includes these multiple distressed assets, one prefers to rely on an extension of (Δ)CoVaR, namely (Δ)MCoVaR, where the "M" refers to "multiple" or "multivariate". This extension was first proposed by Cao (2013) to replace the (Δ)CoVaR, which only involves a single conditioning asset being in either distress or a normal condition. The author defined the MCoVaR for a targeted asset by accounting for the joint distressing events of all the remaining assets at the same time. Meanwhile, Torri et al. (2021) took account of the distressing event of one conditioning asset and the joint normal conditions of the remaining assets. These frameworks were generalized by Bernardi and Petrella (2015) and Bernardi et al. (2017) by considering the condition that multiple assets are jointly in distress and that the remaining assets are in their median or normal states. The resulting ΔMCoVaR can then be utilized to measure the joint transmissions of systemic risk across the analyzed financial markets.

The above (Δ)MCoVaR definitions led previous studies to make use of multivariate or multidimensional risk models. For instance, Cao (2013) computed the proposed (Δ)MCoVaR using a multivariate Student's *t* model when investigating systemic risk in the French and Chinese banking systems. By relying on a finite mixture of multivariate normal and Student's *t* models, Bernardi and Petrella (2015) and Bernardi et al. (2017) computed the (Δ)MCoVaR they proposed for the US financial entities. Meanwhile, Torri et al. (2021) and Chen et al. (2022) implemented the ΔMCoVaR they formulated using multivariate normal and Student's *t* distributions to construct network models for the European and Chinese financial systems, respectively. A similar ΔMCoVaR-based network was also developed by Hakim et al. (2022) using a multivariate Johnson's SU model and its conditional moments with an application to global foreign exchange markets. In addition, Torri et al. (2021) also considered a multiple-quantile regression-based MCoVaR, similar to what Bonaccolto et al. (2023) proposed.

In this study, we aimed to formulate the (Δ)MCoVaR of Bernardi and Petrella (2015) and Bernardi et al. (2017) to measure systemic risk in crypto and non-crypto markets.[1] The

MCoVaR was computed for each asset from these markets when all the (remaining) assets from different (same) markets are jointly distressed. We then determined the ΔMCoVaR by computing the difference between (1) the MCoVaR when considering distressed conditioning assets and (2) the MCoVaR when all the conditioning assets are simultaneously in normal situations. This framework allows us to quantify the joint transmissions of systemic risk within the same markets and across different markets. We did the (Δ)MCoVaR formulation by modeling the returns of these assets using a multivariate Johnson's SU model, which has finite and explicit moments for all orders and permits us to capture their asymmetry and leptokurticity. Furthermore, we proposed more sophisticated multivariate risk models determined based on copulas, particularly normal and Student's *t* copulas. The reason for considering these two copulas is that they remain analytically tractable and closed under marginalization and multivariate conditioning when extended to a multivariate setting. For the comparisons, we also employed classical models distributed according to a multivariate normal or Student's *t* distribution as benchmarks. The performances of the aforementioned models were assessed and compared by evaluating the conditional coverage and backtesting performances of the resulting MCoVaR forecasts. For the empirical study, we selected Bitcoin, Ethereum, Ripple, Litecoin, and Monero as representations of crypto assets. In addition, we chose the following non-crypto assets: the S&P 500 composite index, the S&P US Treasury Bond index, the US dollar index, West Texas Intermediate (WTI) crude oil, and gold. Their daily closing (spot) prices were sampled over a period from 16 January 2018 to 23 February 2022, which encompasses (1) the global COVID-19 crisis, the first major crisis since the invention of crypto assets (Almeida et al. 2022), and (2) the 2021 crypto bubble (Bazán-Palomino 2022).

In contrast to other crises (such as the 2008 global financial crisis and the subsequent European sovereign debt crisis), the COVID-19 pandemic was a major global public health emergency with unique urgency and uncertainty that has brought considerable challenges to global financial markets. It not only impacted people's lives, healths, and properties, but also affected the global economic systems (Li et al. 2021). For instance, Syuhada et al. (2022a, 2022b) demonstrated that the COVID-19 outbreak led the prices of oils and petroleum to exhibit downward volatile movements and even reach the lowest level during the first quarter of the COVID-19 period, suggesting more acute losses. In early March 2020, gold also showed a massive spiking as global travel restrictions and supply chain disruptions impacted its supply (Corbet et al. 2020). Sharif et al. (2020) highlighted that the COVID-19 and oil price shocks unprecedentedly impacted the geopolitical risk levels, economic policy uncertainty, and stock market volatility. Caferra and Vidal-Tomás's (2021) findings provided evidence of a financial contagion in March 2020 as cryptocurrency and stock prices exhibited dramatic declines. While stock markets were stuck in the bear phase, cryptocurrencies quickly rebounded, resulting in the 2021 crypto bubble starting from the first week of November 2020 to the second week of May 2021, as documented by Bazán-Palomino (2022). Bazán-Palomino (2022) also found the volatility of crypto-portfolio returns to increase due to this bubble event. The cryptocurrency systemic risk contagion networks of Akhtaruzzaman et al. (2022) revealed that the COVID-19 pandemic induced increased interconnections, highlighting a higher number of systemic risk contagion channels. In this study, we attempted to investigate the impacts of the COVID-19 pandemic and the 2021 crypto bubble on the mechanism of joint systemic risk transmissions across crypto and non-crypto markets.

In summary, the main contribution of this study to the literature is three-fold. First, we derive analytic (Δ)MCoVaR formulas by taking multivariate Johnson's SU and copula-based models into consideration. They overcome the existing asymmetric and leptokurtic models, whose moments, distributional properties, and tail dependence structures may be analytically intractable. Second, we assess the MCoVaR forecast accuracy by investigating the closeness between its conditional coverage probability and the significance level under consideration. We also perform the assessment by introducing a conditional asymmetric loss function, which asymmetrically penalizes observations below and above the MCoVaR forecast. This attempt complements previous studies, e.g., Cao (2013), Torri et al. (2021), Chen et al. (2022), Bernardi and Petrella (2015), and Bernardi et al. (2017), which were only concerned with the MCoVaR magnitude. Third, using ΔMCoVaR, we quantify the systemic risk contributions of jointly distressed (crypto/non-crypto) assets transmitted to the targeted (crypto/non-crypto) asset. In particular, the mechanism of joint systemic risk transmissions from the crypto assets towards the non-crypto assets permits us to examine whether the crypto markets, well known to have speculative bubble behavior, really become potential sources of financial instability. This framework is contrary to previous works, i.e., Borri (2019), Xu et al. (2021), and Akhtaruzzaman et al. (2022), which solely focused on the systemic risk transmissions from one crypto asset to the other within the crypto markets on the basis of ΔCoVaR.

After this introduction section, we organize the remainder of this paper as follows. We outline multivariate risk models in Section 2. Using these models, we formulate (Δ)MCoVaR in Section 3 and examine the conditional coverage and backtesting performances of its forecasts in Section 4. We implement these theoretical results for crypto and non-crypto assets and provide empirical findings in Section 5. We then conclude our study in Section 6.

2. Multivariate Risk Models

For a fixed $I \in \mathbb{N}$, $I \geq 2$, let $\mathscr{I} = \{1, 2, \ldots, I\}$. Suppose that $\mathbf{X} = (X_i)_{i\in\mathscr{I}}$ denotes a vector of I real-valued random variables defined on the same probability space $(\Omega, \mathscr{F}, \mathbb{P})$. We consider that these random variables are continuously distributed for representing I assets' risks or returns such that $\mathbf{X}(\Omega) = \mathbb{R}^I$. Provided that $\mathbb{E}\big(|X_i|^2\big) < \infty$ for all $i \in \mathscr{I}$, the random vector $\mathbf{X}$ can be expressed as follows:

$$\mathbf{X} = (\mu_i + \sigma_i Z_i)_{i\in\mathscr{I}} = \boldsymbol{\mu} + \mathbf{D}^{\frac{1}{2}}\mathbf{Z}, \tag{1}$$

with $\boldsymbol{\mu} = (\mu_i)_{i\in\mathscr{I}} = \big(\mathbb{E}(X_i)\big)_{i\in\mathscr{I}}$ symbolizing a vector of marginal means and $\mathbf{D} = \operatorname{diag}\{\sigma_i^2\}_{i\in\mathscr{I}} = \operatorname{diag}\{\mathbb{V}(X_i)\}_{i\in\mathscr{I}}$ denoting a diagonal matrix, whose diagonal entries are marginal variances assumed to be positive. Meanwhile, $\mathbf{Z} = (Z_i)_{i\in\mathscr{I}}$ is a random vector following a standardized I-variate distribution, i.e., $\mathbf{Z} \sim \mathcal{D}_I(\mathbf{0}, \mathbf{P}, \boldsymbol{\omega})$, with a joint distribution function $G_{(\mathbf{0},\mathbf{P},\boldsymbol{\omega})}$ characterized by Pearson's correlation matrix $\mathbf{P} = (\rho_{ij})_{i,j\in\mathscr{I}} = \big(\operatorname{Corr}(Z_i, Z_j)\big)_{i,j\in\mathscr{I}}$ being nonsingular and possibly by a vector $\boldsymbol{\omega} = (\boldsymbol{\omega}_i)_{i\in\mathscr{I}}$ of shape parameters. This implies that $\mathbf{X} \sim \mathcal{D}_I(\boldsymbol{\mu}, \boldsymbol{\Sigma}, \boldsymbol{\omega})$, with $\boldsymbol{\Sigma} = \operatorname{Cov}(\mathbf{X}, \mathbf{X}) = \mathbf{D}^{\frac{1}{2}}\mathbf{P}\mathbf{D}^{\frac{1}{2}}$ being its covariance matrix. Its joint distribution function $F_{(\boldsymbol{\mu},\boldsymbol{\Sigma},\boldsymbol{\omega})}$ can be written as follows:

$$F_{(\boldsymbol{\mu},\boldsymbol{\Sigma},\boldsymbol{\omega})}(\mathbf{x}) = G_{(\mathbf{0},\mathbf{P},\boldsymbol{\omega})}\left[\left(\frac{x_i - \mu_i}{\sigma_i}\right)_{i\in\mathscr{I}}\right], \quad \mathbf{x} = (x_i)_{i\in\mathscr{I}} \in \mathbb{R}^I. \tag{2}$$

For each $i \in \mathscr{I}$, its margin X_i admits $\mathcal{D}\big(\mu_i, \sigma_i^2, \boldsymbol{\omega}_i\big)$ with a marginal distribution function $F_{i;(\mu_i,\sigma_i^2,\boldsymbol{\omega}_i)}$ given by $F_{i;(\mu_i,\sigma_i^2,\boldsymbol{\omega}_i)}(x_i) = G_{i;\boldsymbol{\omega}_i}\left(\frac{x_i-\mu_i}{\sigma_i}\right)$, $x_i \in \mathbb{R}$, where $G_{i;\boldsymbol{\omega}_i} = G_{i;(0,1,\boldsymbol{\omega}_i)}$ is the marginal distribution function of $Z_i \sim \mathcal{D}(0, 1, \boldsymbol{\omega}_i)$.[2]

It is worth noting that $\mathbf{P}$ is the common Pearson's correlation matrix of $\mathbf{Z}$ and $\mathbf{X}$ due to the invariance property of Pearson's correlation coefficient ρ under any increasing linear transformation. To overcome its incapability to capture nonlinear dependence, we can employ a rank-based correlation coefficient, namely, Kendall's τ. In contrast to Pearson's ρ, Kendall's τ is invariant under any increasing transformation, which is linear or nonlinear. The similarity between these two correlation coefficients is that they measure dependence in the entire values of the random variables of interest. When dealing with systemic risk quantification by considering the extreme or distressing event of the conditioning random variable, we prefer to measure dependence only in their tails or extreme parts. We can do this using tail dependence coefficients. For all $i, j \in \mathscr{I}$, $i \neq j$, the coefficients of lower and upper tail dependence between X_i and X_j are defined as follows (Embrechts et al. 2003b):[3]

$$\lambda^{\mathrm{L}}_{ij;\boldsymbol{\theta}_{ij}} = \lim_{u \to 0+} \mathbb{P}\left(\left\{X_j < F^{-1}_{j;\boldsymbol{\theta}_j}(u)\right\} \,\middle|\, \left\{X_i < F^{-1}_{i;\boldsymbol{\theta}_i}(u)\right\}\right), \tag{3}$$

$$\lambda^{\mathrm{U}}_{ij;\boldsymbol{\theta}_{ij}} = \lim_{u \to 1-} \mathbb{P}\left(\left\{X_j > F^{-1}_{j;\boldsymbol{\theta}_j}(u)\right\} \,\middle|\, \left\{X_i > F^{-1}_{i;\boldsymbol{\theta}_i}(u)\right\}\right), \tag{4}$$

respectively, provided that the limits exist. We can say that $\lambda^{\mathrm{L}}_{ij;\boldsymbol{\theta}_{ij}}$ ($\lambda^{\mathrm{U}}_{ij;\boldsymbol{\theta}_{ij}}$) measures the tendency of their lower (upper) extreme events to take place simultaneously. Similarly to Kendall's τ, the coefficients of lower and upper tail dependence are invariant under any increasing transformation (Embrechts et al. 2003b).

2.1. Benchmark Models

One commonly assumes that $\mathbf{Z}$, which determines $\mathbf{X}$ in Equation (1), obeys a standardized I-variate normal distribution, i.e., $\mathbf{Z} \sim \mathcal{N}_I(\mathbf{0}, \mathbf{P})$, with a joint distribution function ${}^{\mathrm{N}}G_{(\mathbf{0},\mathbf{P})} = \Phi_{(\mathbf{0},\mathbf{P})}$ given by

$$\Phi_{(\mathbf{0},\mathbf{P})}(\mathbf{z}) = \int \cdots \int_{\times_{i \in \mathscr{I}} (-\infty, z_i]} \frac{1}{\sqrt{(2\pi)^I |\mathbf{P}|}} \mathrm{e}^{-\frac{1}{2}\mathbf{w}^\top \mathbf{P}^{-1} \mathbf{w}} \,\mathrm{d}\mathbf{w}, \quad \mathbf{z} = (z_i)_{i \in \mathscr{I}} \in \mathbb{R}^I, \tag{5}$$

where $\mathbf{P} \in (-1, 1)^{I \times I}$. This assumption leads to $\mathbf{X} \sim \mathcal{N}_I(\boldsymbol{\mu}, \boldsymbol{\Sigma})$ that has the following joint distribution function:

$$\begin{aligned} {}^{\mathrm{N}}F_{(\boldsymbol{\mu},\boldsymbol{\Sigma})}(\mathbf{x}) &= \Phi_{(\mathbf{0},\mathbf{P})}\left[\left(\frac{x_i - \mu_i}{\sigma_i}\right)_{i \in \mathscr{I}}\right] \\ &= \int \cdots \int_{\times_{i \in \mathscr{I}} (-\infty, x_i]} \frac{1}{\sqrt{(2\pi)^I |\boldsymbol{\Sigma}|}} \mathrm{e}^{-\frac{1}{2}(\mathbf{w}-\boldsymbol{\mu})^\top \boldsymbol{\Sigma}^{-1} (\mathbf{w}-\boldsymbol{\mu})} \,\mathrm{d}\mathbf{w}, \quad \mathbf{x} = (x_i)_{i \in \mathscr{I}} \in \mathbb{R}^I. \end{aligned} \tag{6}$$

Proposition 1 (Tong 1990)**.** *Let* $\mathbf{X} = (X_i)_{i \in \mathscr{I}} \sim \mathcal{N}_I(\boldsymbol{\mu}, \boldsymbol{\Sigma})$. *For each* $K \in \mathbb{N}$, $K < I$, *if* $\mathbf{X} = \begin{pmatrix} \mathbf{X}_1 \\ \mathbf{X}_2 \end{pmatrix}$, $\boldsymbol{\mu} = \begin{pmatrix} \boldsymbol{\mu}_1 \\ \boldsymbol{\mu}_2 \end{pmatrix}$, *and* $\boldsymbol{\Sigma} = \begin{pmatrix} \boldsymbol{\Sigma}_{11} & \boldsymbol{\Sigma}_{12} \\ \boldsymbol{\Sigma}_{21} & \boldsymbol{\Sigma}_{22} \end{pmatrix}$ *such that* $\mathbf{X}_1 \sim \mathcal{N}_K(\boldsymbol{\mu}_1, \boldsymbol{\Sigma}_{11})$ *and* $\mathbf{X}_2 \sim \mathcal{N}_{I-K}(\boldsymbol{\mu}_2, \boldsymbol{\Sigma}_{22})$, *then for all* $\mathbf{x}_1 \in \mathbb{R}^K$, $\mathbf{X}_2 \mid \{\mathbf{X}_1 = \mathbf{x}_1\} \sim \mathcal{N}_{I-K}\left(\boldsymbol{\mu}_{2|1}, \boldsymbol{\Sigma}_{2|1}\right)$, *where* $\boldsymbol{\mu}_{2|1} = \boldsymbol{\mu}_2 + \boldsymbol{\Sigma}_{21} \boldsymbol{\Sigma}_{11}^{-1} (\mathbf{x}_1 - \boldsymbol{\mu}_1)$ *and* $\boldsymbol{\Sigma}_{2|1} = \boldsymbol{\Sigma}_{22} - \boldsymbol{\Sigma}_{21} \boldsymbol{\Sigma}_{11}^{-1} \boldsymbol{\Sigma}_{12}$.

For each $i \in \mathscr{I}$, the random variable X_i obeys a univariate normal distribution $\mathcal{N}(\mu_i, \sigma_i^2)$ and has a zero skewness and a zero excess-kurtosis. This suggests its incapability to accommodate asymmetric and leptokurtic returns. For all $i, j \in \mathscr{I}$, $i \neq j$, the random variables X_i and X_j are distributed according to a bivariate normal distribution $\mathcal{N}_2(\boldsymbol{\mu}_{ij}, \boldsymbol{\Sigma}_{ij})$ and have Kendall's correlation coefficient ${}^{\mathrm{N}}\tau_{ij;\rho_{ij}} = \frac{2}{\pi} \sin^{-1}(\rho_{ij})$ (McNeil et al. 2015). The coefficient ${}^{\mathrm{N}}\lambda^{\mathrm{L}}_{ij}$ of their lower tail dependence can be derived as follows:

$${}^{\mathrm{N}}\lambda^{\mathrm{L}}_{ij} = 2 \lim_{u \to 0+} \Phi\left(\frac{\Phi^{-1}(u) - \rho_{ij}\,\Phi^{-1}(u)}{\sqrt{1 - \rho_{ij}^2}}\right) = 2 \lim_{u \to 0+} \Phi\left(\Phi^{-1}(u)\sqrt{\frac{1 - \rho_{ij}}{1 + \rho_{ij}}}\right) = 0,$$

where $\Phi = \Phi_{(0,1)}$ is the distribution function of a standardized univariate normal distribution. Similarly, we can derive ${}^{\mathrm{N}}\lambda^{\mathrm{U}}_{ij} = 0$. This means that the above normal model exhibits lower and upper tail independence. In other words, extreme returns comove independently under the normality assumption.

As an alternative, one can consider $\mathbf{Z}$ derived through the following transformation:

$$\mathbf{Z} = \frac{1}{\sqrt{Q}}\mathbf{Y}, \tag{7}$$

where $\mathbf{Y} = (Y_i)_{i\in\mathscr{I}}$ denotes a random vector obeying $\mathcal{N}_I(\mathbf{0}, \mathbf{P})$, and Q is a random variable having a scaled chi-square distribution, with a shape parameter $\nu \in (2, \infty)$ denoting degrees of freedom and a scale parameter $\nu - 2$; that is, $Q \sim \chi^2(\nu, \nu - 2)$. Assuming that they are independent, we find $\mathbf{Z}$ to follow a standardized I-variate Student's t distribution, with Pearson's correlation matrix $\mathbf{P}$ and degrees of freedom ν; that is, $\mathbf{Z} \sim \mathcal{T}_I(\mathbf{0}, \mathbf{P}, \nu)$ (Demarta and McNeil 2005; Ding 2016; Nadarajah and Kotz 2005). Its joint distribution function ${}^{\mathrm{T}}G_{(\mathbf{0},\mathbf{P},\nu)} = T_{(\mathbf{0},\mathbf{P},\nu)}$ is given by

$$T_{(\mathbf{0},\mathbf{P},\nu)}(\mathbf{z}) = \int\cdots\int_{\times_{i\in\mathscr{I}}(-\infty,z_i]} \frac{\Gamma(\frac{\nu+I}{2})}{\Gamma(\frac{\nu}{2})\sqrt{[(\nu-2)\pi]^I|\mathbf{P}|}} \left(1 + \frac{\mathbf{w}^\top\mathbf{P}^{-1}\mathbf{w}}{\nu-2}\right)^{-\frac{\nu+I}{2}} \mathrm{d}\mathbf{w}, \quad \mathbf{z} \in \mathbb{R}^I, \tag{8}$$

where Γ denotes the gamma function defined by $\Gamma(a) = \int_{\mathbb{R}_+} w^{a-1}\,\mathrm{e}^{-w}\,\mathrm{d}w$, $a \in \mathbb{R}_+$. As a result, we have $\mathbf{X} \sim \mathcal{T}_I(\boldsymbol{\mu}, \boldsymbol{\Sigma}, \nu)$ with the following joint distribution function:

$$\begin{aligned}
&{}^{\mathrm{T}}F_{(\boldsymbol{\mu},\boldsymbol{\Sigma},\nu)}(\mathbf{x}) \\
&= T_{(\mathbf{0},\mathbf{P},\nu)}\left[\left(\frac{x_i-\mu_i}{\sigma_i}\right)_{i\in\mathscr{I}}\right] \\
&= \int\cdots\int_{\times_{i\in\mathscr{I}}(-\infty,x_i]} \frac{\Gamma(\frac{\nu+I}{2})}{\Gamma(\frac{\nu}{2})\sqrt{[(\nu-2)\pi]^I|\boldsymbol{\Sigma}|}} \left[1 + \frac{(\mathbf{w}-\boldsymbol{\mu})^\top\boldsymbol{\Sigma}^{-1}(\mathbf{w}-\boldsymbol{\mu})}{\nu-2}\right]^{-\frac{\nu+I}{2}} \mathrm{d}\mathbf{w}, \quad \mathbf{x} \in \mathbb{R}^I.
\end{aligned} \tag{9}$$

Remark 1. *In this study, we set $Q \sim \chi^2(\nu, \nu-2)$, with a distribution function proportional to $\int_{(-\infty,q]} w^{\frac{\nu}{2}-1}\,\mathrm{e}^{-\frac{1}{2}(\nu-2)w}\,\mathrm{d}w$, $q \in \mathbb{R}_+$, to ensure that the resulting random vector $\mathbf{Z}$ has a standardized joint distribution, more specifically a standardized multivariate Student's t distribution, with Pearson's correlation matrix $\mathbf{P}$. This assumption results in a multivariate Student's t distribution for the random vector $\mathbf{X}$ with the same Pearson's correlation matrix $\mathbf{P}$ and a covariance matrix $\mathrm{Cov}(\mathbf{X},\mathbf{X}) = \boldsymbol{\Sigma}$. This proposed multivariate Student's t distribution is different from the one discussed in previous studies (e.g., Demarta and McNeil 2005; Ding 2016; Nadarajah and Kotz 2005). More specifically, these studies considered $Q \sim \chi^2(\nu, \nu)$, with a distribution function proportional to $\int_{(-\infty,q]} w^{\frac{\nu}{2}-1}\,\mathrm{e}^{-\frac{1}{2}\nu w}\,\mathrm{d}w$, $q \in \mathbb{R}_+$, resulting in a multivariate Student's t distribution with Pearson's correlation matrix $\frac{\nu}{\nu-2}\mathbf{P} \neq \mathbf{P}$ and a covariance matrix $\frac{\nu}{\nu-2}\boldsymbol{\Sigma} \neq \boldsymbol{\Sigma}$.*

Proposition 2 (Ding 2016)**.** *Let $\mathbf{X} = (X_i)_{i\in\mathscr{I}} \sim \mathcal{T}_I(\boldsymbol{\mu}, \boldsymbol{\Sigma}, \nu)$. For each $K \in \mathbb{N}$, $K < I$, if $\mathbf{X} = \begin{pmatrix}\mathbf{X}_1\\ \mathbf{X}_2\end{pmatrix}$, $\boldsymbol{\mu} = \begin{pmatrix}\boldsymbol{\mu}_1\\ \boldsymbol{\mu}_2\end{pmatrix}$, and $\boldsymbol{\Sigma} = \begin{pmatrix}\boldsymbol{\Sigma}_{11} & \boldsymbol{\Sigma}_{12}\\ \boldsymbol{\Sigma}_{21} & \boldsymbol{\Sigma}_{22}\end{pmatrix}$ such that $\mathbf{X}_1 \sim \mathcal{T}_K(\boldsymbol{\mu}_1, \boldsymbol{\Sigma}_{11}, \nu)$ and $\mathbf{X}_2 \sim \mathcal{T}_{I-K}(\boldsymbol{\mu}_2, \boldsymbol{\Sigma}_{22}, \nu)$, then for all $\mathbf{x}_1 \in \mathbb{R}^K$, $\mathbf{X}_2 \mid \{\mathbf{X}_1 = \mathbf{x}_1\} \sim \mathcal{T}_{I-K}\left(\boldsymbol{\mu}_{2|1}, \boldsymbol{\Sigma}_{2|1}, \nu + K\right)$, with $\boldsymbol{\mu}_{2|1} = \boldsymbol{\mu}_2 + \boldsymbol{\Sigma}_{21}\,\boldsymbol{\Sigma}_{11}^{-1}(\mathbf{x}_1 - \boldsymbol{\mu}_1)$ and $\boldsymbol{\Sigma}_{2|1} = \frac{\nu + (\mathbf{x}_1-\boldsymbol{\mu}_1)^\top\boldsymbol{\Sigma}_{11}^{-1}(\mathbf{x}_1-\boldsymbol{\mu}_1) - 2}{\nu+K-2}\left(\boldsymbol{\Sigma}_{22} - \boldsymbol{\Sigma}_{21}\,\boldsymbol{\Sigma}_{11}^{-1}\,\boldsymbol{\Sigma}_{12}\right)$.*[4]

For each $i \in \mathscr{I}$, X_i is distributed according to $\mathcal{T}\left(\mu_i, \sigma_i^2, \nu\right)$ and has a zero skewness, which is only defined if $\nu \in (3, \infty)$, and an excess kurtosis equal to $\frac{6}{\nu-4}$, which is only defined when $\nu \in (4, \infty)$. These moments (and other statistical properties) are controlled by the same degrees of freedom ν for each margin, indicating its inflexibility to capture asymmetric and leptokurtic returns. For all $i, j \in \mathscr{I}$, $i \neq j$, X_i and X_j admits $\mathcal{T}_2(\boldsymbol{\mu}_{ij}, \boldsymbol{\Sigma}_{ij}, \nu)$ and have Kendall's ${}^{\mathrm{T}}\tau_{ij;\rho_{ij}}$ equal to $\frac{2}{\pi}\sin^{-1}(\rho_{ij})$, as the normal model possesses (McNeil et al. 2015). The coefficient ${}^{\mathrm{T}}\lambda^{\mathrm{L}}_{ij;(\rho_{ij},\nu)}$ of their lower tail dependence can be obtained as follows:

$$\begin{aligned} {}^{\mathrm{T}}\lambda^{\mathrm{L}}_{ij;(\rho_{ij},\nu)} &= 2\lim_{u\to 0+} T_{\nu+1}\left(\frac{T_\nu^{-1}(u)-\rho_{ij}\,T_\nu^{-1}(u)}{\sqrt{1-\rho_{ij}^2}}\sqrt{\frac{\nu-1}{\nu+T_\nu^{-1}(u)^2-2}}\right) \\ &= 2\lim_{u\to 0+} T_{\nu+1}\left(\frac{T_\nu^{-1}(u)}{\left|T_\nu^{-1}(u)\right|}\sqrt{\frac{1-\rho_{ij}}{1+\rho_{ij}}\times\frac{\nu-1}{\frac{\nu-2}{T_\nu^{-1}(u)^2}+1}}\right) \\ &= 2T_{\nu+1}\left(-\sqrt{\frac{1-\rho_{ij}}{1+\rho_{ij}}(\nu-1)}\right), \end{aligned}$$

where $T_\nu = T_{(0,1,\nu)}$ is the distribution function of a standardized univariate Student's t distribution, with degrees of freedom ν. Similarly, we can find ${}^{\mathrm{T}}\lambda^{\mathrm{U}}_{ij;(\rho_{ij},\nu)} = {}^{\mathrm{T}}\lambda^{\mathrm{L}}_{ij;(\rho_{ij},\nu)}$.[5] This suggests that the above Student's t model exhibits lower and upper tail dependence. It is noteworthy that if $\nu \to \infty$, then $\mathcal{T}_I(\boldsymbol{\mu},\boldsymbol{\Sigma},\nu) \to \mathcal{N}_I(\boldsymbol{\mu},\boldsymbol{\Sigma})$, in line with the fact that ${}^{\mathrm{T}}\lambda^{\mathrm{L}}_{ij;(\rho_{ij},\nu)} \to 0 = {}^{\mathrm{N}}\lambda^{\mathrm{L}}_{ij}$ and ${}^{\mathrm{T}}\lambda^{\mathrm{U}}_{ij;(\rho_{ij},\nu)} \to 0 = {}^{\mathrm{N}}\lambda^{\mathrm{U}}_{ij}$.

2.2. Johnson's Models

To find a more appropriate distribution for $\mathbf{Z}$ (and for $\mathbf{X}$), we follow Johnson (1949) to propose a set of transformations (or in Johnson's terminology, translations) with the following general form:

$$Y_i = \gamma_i + \delta_i\, h\left(\frac{Z_i-\zeta_i}{\eta_i}\right), \quad i \in \mathscr{I}, \tag{10}$$

or equivalently

$$Z_i = \zeta_i + \eta_i\, h^{-1}\left(\frac{Y_i-\gamma_i}{\delta_i}\right), \quad i \in \mathscr{I}, \tag{11}$$

for some monotone real-valued function h (called the translation function), location parameter vector $\boldsymbol{\zeta} = (\zeta_i)_{i\in\mathscr{I}} \in \mathbb{R}^I$, scale parameter vector $\boldsymbol{\eta} = (\eta_i)_{i\in\mathscr{I}} \in \mathbb{R}^I_+$, and shape parameter vectors $\boldsymbol{\gamma} = (\gamma_i)_{i\in\mathscr{I}} \in \mathbb{R}^I$ and $\boldsymbol{\delta} = (\delta_i)_{i\in\mathscr{I}} \in \mathbb{R}^I_+$ such that $\mathbf{Y} = (Y_i)_{i\in\mathscr{I}}$ is a random vector obeying $\mathcal{N}_I(\mathbf{0},\mathbf{P})$. It is hoped that the translation function h preserves the theoretical importance and advantages of the (multivariate) normal distribution while eliminating its drawbacks (Johnson 1949). The monotonicity of h is required to ensure the existence of h^{-1} and thus make the statistical properties of $\mathbf{Z}$ analytically tractable. In particular, if h is increasing, we can verify that its joint distribution function is given by

$$G_{(\boldsymbol{\zeta},\boldsymbol{\eta},\boldsymbol{\gamma},\boldsymbol{\delta},\mathbf{P})}(\mathbf{z}) = \Phi_{(\mathbf{0},\mathbf{P})}\left[\left(\gamma_i + \delta_i\, h\left(\frac{z_i-\zeta_i}{\eta_i}\right)\right)_{i\in\mathscr{I}}\right], \quad \mathbf{z} \in \mathbb{R}^I. \tag{12}$$

Furthermore, we can obtain the quantile function of Z_i as follows:

$$G^{-1}_{i;(\zeta_i,\eta_i,\gamma_i,\delta_i)}(\alpha) = \zeta_i + \eta_i\, h^{-1}\left(\frac{\Phi^{-1}(\alpha)-\gamma_i}{\delta_i}\right), \quad \alpha \in (0,1). \tag{13}$$

By choosing any translation function h, we can define a multiply infinite system of distributions. In particular, Johnson (1949) considered three types of increasing translation function h, resulting in three special systems of distributions described as follows.

1. System of Bounded Distributions (SB)
   This system is derived using $h : (0,1) \to \mathbb{R}$, with $h(z) = \ln(\frac{z}{1-z})$ and $h^{-1}(y) = \frac{e^y}{1+e^y}$. The resulting distribution for Z_i is bounded since

$$Z_i = \zeta_i + \eta_i \frac{e^{\frac{Y_i-\gamma_i}{\delta_i}}}{1 + e^{\frac{Y_i-\gamma_i}{\delta_i}}} \in (\zeta_i, \zeta_i + \eta_i). \tag{14}$$

2. System of Lognormal Distributions (SL)
   This system is constructed using $h : \mathbb{R}_+ \to \mathbb{R}$, with $h(z) = \ln(z)$ and $h^{-1}(y) = e^y$. The resulting distribution for Z_i is bounded from below since

$$Z_i = \zeta_i + \eta_i \, e^{\frac{Y_i-\gamma_i}{\delta_i}} \in (\zeta_i, \infty). \tag{15}$$

3. System of Unbounded Distributions (SU)
   This system is determined using $h : \mathbb{R} \to \mathbb{R}$, with $h(z) = \sinh^{-1}(z) = \ln\left(z + \sqrt{1+z^2}\right)$ and $h^{-1}(y) = \sinh(y) = \frac{1}{2}(e^y - e^{-y})$. The resulting distribution for Z_i is unbounded since

$$Z_i = \zeta_i + \eta_i \sinh\left(\frac{Y_i - \gamma_i}{\delta_i}\right) \in (-\infty, \infty). \tag{16}$$

In this study, since we focus on modeling financial returns defined on the entire real number line $\mathbb{R} = (-\infty, \infty)$, we choose Johnson's SU translation function. This choice implies that the random vector $\mathbf{Z} = (Z_i)_{i \in \mathscr{I}}$ is said to admit an I-variate Johnson's SU distribution, parameterized by $\boldsymbol{\zeta}$, $\boldsymbol{\eta}$, $\boldsymbol{\gamma}$, $\boldsymbol{\delta}$, and $\mathbf{P}$; see Johnson (1949), Choi and Nam (2008), Choi et al. (2012), and van Dorp and Jones (2020). We can find that

$$\mathbb{E}(Z_i) = \zeta_i - \eta_i \, e^{\frac{1}{2\delta_i^2}} \sinh\left(\frac{\gamma_i}{\delta_i}\right), \tag{17}$$

$$\mathbb{V}(Z_i) = \frac{1}{2}\eta_i^2 \left(e^{\frac{1}{\delta_i^2}} - 1\right)\left[e^{\frac{1}{\delta_i^2}} \cosh\left(2\frac{\gamma_i}{\delta_i}\right) + 1\right], \tag{18}$$

with $\cosh(a) = \frac{1}{2}(e^a + e^{-a})$. Following the work of Hakim et al. (2022), we set $\zeta_i = \zeta(\gamma_i, \delta_i) = \eta(\gamma_i, \delta_i) \, e^{\frac{1}{2\delta_i^2}} \sinh\left(\frac{\gamma_i}{\delta_i}\right)$, $\eta_i = \eta(\gamma_i, \delta_i) = \left\{\frac{1}{2}\left(e^{\frac{1}{\delta_i^2}} - 1\right)\left[e^{\frac{1}{\delta_i^2}} \cosh\left(2\frac{\gamma_i}{\delta_i}\right) + 1\right]\right\}^{-\frac{1}{2}}$, with $\zeta(\cdot,\cdot), \eta(\cdot,\cdot) : \mathbb{R} \times \mathbb{R}_+ \to \mathbb{R}$, to obtain a standardized I-variate Johnson's SU distribution for $\mathbf{Z}$ written by $\mathbf{Z} \sim \mathcal{J}_I^{\text{SU}}(\mathbf{0}, {}^{\text{SU}}\mathbf{P}, \boldsymbol{\gamma}, \boldsymbol{\delta})$. Accordingly, the random vector $\mathbf{X}$ defined in Equation (1) follows $\mathcal{J}_I^{\text{SU}}(\boldsymbol{\mu}, {}^{\text{SU}}\boldsymbol{\Sigma}, \boldsymbol{\gamma}, \boldsymbol{\delta})$, with a joint distribution function ${}^{\text{SU}}F_{(\boldsymbol{\mu}, {}^{\text{SU}}\boldsymbol{\Sigma}, \boldsymbol{\gamma}, \boldsymbol{\delta})}$ given by

$${}^{\text{SU}}F_{(\boldsymbol{\mu}, {}^{\text{SU}}\boldsymbol{\Sigma}, \boldsymbol{\gamma}, \boldsymbol{\delta})}(\mathbf{x}) = \Phi_{(\mathbf{0},\mathbf{P})}\left[\left(\gamma_i + \delta_i \sinh^{-1}\left(\frac{\frac{x_i - \mu_i}{\sigma_i} - \zeta(\gamma_i, \delta_i)}{\eta(\gamma_i, \delta_i)}\right)\right)_{i \in \mathscr{I}}\right], \quad \mathbf{x} \in \mathbb{R}^I, \tag{19}$$

where ${}^{\text{SU}}\boldsymbol{\Sigma} = \left(\mathbf{D}^{\frac{1}{2}}\right)\left({}^{\text{SU}}\mathbf{P}\right)\left(\mathbf{D}^{\frac{1}{2}}\right)$.

For each $i \in \mathscr{I}$, X_i has finite moments for all orders. In particular, its skewness ξ_i and excess kurtosis κ_i can be expressed as follows (Hakim et al. 2022):

$$\begin{aligned} \xi_i = & -2\zeta(\gamma_i, \delta_i)^3 + \frac{3}{2}\zeta(\gamma_i, \delta_i)\,\eta(\gamma_i, \delta_i)^2 \left[e^{\frac{2}{\delta_i^2}} \cosh\left(2\frac{\gamma_i}{\delta_i}\right) - 1\right] \\ & - \frac{1}{4}\eta(\gamma_i, \delta_i)^3 \, e^{\frac{1}{2\delta_i^2}} \left[e^{\frac{4}{\delta_i^2}} \sinh\left(3\frac{\gamma_i}{\delta_i}\right) - 3\sinh\left(\frac{\gamma_i}{\delta_i}\right)\right], \end{aligned} \tag{20}$$

$$\begin{aligned}\kappa_i = &-3 - 3\zeta(\gamma_i,\delta_i)^4 + 3\zeta(\gamma_i,\delta_i)^2\,\eta(\gamma_i,\delta_i)^2\left[\mathrm{e}^{\frac{2}{\delta_i^2}}\cosh\left(2\frac{\gamma_i}{\delta_i}\right) - 1\right] \\ &-\zeta(\gamma_i,\delta_i)\,\eta(\gamma_i,\delta_i)^3\,\mathrm{e}^{\frac{1}{2\delta_i^2}}\left[\mathrm{e}^{\frac{4}{\delta_i^2}}\sinh\left(3\frac{\gamma_i}{\delta_i}\right) - 3\sinh\left(\frac{\gamma_i}{\delta_i}\right)\right] \\ &+\frac{1}{8}\eta(\gamma_i,\delta_i)^4\left[\mathrm{e}^{\frac{8}{\delta_i^2}}\cosh\left(4\frac{\gamma_i}{\delta_i}\right) - 4\mathrm{e}^{\frac{2}{\delta_i^2}}\cosh\left(2\frac{\gamma_i}{\delta_i}\right) + 3\right],\end{aligned} \tag{21}$$

whose values are controlled by γ_i and δ_i, respectively, (Choi and Nam 2008). More specifically, $\xi_i < 0$ for all $(\gamma_i,\delta_i) \in \mathbb{R}_+ \times \mathbb{R}_+$, $\xi_i = 0$ for all $(\gamma_i,\delta_i) \in \{0\} \times \mathbb{R}_+$, and $\xi_i > 0$ for all $(\gamma_i,\delta_i) \in \mathbb{R}_- \times \mathbb{R}_+$. Furthermore, $\kappa_i > 0$ for all $(\gamma_i,\delta_i) \in \mathbb{R} \times \mathbb{R}_+$. This suggests that Johnson's SU model is a suitable choice for more flexibly modeling asset returns that frequently exhibit asymmetry and leptokurticity. For all $i,j \in \mathscr{I}$, Pearson's correlation coefficient ${}^{\mathrm{SU}}\rho_{ij;(\rho_{ij},\boldsymbol{\gamma}_{ij},\boldsymbol{\delta}_{ij})}$ between X_i and X_j, which is the entry of Pearson's correlation matrix ${}^{\mathrm{SU}}\mathbf{P}$, is different from the entry ρ_{ij} of $\mathbf{P}$ due to the nonlinearity of the translation function $h = \sinh^{-1}$. These are related through the following formula (Hakim et al. 2022):

$$\begin{aligned}{}^{\mathrm{SU}}\rho_{ij;(\rho_{ij},\boldsymbol{\gamma}_{ij},\boldsymbol{\delta}_{ij})} = &\frac{1}{2}\eta(\gamma_i,\delta_i)\,\eta(\gamma_j,\delta_j)\,\mathrm{e}^{\frac{1}{2(\delta_i^2+\delta_j^2)}} \\ &\times\left[\left(\mathrm{e}^{\frac{\rho_{ij}}{\delta_i\delta_j}} - 1\right)\cosh\left(\frac{\gamma_i}{\delta_i} + \frac{\gamma_j}{\delta_j}\right) - \left(\mathrm{e}^{-\frac{\rho_{ij}}{\delta_i\delta_j}} - 1\right)\cosh\left(\frac{\gamma_i}{\delta_i} - \frac{\gamma_j}{\delta_j}\right)\right].\end{aligned} \tag{22}$$

However, since $h = \sinh^{-1}$ is increasing and δ_i is positive, Johnson's SU translation (16) leads us to have Kendall's correlation coefficient ${}^{\mathrm{SU}}\tau_{ij;(\rho_{ij},\boldsymbol{\gamma}_{ij},\boldsymbol{\delta}_{ij})} = {}^{\mathrm{N}}\tau_{ij;\rho_{ij}} = \frac{2}{\pi}\sin^{-1}(\rho_{ij})$ and the following lower and upper tail dependence coefficients: ${}^{\mathrm{SU}}\lambda_{ij}^{\mathrm{L}} = {}^{\mathrm{N}}\lambda_{ij}^{\mathrm{L}} = 0$ and ${}^{\mathrm{SU}}\lambda_{ij}^{\mathrm{U}} = {}^{\mathrm{N}}\lambda_{ij}^{\mathrm{U}} = 0$. This indicates the incapability of Johnson's SU model to accommodate tail dependence in both lower and upper tails, as the normal model does.

2.3. Copulas

More sophisticated multivariate risk models can be constructed using another approach based on the so-called copula defined as follows.

Definition 1 (McNeil et al. 2015)**.** *An I-variate copula is a joint distribution function, restricted to $[0,1]^I$, for a vector of I random variables uniformly distributed over $[0,1]$.*

From the above definition, we can denote an I-variate copula for a random vector $\mathbf{U} = (U_i)_{i\in\mathscr{I}}$ as a function $C_{\boldsymbol{\vartheta}} : [0,1]^I \to [0,1]$, with[6]

$$C_{\boldsymbol{\vartheta}}(\mathbf{u}) = \mathbb{P}\big(\{U_i \le u_i\}_{i\in\mathscr{I}}\big), \quad \mathbf{u} = (u_i)_{i\in\mathscr{I}} \in [0,1]^I, \tag{23}$$

characterized by a parameter $\boldsymbol{\vartheta}$. For a given vector $\mathbf{X} = (X_i)_{i\in\mathscr{I}}$ of continuous random variables, with a joint distribution function $F_{\boldsymbol{\theta}}$ and marginal distribution functions $F_{i;\boldsymbol{\theta}_i}$, $i \in \mathscr{I}$, we can find that $F_{i;\boldsymbol{\theta}_i}(X_i) \sim \mathcal{U}(0,1)$, $i \in \mathscr{I}$, known as the probability integral transform. This implies that there exists a copula $C_{\boldsymbol{\vartheta}}$ that can determine the joint distribution function $F_{\boldsymbol{\theta}}$. Conversely, for a given vector $\mathbf{U} = (U_i)_{i\in\mathscr{I}}$ of random variables following $\mathcal{U}(0,1)$ with a copula $C_{\boldsymbol{\vartheta}}$, and for specified continuous marginal distribution functions $F_{i;\boldsymbol{\theta}_i}$, $i \in \mathscr{I}$, we can verify that $F_{i;\boldsymbol{\theta}_i}^{-1}(U_i)$, $i \in \mathscr{I}$, are continuous random variables, whose marginal distribution functions are $F_{i;\boldsymbol{\theta}_i}$, $i \in \mathscr{I}$; this is known as the inverse probability integral transform. Consequently, there exists a joint distribution function $F_{\boldsymbol{\theta}}$ for such random variables. These notions were introduced by Sklar (1959), as completely stated in the following theorem.

Theorem 1 (Sklar 1959)**.** *If $F_{\boldsymbol{\theta}}$ is a continuous I-variate distribution function with marginal distribution functions $F_{i;\boldsymbol{\theta}_i}$, $i \in \mathscr{I}$, then there uniquely exists an I-variate copula $C_{\boldsymbol{\vartheta}}$ such that*

$$F_{\boldsymbol{\theta}}(\mathbf{x}) = C_{\boldsymbol{\vartheta}}\left[\left(F_{i;\boldsymbol{\theta}_i}(x_i)\right)_{i\in\mathscr{I}}\right], \quad \mathbf{x} = (x_i)_{i\in\mathscr{I}} \in \mathbb{R}^I. \tag{24}$$

Conversely, if $C_{\boldsymbol{\vartheta}}$ is an I-variate copula, and $F_{i;\boldsymbol{\theta}_i}$, $i \in \mathscr{I}$, are continuous univariate distribution functions, then the function $F_{\boldsymbol{\theta}}$ defined in Equation (24) is an I-variate distribution function with marginal distribution functions $F_{i;\boldsymbol{\theta}_i}$, $i \in \mathscr{I}$.

We see from Equation (24) that the distribution function $F_{\boldsymbol{\theta}}$ can be determined using a composition of the copula $C_{\boldsymbol{\vartheta}}$ and the marginal distribution functions $F_{i;\boldsymbol{\theta}_i}$, $i \in \mathscr{I}$. This means that $C_{\boldsymbol{\vartheta}}$ represents the dependence structure of random variables having a joint distribution function $F_{\boldsymbol{\theta}}$. This copula has the following expression:

$$C_{\boldsymbol{\vartheta}}(\mathbf{u}) = F_{\boldsymbol{\theta}}\left[\left(F^{-1}_{i;\boldsymbol{\theta}_i}(u_i)\right)_{i\in\mathscr{I}}\right], \quad \mathbf{u} = (u_i)_{i\in\mathscr{I}} \in [0,1]^I. \tag{25}$$

Based on the above formula, an I-variate copula can be constructed from a given I-variate distribution function and its margins; this is known as the inversion copula. According to the second part of Sklar's Theorem 1, this copula can be employed to determine another I-variate distribution function when given some margins. Due to the invariance properties of Kendall's correlation coefficient and tail dependence coefficients under any increasing transformation, these coefficients are preserved in the resulting copula $C_{\boldsymbol{\vartheta}}$.

In this study, the copulas we take into consideration are the members of the elliptical copula family. Two popular members of this copula family are the following:

1. Gaussian or normal copula ${}^{\mathrm{N}}C_{\mathbf{P}}$, which is derived from $\mathcal{N}_I(\mathbf{0}, \mathbf{P})$ as follows:

$$^{\mathrm{N}}C_{\mathbf{P}}(\mathbf{u}) = \Phi_{(\mathbf{0},\mathbf{P})}\left[\left(\Phi^{-1}(u_i)\right)_{i\in\mathscr{I}}\right], \quad \mathbf{u} \in [0,1]^I; \tag{26}$$

2. Student's t copula ${}^{\mathrm{T}}C_{(\mathbf{P},\nu)}$, which is obtained from $\mathcal{T}_I(\mathbf{0}, \mathbf{P}, \nu)$ as follows:[7]

$$^{\mathrm{T}}C_{(\mathbf{P},\nu)}(\mathbf{u}) = T_{(\mathbf{0},\mathbf{P},\nu)}\left[\left(T_\nu^{-1}(u_i)\right)_{i\in\mathscr{I}}\right], \quad \mathbf{u} \in [0,1]^I. \tag{27}$$

For all $i, j \in \mathscr{I}$, due to the invariance properties of Kendall's correlation coefficient and tail dependence coefficients under any increasing transformation, the normal copula has the coefficients of ${}^{\mathrm{N}}\tau_{ij;\rho_{ij}} = \frac{2}{\pi}\sin^{-1}(\rho_{ij})$ and ${}^{\mathrm{N}}\lambda^{\mathrm{L}}_{ij} = {}^{\mathrm{N}}\lambda^{\mathrm{U}}_{ij} = 0$, as the normal distribution possesses. Similar to Student's t distribution, Student's t copula has the coefficients of ${}^{\mathrm{T}}\tau_{ij;\rho_{ij}} = \frac{2}{\pi}\sin^{-1}(\rho_{ij})$ and ${}^{\mathrm{T}}\lambda^{\mathrm{L}}_{ij;(\rho_{ij},\nu)} = {}^{\mathrm{T}}\lambda^{\mathrm{U}}_{ij;(\rho_{ij},\nu)} = 2T_{\nu+1}\left(-\sqrt{\frac{1-\rho_{ij}}{1+\rho_{ij}}(\nu-1)}\right)$.[8] If $\nu \to \infty$, we have ${}^{\mathrm{T}}C_{(\mathbf{P},\nu)} \to {}^{\mathrm{N}}C_{\mathbf{P}}$, in line with evidence that $\mathcal{T}_I(\boldsymbol{\mu}, \boldsymbol{\Sigma}, \nu) \to \mathcal{N}_I(\boldsymbol{\mu}, \boldsymbol{\Sigma})$.

Note that if we construct an I-variate normal copula ${}^{\mathrm{N}}C_{\mathbf{P}}$ with normal margins $\mathcal{N}(\mu_i, \sigma_i^2)$, $i \in \mathscr{I}$, then the resulting distribution is $\mathcal{N}_I(\boldsymbol{\mu}, \boldsymbol{\Sigma})$, as discussed in Section 2.1. Furthermore, if we combine an I-variate normal copula ${}^{\mathrm{N}}C_{\mathbf{P}}$ and Johnson's SU margins $\mathcal{J}^{\mathrm{SU}}(\mu_i, \sigma_i^2, \gamma_i, \delta_i)$, $i \in \mathscr{I}$, we then derive $\mathcal{J}_I^{\mathrm{SU}}(\boldsymbol{\mu}, {}^{\mathrm{SU}}\boldsymbol{\Sigma}, \boldsymbol{\gamma}, \boldsymbol{\delta})$, as described in Section 2.2. Therefore, this study considers four copula-based multivariate models provided in the following proposition.

Proposition 3. *Let ${}^{\mathrm{N}}C_{\mathbf{P}}$ and ${}^{\mathrm{T}}C_{(\mathbf{P},\nu)}$ symbolize an I-variate normal and Student's t copulas, respectively.*

1. *A combination of the normal copula ${}^{\mathrm{N}}C_{\mathbf{P}}$ and Student's t margins $\mathcal{T}(\mu_i, \sigma_i^2, \nu_i)$, $i \in \mathscr{I}$, results in an I-variate model with the following joint distribution function:*

$$^{\mathrm{N-T}}F_{\boldsymbol{\theta}}(\mathbf{x}) = \Phi_{(\mathbf{0},\mathbf{P})}\left[\left(\Phi^{-1} \circ T_{\nu_i}\left(\frac{x_i - \mu_i}{\sigma_i}\right)\right)_{i\in\mathscr{I}}\right], \quad \mathbf{x} \in \mathbb{R}^I. \tag{28}$$

2. *A combination of Student's t copula* ${}^{\mathrm{T}}C_{(\mathbf{P},\nu)}$ *and normal margins* $\mathcal{N}(\mu_i,\sigma_i^2)$, $i \in \mathscr{I}$, *results in an I-variate model with the following joint distribution function:*

$$ {}^{\mathrm{T-N}}F_{\boldsymbol{\theta}}(\mathbf{x}) = T_{(\mathbf{0},\mathbf{P},\nu)}\left[\left(T_\nu^{-1}\circ\Phi\left(\frac{x_i-\mu_i}{\sigma_i}\right)\right)_{i\in\mathscr{I}}\right], \quad \mathbf{x}\in\mathbb{R}^I. \tag{29}$$

3. *A combination of Student's t copula* ${}^{\mathrm{T}}C_{(\mathbf{P},\nu)}$ *and Student's t margins* $\mathcal{T}(\mu_i,\sigma_i^2,\nu_i)$, $i \in \mathscr{I}$, *results in an I-variate model with the following joint distribution function:*[9]

$$ {}^{\mathrm{T-T}}F_{\boldsymbol{\theta}}(\mathbf{x}) = T_{(\mathbf{0},\mathbf{P},\nu)}\left[\left(T_\nu^{-1}\circ T_{\nu_i}\left(\frac{x_i-\mu_i}{\sigma_i}\right)\right)_{i\in\mathscr{I}}\right], \quad \mathbf{x}\in\mathbb{R}^I. \tag{30}$$

4. *A combination of Student's t copula* ${}^{\mathrm{T}}C_{(\mathbf{P},\nu)}$ *and Johnson's SU margins* $\mathcal{J}^{\mathrm{SU}}(\mu_i,\sigma_i^2,\gamma_i,\delta_i)$, $i \in \mathscr{I}$, *results in an I-variate model with the following joint distribution function:*

$$ \begin{aligned} &{}^{\mathrm{T-SU}}F_{\boldsymbol{\theta}}(\mathbf{x}) \\ &= T_{(\mathbf{0},\mathbf{P},\nu)}\left\{\left(T_\nu^{-1}\circ\Phi\left[\gamma_i+\delta_i\sinh^{-1}\left(\frac{\frac{x_i-\mu_i}{\sigma_i}-\zeta(\gamma_i,\delta_i)}{\eta(\gamma_i,\delta_i)}\right)\right]\right)_{i\in\mathscr{I}}\right\}, \quad \mathbf{x}\in\mathbb{R}^I. \end{aligned} \tag{31}$$

Overall, the seven models proposed in this study are summarized in Table 1. We see that Model 7 constructed using Student's t copula and Johnson's SU margins has the most complete ability to capture asymmetry, leptokurticity, and tail dependence.

Table 1. Seven multivariate models.

	Model	Abbreviation	Asymmetry	Leptokurticity	Tail Dependence
1	Normal	N	No	No	No
2	Student's t	T	No	**Yes**	**Yes**
3	Johnson's SU	SU	**Yes**	**Yes**	No
4	Normal copula with Student's t margins	N–T	No	**Yes**	No
5	Student's t copula with normal margins	T–N	No	No	**Yes**
6	Student's t copula with Student's t margins	T–T	No	**Yes**	**Yes**
7	Student's t copula with Johnson's SU margins	T–SU	**Yes**	**Yes**	**Yes**

Student's t copula and Student's t margins constructing Model 6 have different degrees of freedom. The last three columns indicate the ability of each model to capture asymmetry, leptokurticity, and tail dependence structure.

3. MCoVaR Formulation

For each $i \in \mathscr{I}$, we measure asset i's tail risk at a specified significance level $\alpha_i \in (0,1)$ using the VaR risk measure we denote by $\mathrm{VaR}^{\alpha_i}(X_i;\boldsymbol{\theta}_i) = \mathrm{VaR}_i^{\alpha_i}(\boldsymbol{\theta}_i)$ or simply $\mathrm{VaR}^{\alpha_i}(X_i) = \mathrm{VaR}_i^{\alpha_i}$. It satisfies the coverage probability equation $\mathbb{P}\{-X_i \le \mathrm{VaR}_i^{\alpha_i}\} = 1-\alpha_i$ or equivalently $\mathbb{P}\{X_i \le -\mathrm{VaR}_i^{\alpha_i}\} = \alpha_i$, and thus equals

$$ \mathrm{VaR}_i^{\alpha_i} = -F^{-1}_{i;(\mu_i,\sigma_i^2,\boldsymbol{\omega}_i)}(\alpha_i) = -\mu_i - \sigma_i\, G^{-1}_{i;\boldsymbol{\omega}_i}(\alpha_i). \tag{32}$$

Given the distressing event $\{X_i = -\mathrm{VaR}_i^{\alpha_i}\}$ of asset i at the α_i level, Adrian and Brunnermeier (2016) introduced CoVaR, defined by

$$ \mathrm{CoVaR}_{j|i}^{\alpha_j}\left(\boldsymbol{\theta}_{j|i}^{\alpha_i}\right) = \mathrm{CoVaR}_{j|i}^{\alpha_j|\alpha_i} = \mathrm{VaR}^{\alpha_j}\left(X_j \mid \{X_i = -\mathrm{VaR}_i^{\alpha_i}\}\right), \tag{33}$$

to measure asset j's tail risk at another fixed significance level $\alpha_j \in (0,1)$. The corresponding ΔCoVaR equal to $\mathrm{CoVaR}_{j|i}^{\alpha_j|\alpha_i} - \mathrm{CoVaR}_{j|i}^{\alpha_j|50\%}$ can be used to quantify the change in asset j's tail risk if asset i moves from a normal state to a distressing situation. However, these measures only account for potential systemic risk transmissions across each pair of targeted asset j and conditioning asset i by disregarding the remaining assets. Instead of involving asset i only, we prefer to account for the joint conditioning events of multiple assets by adopting the (Δ)MCoVaR systemic risk measure of Bernardi and Petrella (2015) and Bernardi et al. (2017). For simplicity in formulating the (Δ)MCoVaR, we introduce the following notations:

- For a given index set $\mathscr{I} = \{1, 2, \ldots, I\}$, we denote $\mathscr{I} \backslash \{j\}$ by $\mathscr{I}_{\backslash j}$ or simply $\backslash j$ for all $j \in \mathscr{I}$.
- For a given matrix $\mathbf{A} = (a_{kl})_{k \in \mathscr{I}_1, l \in \mathscr{I}_2}$, we denote $(a_{kj})_{k \in \mathscr{I}_1^*}$ and $(a_{kl})_{k \in \mathscr{I}_1^*, l \in \mathscr{I}_2^*}$ by $\mathbf{A}_{\mathscr{I}_1^*, j}$ and $\mathbf{A}_{\mathscr{I}_1^*, \mathscr{I}_2^*}$, respectively, for all $j \in \mathscr{I}_2$, $\mathscr{I}_1^* \subseteq \mathscr{I}_1$, and $\mathscr{I}_2^* \subseteq \mathscr{I}_2$.
- For a given function $h : A \to B$, we denote $\big(h(a_{kl})\big)_{k \in \mathscr{I}_1, l \in \mathscr{I}_2}$ by $h(\mathbf{A})$ for all $\mathbf{A} = (a_{kl})_{k \in \mathscr{I}_1, l \in \mathscr{I}_2} \in A^{I_1 \times I_2}$.

Definition 2 (Bernardi and Petrella 2015; Bernardi et al. 2017)**.** *Let $\mathbf{X} = (X_i)_{i \in \mathscr{I}}$. For each $j \in \mathscr{I}$, suppose that $\mathscr{I}_{\backslash j} = \mathscr{I}_{\backslash j}^{\mathrm{D}} \cup \mathscr{I}_{\backslash j}^{\mathrm{N}}$ such that $\mathscr{I}_{\backslash j}^{\mathrm{D}} \cap \mathscr{I}_{\backslash j}^{\mathrm{N}} = \varnothing$. For all $\alpha_j \in (0,1)$ and $\boldsymbol{\alpha}_{\backslash j}^{\mathrm{D}} = (\alpha_i)_{i \in \mathscr{I}_{\backslash j}^{\mathrm{D}}} \in (0,1)^{\left|\mathscr{I}_{\backslash j}^{\mathrm{D}}\right|}$, the MCoVaR of X_j at the α_j level is defined by*[10]

$$
\begin{aligned}
&\mathrm{MCoVaR}_{j|\backslash j}^{\alpha_j}\left(\boldsymbol{\theta}_{j|\backslash j}^{\boldsymbol{\alpha}_{\backslash j}^{\mathrm{D}}, 50\%}\right) \\
&= \mathrm{MCoVaR}_{j|\backslash j}^{\alpha_j | \boldsymbol{\alpha}_{\backslash j}^{\mathrm{D}}, 50\%} \\
&= \mathrm{VaR}^{\alpha_j}\left(X_j \;\middle|\; \{X_i = -\mathrm{VaR}_i^{\alpha_i}\}_{i \in \mathscr{I}_{\backslash j}^{\mathrm{D}}} \bigcap \left\{X_k = -\mathrm{VaR}_k^{50\%}\right\}_{k \in \mathscr{I}_{\backslash j}^{\mathrm{N}}}\right),
\end{aligned} \tag{34}
$$

which has the following conditional coverage probability:

$$
\begin{aligned}
&\mathbb{P}\left(\left\{X_j \leq -\mathrm{MCoVaR}_{j|\backslash j}^{\alpha_j | \boldsymbol{\alpha}_{\backslash j}^{\mathrm{D}}, 50\%}\right\} \;\middle|\; \{X_i = -\mathrm{VaR}_i^{\alpha_i}\}_{i \in \mathscr{I}_{\backslash j}^{\mathrm{D}}} \bigcap \left\{X_k = -\mathrm{VaR}_k^{50\%}\right\}_{k \in \mathscr{I}_{\backslash j}^{\mathrm{N}}}\right) \\
&= \alpha_j.
\end{aligned} \tag{35}
$$

The corresponding ΔMCoVaR is defined as the difference

$$
\Delta\mathrm{MCoVaR}_{j|\backslash j}^{\alpha_j | \boldsymbol{\alpha}_{\backslash j}^{\mathrm{D}}, 50\%} = \mathrm{MCoVaR}_{j|\backslash j}^{\alpha_j | \boldsymbol{\alpha}_{\backslash j}^{\mathrm{D}}, 50\%} - \mathrm{MCoVaR}_{j|\backslash j}^{\alpha_j | 50\%, 50\%}. \tag{36}
$$

Remark 2. *MCoVaR was first introduced by Cao (2013) by assuming that $\mathscr{I}_{\backslash j}^{\mathrm{D}} = \mathscr{I}_{\backslash j}$; that is, all assets, except for targeted asset j, are jointly distressed. Meanwhile, Torri et al. (2021) proposed MCoVaR by taking $\mathscr{I}_{\backslash j}^{\mathrm{D}} = \{i\}$ and $\mathscr{I}_{\backslash j}^{\mathrm{N}} = \mathscr{I} \backslash \{i, j\}$ into consideration.*

We can say that the MCoVaR in Equation (34) measures asset j's tail risk under the condition that all the assets in $\mathscr{I}_{\backslash j}^{\mathrm{D}}$ are jointly in distress and that all the assets in $\mathscr{I}_{\backslash j}^{\mathrm{N}}$ are jointly in their median or normal states. Meanwhile, the ΔMCoVaR in Equation (36) quantifies the joint systemic risk contributions of all the assets in $\mathscr{I}_{\backslash j}^{\mathrm{D}}$ to the targeted asset j. These systemic risk measures can be derived by determining and inverting the conditional distribution function $F_{j|\backslash j; \boldsymbol{\theta}_{j|\backslash j}}$ of X_j, given the joint conditioning events involving the vector $\mathbf{X}_{\backslash j} = (X_i)_{i \in \mathscr{I}_{\backslash j}}$ of the remaining random variables; that is,

$$
\mathrm{MCoVaR}_{j|\backslash j}^{\alpha_j | \boldsymbol{\alpha}_{\backslash j}^{\mathrm{D}}, 50\%} = -F_{j|\backslash j; \boldsymbol{\theta}_{j|\backslash j}}^{-1}(\alpha_j \mid \cdot). \tag{37}
$$

In this study, we perform the MCoVaR formulation when the asset returns are modeled using classical multivariate risk models, including multivariate normal and Student's t benchmark models and a multivariate Johnson's SU model. Some multivariate copulas with normal, Student's t, or Johnson's SU margins are also taken into consideration.

3.1. MCoVaR Based on Benchmark Models

The following theorems provide analytic MCoVaR formulas determined based on two benchmark models distributed according to multivariate normal and Student's t distributions. While previous studies (e.g., Bernardi and Petrella 2015; Bernardi et al. 2017; Torri et al. 2021) directly partitioned the covariance matrices of these models, this study considers the partitions of their correlation matrices, resulting in simpler formulas.

Theorem 2. *Let $\mathbf{X} = (X_i)_{i\in\mathscr{I}} \sim \mathcal{N}_I(\boldsymbol{\mu}, \boldsymbol{\Sigma})$, as determined by $\mathbf{Z} = (Z_i)_{i\in\mathscr{I}} \sim \mathcal{N}_I(\mathbf{0}, \mathbf{P})$ through Equation (1). For all $j \in \mathscr{I}$ and $\alpha_j \in (0,1)$, the MCoVaR of X_j at the α_j level, defined in Definition 2, is given by*

$$\begin{aligned}{}^{\mathrm{N}}\mathrm{MCoVaR}_{j|\backslash j}^{\alpha_j|\boldsymbol{\alpha}_{\backslash j}^{\mathrm{D}},50\%} &= -\mu_j - \sigma_j \left(\mathbf{P}_{j,\backslash j}\,\mathbf{P}_{\backslash j,\backslash j}^{-1}\right)_{\mathscr{I}_{\backslash j}^{\mathrm{D}}} \Phi^{-1}\left(\boldsymbol{\alpha}_{\backslash j}^{\mathrm{D}}\right) \\ &\quad - \sigma_j \sqrt{1 - \mathbf{P}_{j,\backslash j}\,\mathbf{P}_{\backslash j,\backslash j}^{-1}\,\mathbf{P}_{\backslash j,j}}\, \Phi^{-1}(\alpha_j).\end{aligned} \tag{38}$$

Proof. Suppose that all the entries of $\mathbf{Z} \sim \mathcal{N}_I(\mathbf{0}, \mathbf{P})$ are rearranged and partitioned as follows:

$$\begin{pmatrix} Z_j \\ \mathbf{Z}_{\backslash j} \end{pmatrix} \sim \mathcal{N}_I\left[\begin{pmatrix} 0 \\ \mathbf{0} \end{pmatrix}, \begin{pmatrix} 1 & \mathbf{P}_{j,\backslash j} \\ \mathbf{P}_{\backslash j,j} & \mathbf{P}_{\backslash j,\backslash j} \end{pmatrix}\right]. \tag{39}$$

According to Proposition 1, for all $\mathbf{z}_{\backslash j} \in \mathbb{R}^{I-1}$, we obtain

$$Z_j \,\Big|\, \left\{\mathbf{Z}_{\backslash j} = \mathbf{z}_{\backslash j}\right\} \sim \mathcal{N}\left(\mathbf{P}_{j,\backslash j}\,\mathbf{P}_{\backslash j,\backslash j}^{-1}\,\mathbf{z}_{\backslash j}, 1 - \mathbf{P}_{j,\backslash j}\,\mathbf{P}_{\backslash j,\backslash j}^{-1}\,\mathbf{P}_{\backslash j,j}\right). \tag{40}$$

For all $\mathbf{x}_{\backslash j} = (x_k)_{k\in\mathscr{I}_{\backslash j}} \in \mathbb{R}^{I-1}$, the conditional random variable $X_j \,\Big|\, \left\{\mathbf{X}_{\backslash j} = \mathbf{x}_{\backslash j}\right\}$ is distributionally equal to $\mu_j + \sigma_j\, Z_j \,\Big|\, \left\{\mathbf{Z}_{\backslash j} = \mathbf{z}_{\backslash j}\right\}$, with $\mathbf{z}_{\backslash j} = \left(\frac{x_k - \mu_k}{\sigma_k}\right)_{k\in\mathscr{I}_{\backslash j}}$. Therefore, we find that it obeys $\mathcal{N}\left[\mu_j + \sigma_j\,\mathbf{P}_{j,\backslash j}\,\mathbf{P}_{\backslash j,\backslash j}^{-1}\,\mathbf{z}_{\backslash j}, \sigma_j^2\left(1 - \mathbf{P}_{j,\backslash j}\,\mathbf{P}_{\backslash j,\backslash j}^{-1}\,\mathbf{P}_{\backslash j,j}\right)\right]$. Its conditional quantile at the α_j level is given by

$${}^{\mathrm{N}}F_{j|\backslash j;\boldsymbol{\theta}_{j|\backslash j}}^{-1}\left(\alpha_j \,\Big|\, \mathbf{x}_{\backslash j}\right) = \mu_j + \sigma_j\,\mathbf{P}_{j,\backslash j}\,\mathbf{P}_{\backslash j,\backslash j}^{-1}\,\mathbf{z}_{\backslash j} + \sigma_j\sqrt{1 - \mathbf{P}_{j,\backslash j}\,\mathbf{P}_{\backslash j,\backslash j}^{-1}\,\mathbf{P}_{\backslash j,j}}\,\Phi^{-1}(\alpha_j).$$

By substituting $x_k = -{}^{\mathrm{N}}\mathrm{VaR}_k^{\alpha_k} = \mu_k + \sigma_k\,\Phi^{-1}(\alpha_k)$ for all $k \in \mathscr{I}_{\backslash j}^{\mathrm{D}}$ and $x_k = -{}^{\mathrm{N}}\mathrm{VaR}_k^{50\%} = \mu_k$ for all $k \in \mathscr{I}_{\backslash j}^{\mathrm{N}}$, we obtain the MCoVaR of X_j, as presented in Equation (38). □

Theorem 3. *Let $\mathbf{X} = (X_i)_{i\in\mathscr{I}} \sim \mathcal{T}_I(\boldsymbol{\mu}, \boldsymbol{\Sigma}, \nu)$, as determined by $\mathbf{Z} = (Z_i)_{i\in\mathscr{I}} \sim \mathcal{T}_I(\mathbf{0}, \mathbf{P}, \nu)$ through Equation (1). For all $j \in \mathscr{I}$ and $\alpha_j \in (0,1)$, the MCoVaR of X_j at the α_j level, defined in Definition 2, is given by*

$$\begin{aligned}&{}^{\mathrm{T}}\mathrm{MCoVaR}_{j|\backslash j}^{\alpha_j|\boldsymbol{\alpha}_{\backslash j}^{\mathrm{D}},50\%} \\ &= -\mu_j - \sigma_j\left(\mathbf{P}_{j,\backslash j}\,\mathbf{P}_{\backslash j,\backslash j}^{-1}\right)_{\mathscr{I}_{\backslash j}^{\mathrm{D}}} T_\nu^{-1}\left(\boldsymbol{\alpha}_{\backslash j}^{\mathrm{D}}\right) \\ &\quad - \sigma_j\sqrt{\frac{\nu + T_\nu^{-1}\left(\boldsymbol{\alpha}_{\backslash j}^{\mathrm{D}}\right)^{\top}\mathbf{P}_{\mathscr{I}_{\backslash j}^{\mathrm{D}},\mathscr{I}_{\backslash j}^{\mathrm{D}}}^{-1}\,T_\nu^{-1}\left(\boldsymbol{\alpha}_{\backslash j}^{\mathrm{D}}\right) - 2}{\nu + I - 3}\left(1 - \mathbf{P}_{j,\backslash j}\,\mathbf{P}_{\backslash j,\backslash j}^{-1}\,\mathbf{P}_{\backslash j,j}\right)}\; T_{\nu+I-1}^{-1}(\alpha_j).\end{aligned} \tag{41}$$

Proof. Suppose that all the entries of $\mathbf{Z} \sim \mathcal{T}_I(\mathbf{0}, \mathbf{P}, \nu)$ are rearranged and partitioned as follows:

$$\begin{pmatrix} Z_j \\ \mathbf{Z}_{\backslash j} \end{pmatrix} \sim \mathcal{T}_I\left[\begin{pmatrix} 0 \\ \mathbf{0} \end{pmatrix}, \begin{pmatrix} 1 & \mathbf{P}_{j,\backslash j} \\ \mathbf{P}_{\backslash j,j} & \mathbf{P}_{\backslash j,\backslash j} \end{pmatrix}, \nu\right]. \tag{42}$$

Based on Proposition 2, for all $\mathbf{z}_{\setminus j} \in \mathbb{R}^{I-1}$, we obtain

$$Z_j \,\Big|\, \Big\{\mathbf{Z}_{\setminus j} = \mathbf{z}_{\setminus j}\Big\} \sim \mathcal{T}\left[\mathbf{P}_{j,\setminus j}\,\mathbf{P}_{\setminus j,\setminus j}^{-1}\,\mathbf{z}_{\setminus j},\, \frac{\nu + \mathbf{z}_{\setminus j}^{\top}\,\mathbf{P}_{\setminus j,\setminus j}^{-1}\,\mathbf{z}_{\setminus j} - 2}{\nu + I - 3}\Big(1 - \mathbf{P}_{j,\setminus j}\,\mathbf{P}_{\setminus j,\setminus j}^{-1}\,\mathbf{P}_{\setminus j,j}\Big), \nu + I - 1\right]. \tag{43}$$

For all $\mathbf{x}_{\setminus j} = (x_k)_{k\in\mathscr{I}_{\setminus j}} \in \mathbb{R}^{I-1}$, we find $X_j \,\Big|\, \Big\{\mathbf{X}_{\setminus j} = \mathbf{x}_{\setminus j}\Big\}$ to be distributionally equal to $\mu_j + \sigma_j\, Z_j \,\Big|\, \Big\{\mathbf{Z}_{\setminus j} = \mathbf{z}_{\setminus j}\Big\}$, where $\mathbf{z}_{\setminus j} = \Big(\frac{x_k - \mu_k}{\sigma_k}\Big)_{k\in\mathscr{I}_{\setminus j}}$. Thus, we obtain that $X_j \,\Big|\, \Big\{\mathbf{X}_{\setminus j} = \mathbf{x}_{\setminus j}\Big\}$ follows

$$\mathcal{T}\left[\mu_j + \sigma_j\,\mathbf{P}_{j,\setminus j}\,\mathbf{P}_{\setminus j,\setminus j}^{-1}\,\mathbf{z}_{\setminus j},\, \frac{\nu + \mathbf{z}_{\setminus j}^{\top}\,\mathbf{P}_{\setminus j,\setminus j}^{-1}\,\mathbf{z}_{\setminus j} - 2}{\nu + I - 3}\sigma_j^2\Big(1 - \mathbf{P}_{j,\setminus j}\,\mathbf{P}_{\setminus j,\setminus j}^{-1}\,\mathbf{P}_{\setminus j,j}\Big), \nu + I - 1\right].$$

Its conditional quantile at the α_j level is given by

$$\begin{aligned} {}^{\mathrm{T}}F^{-1}_{j|\setminus j;\boldsymbol{\theta}_{j|\setminus j}}\Big(\alpha_j \,\Big|\, \mathbf{x}_{\setminus j}\Big) &= \mu_j + \sigma_j\,\mathbf{P}_{j,\setminus j}\,\mathbf{P}_{\setminus j,\setminus j}^{-1}\,\mathbf{z}_{\setminus j} \\ &\quad + \sigma_j\sqrt{\frac{\nu + \mathbf{z}_{\setminus j}^{\top}\,\mathbf{P}_{\setminus j,\setminus j}^{-1}\,\mathbf{z}_{\setminus j} - 2}{\nu + I - 3}\Big(1 - \mathbf{P}_{j,\setminus j}\,\mathbf{P}_{\setminus j,\setminus j}^{-1}\,\mathbf{P}_{\setminus j,j}\Big)}\; T^{-1}_{\nu+I-1}(\alpha_j). \end{aligned}$$

By substituting $x_k = -{}^{\mathrm{T}}\mathrm{VaR}_k^{\alpha_k} = \mu_k + \sigma_k\, T_\nu^{-1}(\alpha_k)$ for all $k \in \mathscr{I}_{\setminus j}^{\mathrm{D}}$ and $x_k = -{}^{\mathrm{T}}\mathrm{VaR}_k^{50\%} = \mu_k$ for all $k \in \mathscr{I}_{\setminus j}^{\mathrm{N}}$, we derive the MCoVaR of X_j, as given in Equation (41). □

3.2. MCoVaR Based on Johnson's SU Models

To formulate the MCoVaR under Johnson's SU distributional assumption, we first determine the conditional distribution of Johnson's SU models as follows.

Proposition 4 (Hakim et al. 2022)**.** *Let* $\mathbf{X} = (X_i)_{i\in\mathscr{I}} \sim \mathcal{J}_I^{\mathrm{SU}}\big(\boldsymbol{\mu}, {}^{\mathrm{SU}}\boldsymbol{\Sigma}, \boldsymbol{\gamma}, \boldsymbol{\delta}\big)$*, as determined by* $\mathbf{Y} = (Y_i)_{i\in\mathscr{I}} \sim \mathcal{N}_I(\mathbf{0}, \mathbf{P})$ *through Equation (1) and Johnson's SU transform (16). For all* $j \in \mathscr{I}$ *and* $\mathbf{x}_{\setminus j} \in \mathbb{R}^{I-1}$*, the conditional distribution of* $X_j \,\Big|\, \Big\{\mathbf{X}_{\setminus j} = \mathbf{x}_{\setminus j}\Big\}$ *is* $\mathcal{J}^{\mathrm{SU}}\Big(\mu_{j|\setminus j}, \sigma^2_{j|\setminus j}, \gamma_{j|\setminus j}, \delta_{j|\setminus j}\Big)$*, where*

$$\mu_{j|\setminus j} = \mu_j + \sigma_j\left[\zeta(\gamma_j,\delta_j) - \eta(\gamma_j,\delta_j)\,\mathrm{e}^{\frac{1}{2(\delta_{j|\setminus j})^2}}\sinh\left(\frac{\gamma_{j|\setminus j}}{\delta_{j|\setminus j}}\right)\right], \tag{44}$$

$$\sigma^2_{j|\setminus j} = \frac{1}{2}\sigma_j^2\,\eta(\gamma_j,\delta_j)^2\left(\mathrm{e}^{\frac{1}{(\delta_{j|\setminus j})^2}} - 1\right)\left[\mathrm{e}^{\frac{1}{(\delta_{j|\setminus j})^2}}\cosh\left(2\frac{\gamma_{j|\setminus j}}{\delta_{j|\setminus j}}\right) + 1\right], \tag{45}$$

$$\gamma_{j|\setminus j} = \frac{\gamma_j - \mathbf{P}_{j,\setminus j}\,\mathbf{P}_{\setminus j,\setminus j}^{-1}\,\mathbf{y}_{\setminus j}}{\sqrt{1 - \mathbf{P}_{j,\setminus j}\,\mathbf{P}_{\setminus j,\setminus j}^{-1}\,\mathbf{P}_{\setminus j,j}}}, \quad \delta_{j|\setminus j} = \frac{\delta_j}{\sqrt{1 - \mathbf{P}_{j,\setminus j}\,\mathbf{P}_{\setminus j,\setminus j}^{-1}\,\mathbf{P}_{\setminus j,j}}}, \tag{46}$$

with

$$\mathbf{y}_{\setminus j} = \left(\gamma_k + \delta_k\sinh^{-1}\left(\frac{\frac{x_k-\mu_k}{\sigma_k} - \zeta(\gamma_k,\delta_k)}{\eta(\gamma_k,\delta_k)}\right)\right)_{k\in\mathscr{I}_{\setminus j}}. \tag{47}$$

Proof. Suppose that all the entries of $\mathbf{Y} \sim \mathcal{N}_I(\mathbf{0}, \mathbf{P})$ are rearranged and partitioned as in Equation (39) such that $Y_j \,\Big|\, \Big\{\mathbf{Y}_{\setminus j} = \mathbf{y}_{\setminus j}\Big\} \sim \mathcal{N}\Big(\mathbf{P}_{j,\setminus j}\,\mathbf{P}_{\setminus j,\setminus j}^{-1}\,\mathbf{y}_{\setminus j}, 1 - \mathbf{P}_{j,\setminus j}\,\mathbf{P}_{\setminus j,\setminus j}^{-1}\,\mathbf{P}_{\setminus j,j}\Big)$ for all

$\mathbf{y}_{\backslash j} \in \mathbb{R}^{I-1}$. This implies that, for all $\mathbf{x}_{\backslash j} \in \mathbb{R}^{I-1}$, the conditional distribution function of $X_j \,\Big|\, \left\{\mathbf{X}_{\backslash j} = \mathbf{x}_{\backslash j}\right\}$ is given by

$$\begin{aligned}
&{}^{\mathrm{SU}}F_{j|\backslash j;\boldsymbol{\theta}_{j|\backslash j}}\left(x_j \,\middle|\, \mathbf{x}_{\backslash j}\right) \\
&= \mathbb{P}\left(\{X_j \leq x_j\} \,\middle|\, \left\{\mathbf{X}_{\backslash j} = \mathbf{x}_{\backslash j}\right\}\right) \\
&= \mathbb{P}\left[\left\{Y_j \leq \gamma_j + \delta_j \sinh^{-1}\left(\frac{\frac{x_j-\mu_j}{\sigma_j} - \zeta(\gamma_j,\delta_j)}{\eta(\gamma_j,\delta_j)}\right)\right\} \,\middle|\, \left\{\mathbf{Y}_{\backslash j} = \mathbf{y}_{\backslash j}\right\}\right] \\
&= \Phi\left[\frac{\gamma_j + \delta_j \sinh^{-1}\left(\frac{\frac{x_j-\mu_j}{\sigma_j} - \zeta(\gamma_j,\delta_j)}{\eta(\gamma_j,\delta_j)}\right) - \mathbf{P}_{j,\backslash j}\,\mathbf{P}^{-1}_{\backslash j,\backslash j}\,\mathbf{y}_{\backslash j}}{\sqrt{1 - \mathbf{P}_{j,\backslash j}\,\mathbf{P}^{-1}_{\backslash j,\backslash j}\,\mathbf{P}_{\backslash j,j}}}\right] \\
&= \Phi\left[\frac{\gamma_j - \mathbf{P}_{j,\backslash j}\,\mathbf{P}^{-1}_{\backslash j,\backslash j}\,\mathbf{y}_{\backslash j}}{\sqrt{1 - \mathbf{P}_{j,\backslash j}\,\mathbf{P}^{-1}_{\backslash j,\backslash j}\,\mathbf{P}_{\backslash j,j}}} + \frac{\delta_j}{\sqrt{1 - \mathbf{P}_{j,\backslash j}\,\mathbf{P}^{-1}_{\backslash j,\backslash j}\,\mathbf{P}_{\backslash j,j}}} \sinh^{-1}\left(\frac{\frac{x_j-\mu_j}{\sigma_j} - \zeta(\gamma_j,\delta_j)}{\eta(\gamma_j,\delta_j)}\right)\right],
\end{aligned}$$

where $\mathbf{y}_{\backslash j}$ is provided in Equation (47). This shows that $X_j \,\Big|\, \left\{\mathbf{X}_{\backslash j} = \mathbf{x}_{\backslash j}\right\}$ admits Johnson's SU distribution, with shape parameters $\gamma_{j|\backslash j}$ and $\delta_{j|\backslash j}$ given in Equation (46). According to Equations (17) and (18), its conditional mean $\mu_{j|\backslash j}$ and conditional variance $\sigma^2_{j|\backslash j}$ are derived as in Equations (44) and (45), respectively. □

The following theorem states an analytic MCoVaR formula determined based on the above multivariate Johnson's SU model.

Theorem 4. *Let $\mathbf{X} = (X_i)_{i\in\mathscr{I}} \sim \mathcal{J}_I^{\mathrm{SU}}(\boldsymbol{\mu}, {}^{\mathrm{SU}}\boldsymbol{\Sigma}, \boldsymbol{\gamma}, \boldsymbol{\delta})$, as determined by $\mathbf{Y} = (Y_i)_{i\in\mathscr{I}} \sim \mathcal{N}_I(\mathbf{0}, \mathbf{P})$ through Equation (1) and Johnson's SU transform (16). For all $j \in \mathscr{I}$ and $\alpha_j \in (0,1)$, the MCoVaR of X_j at the α_j level, defined in Definition 2, is given by*

$$\begin{aligned}
&{}^{\mathrm{SU}}\mathrm{MCoVaR}_{j|\backslash j}^{\alpha_j|\boldsymbol{\alpha}^{\mathrm{D}}_{\backslash j},50\%} \\
&= -\mu_j - \sigma_j\left[\zeta(\gamma_j,\delta_j) - \eta(\gamma_j,\delta_j)\, \mathrm{e}^{\frac{1}{2(\delta_{j|\backslash j})^2}} \sinh\left(\frac{\gamma_{j|\backslash j}^{\boldsymbol{\alpha}^{\mathrm{D}}_{\backslash j},50\%}}{\delta_{j|\backslash j}}\right)\right] \\
&\quad - \sigma_j\,\eta(\gamma_j,\delta_j)\sqrt{\frac{1}{2}\left(\mathrm{e}^{\frac{1}{(\delta_{j|\backslash j})^2}} - 1\right)\left[\mathrm{e}^{\frac{1}{(\delta_{j|\backslash j})^2}} \cosh\left(2\frac{\gamma_{j|\backslash j}^{\boldsymbol{\alpha}^{\mathrm{D}}_{\backslash j},50\%}}{\delta_{j|\backslash j}}\right) + 1\right]} \\
&\quad \times \left[\zeta\left(\gamma_{j|i,\backslash j}^{\boldsymbol{\alpha}^{\mathrm{D}}_{\backslash j},50\%}, \delta_{j|\backslash j}\right) + \eta\left(\gamma_{j|\backslash j}^{\boldsymbol{\alpha}^{\mathrm{D}}_{\backslash j},50\%}, \delta_{j|\backslash j}\right) \sinh\left(\frac{\Phi^{-1}(\alpha_j) - \gamma_{j|\backslash j}^{\boldsymbol{\alpha}^{\mathrm{D}}_{\backslash j},50\%}}{\delta_{j|\backslash j}}\right)\right],
\end{aligned} \tag{48}$$

where

$$\gamma_{j|i,\backslash j}^{\boldsymbol{\alpha}^{\mathrm{D}}_{\backslash j},50\%} = \frac{\gamma_j - \left(\mathbf{P}_{j,\backslash j}\,\mathbf{P}^{-1}_{\backslash j,\backslash j}\right)_{\mathscr{I}^{\mathrm{D}}_{\backslash j}} \Phi^{-1}\left(\boldsymbol{\alpha}^{\mathrm{D}}_{\backslash j}\right)}{\sqrt{1 - \mathbf{P}_{j,\backslash j}\,\mathbf{P}^{-1}_{\backslash j,\backslash j}\,\mathbf{P}_{\backslash j,j}}}, \quad \delta_{j|\backslash j} = \frac{\delta_j}{\sqrt{1 - \mathbf{P}_{j,\backslash j}\,\mathbf{P}^{-1}_{\backslash j,\backslash j}\,\mathbf{P}_{\backslash j,j}}}. \tag{49}$$

Proof. According to Proposition 4, the conditional quantile of $X_j \,\Big|\, \left\{\mathbf{X}_{\setminus j} = \mathbf{x}_{\setminus j}\right\}$ at the α_j level is formulated as follows:

$$\begin{aligned}
{}^{\mathrm{SU}}F^{-1}_{j|\setminus j;\boldsymbol{\vartheta}_{j|\setminus j}}\left(\alpha_j \,\Big|\, \mathbf{x}_{\setminus j}\right) &= \mu_j + \sigma_j \left[\zeta(\gamma_j,\delta_j) - \eta(\gamma_j,\delta_j)\, \mathrm{e}^{\frac{1}{2(\delta_{j|\setminus j})^2}} \sinh\left(\frac{\gamma_{j|\setminus j}}{\delta_{j|\setminus j}}\right)\right] \\
&\quad + \sigma_j\, \eta(\gamma_j,\delta_j) \sqrt{\frac{1}{2}\left(\mathrm{e}^{\frac{1}{(\delta_{j|\setminus j})^2}} - 1\right)\left[\mathrm{e}^{\frac{1}{(\delta_{j|\setminus j})^2}} \cosh\left(2\frac{\gamma_{j|\setminus j}}{\delta_{j|\setminus j}}\right) + 1\right]} \\
&\quad \times \left[\zeta\left(\gamma_{j|i,\setminus j}, \delta_{j|\setminus j}\right) + \eta\left(\gamma_{j|\setminus j}, \delta_{j|\setminus j}\right) \sinh\left(\frac{\Phi^{-1}(\alpha_j) - \gamma_{j|\setminus j}}{\delta_{j|\setminus j}}\right)\right],
\end{aligned}$$

where the two shape parameters $\gamma_{j|\setminus j}$ and $\delta_{j|\setminus j}$ are given in Equation (46); these parameters depend on $\mathbf{y}_{\setminus j} = \left(\gamma_k + \delta_k \sinh^{-1}\left(\frac{\frac{x_k-\mu_k}{\sigma_k} - \zeta(\gamma_k,\delta_k)}{\eta(\gamma_k,\delta_k)}\right)\right)_{k\in\mathscr{I}_{\setminus j}}$ stated in Equation (47). If we substitute $x_k = -{}^{\mathrm{SU}}\mathrm{VaR}_k^{\alpha_k} = \mu_k + \sigma_k\left[\zeta(\gamma_k,\delta_k) + \eta(\gamma_k,\delta_k)\sinh\left(\frac{\Phi^{-1}(\alpha_k)-\gamma_k}{\delta_k}\right)\right]$ for all $k \in \mathscr{I}^{\mathrm{D}}_{\setminus j}$ and $x_k = -{}^{\mathrm{SU}}\mathrm{VaR}_k^{50\%} = \mu_k + \sigma_k\left[\zeta(\gamma_k,\delta_k) + \eta(\gamma_k,\delta_k)\sinh\left(\frac{-\gamma_k}{\delta_k}\right)\right]$ for all $k \in \mathscr{I}^{\mathrm{N}}_{\setminus j}$, we obtain the MCoVaR of X_j, as formulated in Equation (48). □

3.3. MCoVaR Based on Copulas

In this subsection, we formulate the MCoVaR systemic risk measure by employing elliptical copulas with normal, Student's t, or Johnson's SU margins. To accomplish this, we first determine conditional copula functions and their inverse as follows.

Theorem 5. *Let $\mathbf{U} = (U_i)_{i\in\mathscr{I}}$ be uniformly distributed over $[0,1]^I$, with a copula $C_{\boldsymbol{\vartheta}}$.*

1. *If $C_{\boldsymbol{\vartheta}} = {}^{\mathrm{N}}C_{\mathbf{P}}$ is a normal copula, then for all $j \in \mathscr{I}$ and $\mathbf{u}_{\setminus j} \in [0,1]^{I-1}$, the conditional distribution function of $U_j \,\Big|\, \left\{\mathbf{U}_{\setminus j} = \mathbf{u}_{\setminus j}\right\}$ and its inverse are given by*

$$ {}^{\mathrm{N}}C_{j|\setminus j;\boldsymbol{\vartheta}_{j|\setminus j}}\left(u_j \,\Big|\, \mathbf{u}_{\setminus j}\right) = \Phi\left[\frac{\Phi^{-1}(u_j) - \mathbf{P}_{j,\setminus j}\,\mathbf{P}^{-1}_{\setminus j,\setminus j}\,\Phi^{-1}(\mathbf{u}_{\setminus j})}{\sqrt{1 - \mathbf{P}_{j,\setminus j}\,\mathbf{P}^{-1}_{\setminus j,\setminus j}\,\mathbf{P}_{\setminus j,j}}}\right], \quad u_j \in [0,1], \tag{50}$$

and

$$\begin{aligned}
{}^{\mathrm{N}}C^{-1}_{j|\setminus j;\boldsymbol{\vartheta}_{j|\setminus j}}\left(\alpha_j \,\Big|\, \mathbf{u}_{\setminus j}\right) &= \Phi\left[\mathbf{P}_{j,\setminus j}\,\mathbf{P}^{-1}_{\setminus j,\setminus j}\,\Phi^{-1}(\mathbf{u}_{\setminus j}) + \sqrt{1 - \mathbf{P}_{j,\setminus j}\,\mathbf{P}^{-1}_{\setminus j,\setminus j}\,\mathbf{P}_{\setminus j,j}}\;\Phi^{-1}(\alpha_j)\right], \\
&\quad \alpha_j \in [0,1].
\end{aligned} \tag{51}$$

2. *If $C_{\boldsymbol{\vartheta}} = {}^{\mathrm{T}}C_{(\mathbf{P},\nu)}$ is Student's t copula, then for all $j \in \mathscr{I}$ and $\mathbf{u}_{\setminus j} \in [0,1]^{I-1}$, the conditional distribution function of $U_j \,\Big|\, \left\{\mathbf{U}_{\setminus j} = \mathbf{u}_{\setminus j}\right\}$ and its inverse are formulated as follows:*

$$\begin{aligned}
&{}^{\mathrm{T}}C_{j|\setminus j;\boldsymbol{\vartheta}_{j|\setminus j}}\left(u_j \,\Big|\, \mathbf{u}_{\setminus j}\right) \\
&= T_{\nu+I-1}\left[\frac{T_\nu^{-1}(u_j) - \mathbf{P}_{j,\setminus j}\,\mathbf{P}^{-1}_{\setminus j,\setminus j}\,T_\nu^{-1}(\mathbf{u}_{\setminus j})}{\sqrt{\frac{\nu + T_\nu^{-1}(\mathbf{u}_{\setminus j})^\top\,\mathbf{P}^{-1}_{\setminus j,\setminus j}\,T_\nu^{-1}(\mathbf{u}_{\setminus j}) - 2}{\nu+I-3}\left(1 - \mathbf{P}_{j,\setminus j}\,\mathbf{P}^{-1}_{\setminus j,\setminus j}\,\mathbf{P}_{\setminus j,j}\right)}}\right], \quad u_j \in [0,1],
\end{aligned} \tag{52}$$

and

$$
\begin{aligned}
&{}^{\mathrm{T}}C^{-1}_{j|\backslash j;\boldsymbol{\vartheta}_{j|\backslash j}}\left(\alpha_j \,\middle|\, \mathbf{u}_{\backslash j}\right) \\
&= T_\nu\Bigg[\mathbf{P}_{j,\backslash j}\,\mathbf{P}^{-1}_{\backslash j,\backslash j}\,T^{-1}_\nu(\mathbf{u}_{\backslash j}) \\
&\quad+\sqrt{\frac{\nu + T^{-1}_\nu(\mathbf{u}_{\backslash j})^\top\,\mathbf{P}^{-1}_{\backslash j,\backslash j}\,T^{-1}_\nu(\mathbf{u}_{\backslash j}) - 2}{\nu + I - 3}\left(1 - \mathbf{P}_{j,\backslash j}\,\mathbf{P}^{-1}_{\backslash j,\backslash j}\,\mathbf{P}_{\backslash j,j}\right)}\;T^{-1}_{\nu+I-1}(\alpha_j)\Bigg],
\end{aligned}
\tag{53}
$$

$\alpha_j \in [0,1]$.

Proof.

1. Based on the inverse probability integral transform, if $\mathbf{U}$ has a normal copula ${}^{\mathrm{N}}C_{\mathbf{P}}$, we find that $\Phi^{-1}(\mathbf{U}) \sim \mathcal{N}_I(\mathbf{0},\mathbf{P})$. By adopting Equations (39) and (40), we obtain

$$
\begin{aligned}
{}^{\mathrm{N}}C_{j|\backslash j;\boldsymbol{\vartheta}_{j|\backslash j}}\left(u_j \,\middle|\, \mathbf{u}_{\backslash j}\right) &= \mathbb{P}\left(\{U_j \le u_j\} \,\middle|\, \left\{\mathbf{U}_{\backslash j} = \mathbf{u}_{\backslash j}\right\}\right) \\
&= \mathbb{P}\left(\left\{\Phi^{-1}(U_j) \le \Phi^{-1}(u_j)\right\} \,\middle|\, \left\{\Phi^{-1}(\mathbf{U}_{\backslash j}) = \Phi^{-1}(\mathbf{u}_{\backslash j})\right\}\right) \\
&= \Phi\left[\frac{\Phi^{-1}(u_j) - \mathbf{P}_{j,\backslash j}\,\mathbf{P}^{-1}_{\backslash j,\backslash j}\,\Phi^{-1}(\mathbf{u}_{\backslash j})}{\sqrt{1 - \mathbf{P}_{j,\backslash j}\,\mathbf{P}^{-1}_{\backslash j,\backslash j}\,\mathbf{P}_{\backslash j,j}}}\right].
\end{aligned}
$$

   Its inverse is straightforward to derive.

2. According to the inverse probability integral transform, if $\mathbf{U}$ possesses Student's t copula ${}^{\mathrm{T}}C_{(\mathbf{P},\nu)}$, we obtain $T^{-1}_\nu(\mathbf{U}) \sim \mathcal{T}_I(\mathbf{0},\mathbf{P},\nu)$. By using Equations (42) and (43), we have

$$
\begin{aligned}
{}^{\mathrm{N}}C_{j|\backslash j;\boldsymbol{\vartheta}_{j|\backslash j}}\left(u_j \,\middle|\, \mathbf{u}_{\backslash j}\right) &= \mathbb{P}\left(\{U_j \le u_j\} \,\middle|\, \left\{\mathbf{U}_{\backslash j} = \mathbf{u}_{\backslash j}\right\}\right) \\
&= \mathbb{P}\left(\left\{T^{-1}_\nu(U_j) \le T^{-1}_\nu(u_j)\right\} \,\middle|\, \left\{T^{-1}_\nu(\mathbf{U}_{\backslash j}) = T^{-1}_\nu(\mathbf{u}_{\backslash j})\right\}\right) \\
&= T_{\nu+I-1}\left[\frac{T^{-1}_\nu(u_j) - \mathbf{P}_{j,\backslash j}\,\mathbf{P}^{-1}_{\backslash j,\backslash j}\,T^{-1}_\nu(\mathbf{u}_{\backslash j})}{\sqrt{\frac{\nu + T^{-1}_\nu(\mathbf{u}_{\backslash j})^\top\,\mathbf{P}^{-1}_{\backslash j,\backslash j}\,T^{-1}_\nu(\mathbf{u}_{\backslash j}) - 2}{\nu+I-3}\left(1 - \mathbf{P}_{j,\backslash j}\,\mathbf{P}^{-1}_{\backslash j,\backslash j}\,\mathbf{P}_{\backslash j,j}\right)}}\right].
\end{aligned}
$$

   Its inverse is straightforward to find.

□

Analytic MCoVaR formulas determined based on the above copulas are provided in the following theorem.

Theorem 6. *Let $\mathbf{X} = (X_i)_{i\in\mathscr{I}}$ have a joint distribution determined by a copula $C_{\boldsymbol{\vartheta}}$ and marginal distribution functions $F_{i;(\mu_i,\sigma_i^2,\boldsymbol{\omega}_i)}(x_i) = G_{i;\boldsymbol{\omega}_i}\left(\frac{x_i-\mu_i}{\sigma_i}\right)$, $x_i \in \mathbb{R}$, $i \in \mathscr{I}$.*

1. *If $C_{\boldsymbol{\vartheta}} = {}^{\mathrm{N}}C_{\mathbf{P}}$ is a normal copula, then for all $j \in \mathscr{I}$ and $\alpha_j \in (0,1)$, the MCoVaR of X_j at the α_j level, defined in Definition 2, is given by*

$$
\begin{aligned}
&{}^{\mathrm{N-X}}\mathrm{MCoVaR}^{\alpha_j|\boldsymbol{\alpha}^{\mathrm{D}}_{\backslash j},50\%}_{j|\backslash j} \\
&= -\mu_j - \sigma_j\,G^{-1}_{j;\boldsymbol{\omega}_j} \circ \Phi\left[\left(\mathbf{P}_{j,\backslash j}\,\mathbf{P}^{-1}_{\backslash j,\backslash j}\right)_{\mathscr{I}^{\mathrm{D}}_{\backslash j}}\Phi^{-1}\left(\boldsymbol{\alpha}^{\mathrm{D}}_{\backslash j}\right) + \sqrt{1 - \mathbf{P}_{j,\backslash j}\,\mathbf{P}^{-1}_{\backslash j,\backslash j}\,\mathbf{P}_{\backslash j,j}}\;\Phi^{-1}(\alpha_j)\right].
\end{aligned}
\tag{54}
$$

2. *If $C_{\boldsymbol{\vartheta}} = {}^{\mathrm{T}}C_{(\mathbf{P},\nu)}$ is Student's t copula, then for all $j \in \mathscr{I}$ and $\alpha_j \in (0,1)$, the MCoVaR of X_j at the α_j level, defined in Definition 2, is given by*

$$
\begin{aligned}
&{}^{\mathrm{T-X}}\mathrm{MCoVaR}_{j|\backslash j}^{\alpha_j|\boldsymbol{\alpha}_{\backslash j}^{\mathrm{D}},50\%} \\
&= -\mu_j - \sigma_j\, G_{j;\boldsymbol{\omega}_j}^{-1} \circ T_\nu \Bigg[\left(\mathbf{P}_{j,\backslash j}\,\mathbf{P}_{\backslash j,\backslash j}^{-1}\right)_{\mathscr{I}_{\backslash j}^{\mathrm{D}}} T_\nu^{-1}\left(\boldsymbol{\alpha}_{\backslash j}^{\mathrm{D}}\right) \\
&\quad + \sqrt{\frac{\nu + T_\nu^{-1}\left(\boldsymbol{\alpha}_{\backslash j}^{\mathrm{D}}\right)^{\top} \mathbf{P}_{\mathscr{I}_{\backslash j}^{\mathrm{D}},\mathscr{I}_{\backslash j}^{\mathrm{D}}}^{-1} T_\nu^{-1}\left(\boldsymbol{\alpha}_{\backslash j}^{\mathrm{D}}\right) - 2}{\nu + I - 3}\left(1 - \mathbf{P}_{j,\backslash j}\,\mathbf{P}_{\backslash j,\backslash j}^{-1}\,\mathbf{P}_{\backslash j,j}\right)}\; T_{\nu+I-1}^{-1}(\alpha_j) \Bigg].
\end{aligned}
\tag{55}
$$

Proof. According to the probability integral transform, we find $U_i = F_{i;\boldsymbol{\theta}_i}(X_i) \sim \mathcal{U}(0,1)$, $i \in \mathscr{I}$, with a copula $C_{\boldsymbol{\vartheta}}$. Based on the MCoVaR definition in Equations (34) and (35), we have

$$
\begin{aligned}
\alpha_j &= \mathbb{P}\left(\left\{X_j \le -\mathrm{MCoVaR}_{j|\backslash j}^{\alpha_j|\boldsymbol{\alpha}_{\backslash j}^{\mathrm{D}},50\%}\right\} \,\middle|\, \left\{X_i = -\mathrm{VaR}_i^{\alpha_i}\right\}_{i\in\mathscr{I}_{\backslash j}^{\mathrm{D}}} \bigcap \left\{X_k = -\mathrm{VaR}_k^{50\%}\right\}_{k\in\mathscr{I}_{\backslash j}^{\mathrm{N}}}\right) \\
&= \mathbb{P}\Bigg[\left\{F_{j;\boldsymbol{\theta}_j}(X_j) \le F_{j;\boldsymbol{\theta}_j}\left(-\mathrm{MCoVaR}_{j|\backslash j}^{\alpha_j|\boldsymbol{\alpha}_{\backslash j}^{\mathrm{D}},50\%}\right)\right\} \,\Bigg|\, \\
&\qquad \left\{F_{i;\boldsymbol{\theta}_i}(X_i) = F_{i;\boldsymbol{\theta}_i}\left(-\mathrm{VaR}_i^{\alpha_i}\right)\right\}_{i\in\mathscr{I}_{\backslash j}^{\mathrm{D}}} \bigcap \left\{F_{k;\boldsymbol{\theta}_k}(X_k) = F_{k;\boldsymbol{\theta}_k}\left(-\mathrm{VaR}_k^{50\%}\right)\right\}_{k\in\mathscr{I}_{\backslash j}^{\mathrm{N}}}\Bigg] \\
&= \mathbb{P}\left[\left\{U_j \le F_{j;\boldsymbol{\theta}_j}\left(-\mathrm{MCoVaR}_{j|\backslash j}^{\alpha_j|\boldsymbol{\alpha}_{\backslash j}^{\mathrm{D}},50\%}\right)\right\} \,\middle|\, \{U_i = \alpha_i\}_{i\in\mathscr{I}_{\backslash j}^{\mathrm{D}}} \bigcap \{U_k = 50\%\}_{k\in\mathscr{I}_{\backslash j}^{\mathrm{N}}}\right] \\
&= C_{j|\backslash j;\boldsymbol{\vartheta}_{j|\backslash j}}\left[F_{j;\boldsymbol{\theta}_j}\left(-\mathrm{MCoVaR}_{j|\backslash j}^{\alpha_j|\boldsymbol{\alpha}_{\backslash j}^{\mathrm{D}},50\%}\right) \,\middle|\, \boldsymbol{\alpha}_{\backslash j}^{\mathrm{D}}, 50\%\right].
\end{aligned}
$$

This implies that

$$
C_{j|\backslash j;\boldsymbol{\vartheta}_{j|\backslash j}}^{-1}\left(\alpha_j \,\middle|\, \boldsymbol{\alpha}_{\backslash j}^{\mathrm{D}}, 50\%\right) = F_{j;\boldsymbol{\theta}_j}\left(-\mathrm{MCoVaR}_{j|\backslash j}^{\alpha_j|\boldsymbol{\alpha}_{\backslash j}^{\mathrm{D}},50\%}\right) = G_{j;\boldsymbol{\omega}_j}\left(\frac{-\mathrm{MCoVaR}_{j|\backslash j}^{\alpha_j|\boldsymbol{\alpha}_{\backslash j}^{\mathrm{D}},50\%} - \mu_j}{\sigma_j}\right)
$$

and thus

$$
\mathrm{MCoVaR}_{j|\backslash j}^{\alpha_j|\boldsymbol{\alpha}_{\backslash j}^{\mathrm{D}},50\%} = -\mu_j - \sigma_j\, G_{j;\boldsymbol{\omega}_j}^{-1} \circ C_{j|\backslash j;\boldsymbol{\vartheta}_{j|\backslash j}}^{-1}\left(\alpha_j \,\middle|\, \boldsymbol{\alpha}_{\backslash j}^{\mathrm{D}}, 50\%\right).
$$

If we substitute $C_{j|\backslash j;\boldsymbol{\vartheta}_{j|\backslash j}}^{-1} = {}^{\mathrm{N}}C_{j|\backslash j;\boldsymbol{\vartheta}_{j|\backslash j}}^{-1}$ given in Equation (51), we have ${}^{\mathrm{N-X}}\mathrm{MCoVaR}_{j|\backslash j}^{\alpha_j|\boldsymbol{\alpha}_{\backslash j}^{\mathrm{D}},50\%}$, as presented in Equation (54). Furthermore, when we substitute $C_{j|\backslash j;\boldsymbol{\vartheta}_{j|\backslash j}}^{-1} = {}^{\mathrm{T}}C_{j|\backslash j;\boldsymbol{\vartheta}_{j|\backslash j}}^{-1}$ given in Equation (53), we derive ${}^{\mathrm{T-X}}\mathrm{MCoVaR}_{j|\backslash j}^{\alpha_j|\boldsymbol{\alpha}_{\backslash j}^{\mathrm{D}},50\%}$, as formulated in Equation (55). □

Based on Theorem 6 and Table 1, we formulate the MCoVaR for four copula-based models as follows:

1. From Equation (54), we obtain the MCoVaR formula for the N–T model by replacing $G_{j;\boldsymbol{\omega}_j}^{-1}$ with $T_{\nu_j}^{-1}$.
2. From Equation (55), we derive the MCoVaR formula for the T–N model by replacing $G_{j;\boldsymbol{\omega}_j}^{-1}$ with Φ^{-1}.
3. From Equation (55), we construct the MCoVaR formula for the T–T model by replacing $G_{j;\boldsymbol{\omega}_j}^{-1}$ with $T_{\nu_j}^{-1}$.

4. From Equation (55), we build the MCoVaR formula for the T–SU model by replacing $G^{-1}_{j;\boldsymbol{\omega}_j}(\cdot)$ with $\zeta(\gamma_j, \delta_j) + \eta(\gamma_j, \delta_j) \sinh\left(\frac{\Phi^{-1}(\cdot)-\gamma_j}{\delta_j}\right)$.

4. MCoVaR Forecasts and Their Conditional Coverage and Backtesting Performances

The true values of $\mathrm{VaR}_i^{\alpha_i} = \mathrm{VaR}_i^{\alpha_i}(\boldsymbol{\theta}_i)$ and $\mathrm{MCoVaR}_{j|\setminus j}^{\alpha_j|\boldsymbol{\alpha}^{\mathrm{D}}_{\setminus j},50\%} = \mathrm{MCoVaR}_{j|\setminus j}^{\alpha_j}\left(\boldsymbol{\theta}_{j|\setminus j}^{\boldsymbol{\alpha}^{\mathrm{D}}_{\setminus j},50\%}\right)$ are unable to be computed in practice since these measures depend on the unknown parameters of the risk models. Consequently, we must first estimate them from an available dataset $\left\{(x_{i;n})_{i\in\mathscr{I}}\right\}_{n\in\mathscr{N}}$, with $\mathscr{N} = \{1, 2, \ldots, N\}$, and then substitute the resulting estimators to the above measures.

- For the multivariate normal model, we estimate its mean vector $\boldsymbol{\mu}$ and covariance matrix $\boldsymbol{\Sigma}$ using the moment matching method as follows: $\hat{\boldsymbol{\mu}} = (\hat{\mu}_i)_{i\in\mathscr{I}}$ and $\hat{\boldsymbol{\Sigma}} = (\hat{\sigma}_{ij})_{i,j\in\mathscr{I}}$, with

$$\begin{cases} \hat{\mu}_i = \dfrac{1}{N} \displaystyle\sum_{n\in\mathscr{N}} x_{i;n} = \bar{x}_i, \\ \hat{\sigma}_i^2 = \dfrac{1}{N} \displaystyle\sum_{n\in\mathscr{N}} (x_{i;n} - \bar{x}_i)^2, \\ \hat{\sigma}_{ij} = \hat{\rho}_{ij}\, \hat{\sigma}_i\, \hat{\sigma}_j = \dfrac{1}{N} \displaystyle\sum_{n\in\mathscr{N}} (x_{i;n} - \bar{x}_i)(x_{j;n} - \bar{x}_j). \end{cases}$$

- For the multivariate Student's t model, we estimate its mean vector $\boldsymbol{\mu}$ and covariance matrix $\boldsymbol{\Sigma}$ using the moment matching method. Once their estimators $\hat{\boldsymbol{\mu}}$ and $\hat{\boldsymbol{\Sigma}}$ have been derived, we then estimate its degrees of freedom ν using the maximum likelihood method as follows:

$$\hat{\nu} = \operatorname*{arg\,max}_{\nu\in(2,\infty)} \prod_{n\in\mathscr{N}} {}^{\mathrm{T}}f_{(\hat{\boldsymbol{\mu}},\hat{\boldsymbol{\Sigma}},\nu)}\big((x_{i;n})_{i\in\mathscr{I}}\big) = \operatorname*{arg\,max}_{\nu\in(2,\infty)} \sum_{n\in\mathscr{N}} \ln\Big[{}^{\mathrm{T}}f_{(\hat{\boldsymbol{\mu}},\hat{\boldsymbol{\Sigma}},\nu)}\big((x_{i;n})_{i\in\mathscr{I}}\big)\Big].$$

- For the multivariate Johnson's SU model, we estimate its mean vector $\boldsymbol{\mu}$, covariance matrix ${}^{\mathrm{SU}}\boldsymbol{\Sigma}$, and shape parameter vectors $\boldsymbol{\gamma}$ and $\boldsymbol{\delta}$ using the moment matching method as follows: $\hat{\boldsymbol{\mu}} = (\hat{\mu}_i)_{i\in\mathscr{I}}$, ${}^{\mathrm{SU}}\hat{\boldsymbol{\Sigma}} = ({}^{\mathrm{SU}}\hat{\sigma}_{ij})_{i,j\in\mathscr{I}}$, $\hat{\boldsymbol{\gamma}} = (\hat{\gamma}_i)_{i\in\mathscr{I}}$, and $\hat{\boldsymbol{\delta}} = (\hat{\delta}_i)_{i\in\mathscr{I}}$, with

$$\begin{cases} \hat{\mu}_i = \dfrac{1}{N} \displaystyle\sum_{n\in\mathscr{N}} x_{i;n} = \bar{x}_i, \\ \hat{\sigma}_i^2 = \dfrac{1}{N} \displaystyle\sum_{n\in\mathscr{N}} (x_{i;n} - \bar{x}_i)^2, \\ {}^{\mathrm{SU}}\hat{\sigma}_{ij} = {}^{\mathrm{SU}}\hat{\rho}_{ij}\, \hat{\sigma}_i\, \hat{\sigma}_j = \dfrac{1}{N} \displaystyle\sum_{n\in\mathscr{N}} (x_{i;n} - \bar{x}_i)(x_{j;n} - \bar{x}_j), \\ \hat{\varsigma}_i\, \hat{\sigma}_i^3 = \dfrac{1}{N} \displaystyle\sum_{n\in\mathscr{N}} (x_{i;n} - \bar{x}_i)^3, \\ \hat{\kappa}_i\, \hat{\sigma}_i^4 = \dfrac{1}{N} \displaystyle\sum_{n\in\mathscr{N}} (x_{i;n} - \bar{x}_i)^4. \end{cases}$$

- For the copula-based multivariate models, we first estimate the parameter vector $\boldsymbol{\theta}_i$ of each margin i using the moment matching or maximum likelihood method and then determine a collection $\left\{(u_{i;n})_{i\in\mathscr{I}}\right\}_{n\in\mathscr{N}}$ of pseudo observations, with $u_{i;n} = F_{i;\hat{\boldsymbol{\theta}}_i}(x_{i;n})$. We estimate the parameter matrix $\mathbf{P}$ of the normal and Student's t copulas by matching the dependence measures as follows: $\hat{\mathbf{P}} = (\hat{\rho}_{ij})_{i,j\in\mathscr{I}}$, with $\hat{\rho}_{ij} = \sin\left(\frac{\pi}{2}\hat{\tau}_{ij}\right)$. We then estimate the degrees of freedom ν of Student's t copula using the maximum likelihood method as follows:

$$\hat{\nu} = \operatorname*{arg\,max}_{\nu\in(2,\infty)} \prod_{n\in\mathscr{N}} {}^{\mathrm{T}}c_{(\hat{\mathbf{P}},\nu)}\big((u_{i;n})_{i\in\mathscr{I}}\big) = \operatorname*{arg\,max}_{\nu\in(2,\infty)} \sum_{n\in\mathscr{N}} \ln\Big[{}^{\mathrm{T}}c_{(\hat{\mathbf{P}},\nu)}\big((u_{i;n})_{i\in\mathscr{I}}\big)\Big].$$

Once the parameter estimators $\hat{\theta}_i$ and $\hat{\theta}_{j|\setminus j}^{\boldsymbol{\alpha}_{\setminus j}^{\mathrm{D}},50\%}$ have been found, an estimative VaR forecast $\mathrm{VaR}_i^{\alpha_i}(\hat{\theta}_i)$ and an estimative MCoVaR forecast $\mathrm{MCoVaR}_{j|\setminus j}^{\alpha_j}\left(\hat{\theta}_{j|\setminus j}^{\boldsymbol{\alpha}_{\setminus j}^{\mathrm{D}},50\%}\right)$ can be obtained.

4.1. Conditional Coverage Performance of MCoVaR Forecasts

We need to examine the coverage probability (CP) of $\mathrm{VaR}_i^{\alpha_i}(\hat{\theta}_i)$ and the conditional coverage probability (MCoCP) of $\mathrm{MCoVaR}_{j|\setminus j}^{\alpha_j}\left(\hat{\theta}_{j|\setminus j}^{\boldsymbol{\alpha}_{\setminus j}^{\mathrm{D}},50\%}\right)$ as follows:

$$\mathrm{CP}_i^{\alpha_i}(\theta_i) = \mathbb{P}\left\{X_i \le -\mathrm{VaR}_i^{\alpha_i}(\hat{\theta}_i)\right\}, \tag{56}$$

which is different from α_i, and

$$\begin{aligned}\mathrm{MCoCP}_{j|\setminus j}^{\alpha_j}\left(\theta_{j|\setminus j}^{\boldsymbol{\alpha}_{\setminus j}^{\mathrm{D}},50\%}\right) = \mathbb{P}\Bigg[\bigg\{X_j \le -\mathrm{MCoVaR}_{j|\setminus j}^{\alpha_j}\left(\hat{\theta}_{j|\setminus j}^{\boldsymbol{\alpha}_{\setminus j}^{\mathrm{D}},50\%}\right)\bigg\} \;\Bigg|\; \\ \left\{X_i = -\mathrm{VaR}_i^{\alpha_i}(\theta_i)\right\}_{i\in\mathscr{I}_{\setminus j}^{\mathrm{D}}} \bigcap \left\{X_k = -\mathrm{VaR}_k^{50\%}(\theta_k)\right\}_{k\in\mathscr{I}_{\setminus j}^{\mathrm{N}}}\Bigg],\end{aligned} \tag{57}$$

which is different from α_j. To assess the accuracy of $\mathrm{VaR}_i^{\alpha_i}(\hat{\theta}_i)$ and $\mathrm{MCoVaR}_{j|\setminus j}^{\alpha_j}\left(\hat{\theta}_{j|\setminus j}^{\boldsymbol{\alpha}_{\setminus j}^{\mathrm{D}},50\%}\right)$, we can thus measure the closeness between $\mathrm{CP}_i^{\alpha_i}(\hat{\theta}_i)$ and α_i and the closeness between $\mathrm{MCoCP}_{j|\setminus j}^{\alpha_j}\left(\hat{\theta}_{j|\setminus j}^{\boldsymbol{\alpha}_{\setminus j}^{\mathrm{D}},50\%}\right)$ and α_j. By adopting the approach of Hakim et al. (2022), we calculate the following root-mean-square errors (RMSEs):

$$\mathrm{RMSE}\left[\mathrm{CP}_i^{\alpha_i}(\hat{\theta}_i)\right] = \sqrt{\frac{1}{M}\sum_{m\in\mathscr{M}}\left[\mathrm{CP}_i^{\alpha_i}(\hat{\theta}_{i;m}) - \alpha_i\right]^2}, \tag{58}$$

$$\mathrm{RMSE}\left[\mathrm{MCoCP}_{j|\setminus j}^{\alpha_j}\left(\hat{\theta}_{j|\setminus j}^{\boldsymbol{\alpha}_{\setminus j}^{\mathrm{D}},50\%}\right)\right] = \sqrt{\frac{1}{M}\sum_{m\in\mathscr{M}}\left[\mathrm{MCoCP}_{j|\setminus j}^{\alpha_j}\left(\hat{\theta}_{j|\setminus j;m}^{\boldsymbol{\alpha}_{\setminus j}^{\mathrm{D}},50\%}\right) - \alpha_j\right]^2}, \tag{59}$$

with $\mathscr{M} = \{1, 2, \ldots, M\}$. For all $m \in \mathscr{M}$, $\mathrm{CP}_i^{\alpha_i}(\hat{\theta}_{i;m})$ is the simulated CP of the VaR forecast, and $\mathrm{MCoCP}_{j|\setminus j}^{\alpha_j}\left(\hat{\theta}_{j|\setminus j;m}^{\boldsymbol{\alpha}_{\setminus j}^{\mathrm{D}},50\%}\right)$ is the simulated MCoCP of the MCoVaR forecast.

4.2. Backtesting Performance of MCoVaR Forecasts

Since $\mathrm{VaR}_i^{\alpha_i}(\theta_i)$ is basically the negative of the α_i-quantile of X_i, it can be derived through the following minimization: $\mathrm{VaR}_i^{\alpha_i}(\theta_i) = -\arg\min_{w\in\mathbb{R}} \mathrm{AL}_i^{\alpha_i}(w;\theta_i)$, with $\mathrm{AL}_i^{\alpha_i}(w;\theta_i) = \mathbb{E}[\varphi^{\alpha_i}(X_i - w)]$ denoting the expected value of an asymmetric piecewise-linear loss function $\varphi^{\alpha_i}(X_i - w) = \left|\alpha_i - \mathbb{I}_{(-\infty,0]}(X_i - w)\right| \cdot |X_i - w|$ (Kuan et al. 2009).[11] This means $\mathrm{AL}_i^{\alpha_i}(w;\theta_i)$ attains its minimum at $w = -\mathrm{VaR}_i^{\alpha_i}(\theta_i)$. Following Syuhada et al. (2021), we estimate $\mathrm{AL}_i^{\alpha_i}(w;\theta_i)$ by

$$\mathrm{AL}_i^{\alpha_i}(w;\hat{\theta}_i) = \frac{\sum_{n\in\mathscr{N}} \varphi^{\alpha_i}(x_{i;n} - w)\, f_{i;\hat{\theta}_i}(x_{i;n})}{\sum_{n\in\mathscr{N}} f_{i;\hat{\theta}_i}(x_{i;n})}. \tag{60}$$

Its value evaluated at $-\mathrm{VaR}_i^{\alpha_i}(\hat{\theta}_i)$, i.e., $\mathrm{AL}_i^{\alpha_i}\left[-\mathrm{VaR}_i^{\alpha_i}(\hat{\theta}_i);\hat{\theta}_i\right]$, is used to examine the VaR backtesting performance.[12] It asymmetrically penalizes observations below and above $-\mathrm{VaR}_i^{\alpha_i}(\hat{\theta}_i)$ by accounting for their magnitude. This is contrary to the VaR backtesting techniques of Kupiec (1995) and Christoffersen (1998) that only rely on the rate or proportion of VaR violations.

Analogous to the above VaR definition, we can define MCoVaR through the following minimization: $\mathrm{MCoVaR}_{j|\setminus j}^{\alpha_j}\left(\boldsymbol{\theta}_{j|\setminus j}^{\boldsymbol{\alpha}_{\setminus j}^{\mathrm{D}},50\%}\right) = -\arg\min_{w\in\mathbb{R}} \mathrm{MCoAL}_{j|\setminus j}^{\alpha_j}\left(w;\boldsymbol{\theta}_{j|\setminus j}^{\boldsymbol{\alpha}_{\setminus j}^{\mathrm{D}},50\%}\right)$, with

$$
\begin{aligned}
&\mathrm{MCoAL}_{j|\setminus j}^{\alpha_j}\left(w;\boldsymbol{\theta}_{j|\setminus j}^{\boldsymbol{\alpha}_{\setminus j}^{\mathrm{D}},50\%}\right)\\
&= \mathbb{E}\left[\varphi^{\alpha_j}(X_j - w) \mid \left\{X_i = -\mathrm{VaR}_i^{\alpha_i}(\boldsymbol{\theta}_i)\right\}_{i\in\mathscr{I}_{\setminus j}^{\mathrm{D}}} \bigcap \left\{X_k = -\mathrm{VaR}_k^{50\%}(\boldsymbol{\theta}_k)\right\}_{k\in\mathscr{I}_{\setminus j}^{\mathrm{N}}}\right]
\end{aligned}
\tag{61}
$$

denoting the expected value of a conditional asymmetric piecewise-linear loss function. If $\mathbf{v}_{\setminus j}^{\mathrm{D}} = \left(\mathrm{VaR}_i^{\alpha_i}(\boldsymbol{\theta}_i)\right)_{i\in\mathscr{I}_{\setminus j}^{\mathrm{D}}}$ and $\mathbf{v}_{\setminus j}^{\mathrm{N}} = \left(\mathrm{VaR}_k^{50\%}(\boldsymbol{\theta}_k)\right)_{k\in\mathscr{I}_{\setminus j}^{\mathrm{N}}}$, then based on Bayes' theorem, $\mathrm{MCoAL}_{j|\setminus j}^{\alpha_j}\left(w;\boldsymbol{\theta}_{j|\setminus j}^{\boldsymbol{\alpha}_{\setminus j}^{\mathrm{D}},50\%}\right)$ can be expressed as follows:

$$
\begin{aligned}
&\mathrm{MCoAL}_{j|\setminus j}^{\alpha_j}\left(w;\boldsymbol{\theta}_{j|\setminus j}^{\boldsymbol{\alpha}_{\setminus j}^{\mathrm{D}},50\%}\right)\\
&= \int_{\mathbb{R}} \varphi^{\alpha_j}(x_j - w)\, f_{j|\setminus j;\boldsymbol{\theta}_{j|\setminus j}}\left(x_j \,\middle|\, \left(-\mathbf{v}_{\setminus j}^{\mathrm{D}}\right)^{\top}, \left(-\mathbf{v}_{\setminus j}^{\mathrm{N}}\right)^{\top}\right) \mathrm{d}x_j\\
&= \int_{\mathbb{R}} \varphi^{\alpha_j}(x_j - w)\, \frac{f_{\setminus j|j;\boldsymbol{\theta}_{\setminus j|j}}\left(\left(-\mathbf{v}_{\setminus j}^{\mathrm{D}}\right)^{\top}, \left(-\mathbf{v}_{\setminus j}^{\mathrm{N}}\right)^{\top} \,\middle|\, x_j\right) f_{j;\boldsymbol{\theta}_j}(x_j)}{f_{\setminus j;\boldsymbol{\theta}_{\setminus j}}\left(\left(-\mathbf{v}_{\setminus j}^{\mathrm{D}}\right)^{\top}, \left(-\mathbf{v}_{\setminus j}^{\mathrm{N}}\right)^{\top}\right)} \mathrm{d}x_j\\
&= \frac{\int_{\mathbb{R}} \left[\varphi^{\alpha_j}(x_j - w)\, f_{\setminus j|j;\boldsymbol{\theta}_{\setminus j|j}}\left(\left(-\mathbf{v}_{\setminus j}^{\mathrm{D}}\right)^{\top}, \left(-\mathbf{v}_{\setminus j}^{\mathrm{N}}\right)^{\top} \,\middle|\, x_j\right)\right] f_{j;\boldsymbol{\theta}_j}(x_j)\,\mathrm{d}x_j}{f_{\setminus j;\boldsymbol{\theta}_{\setminus j}}\left(\left(-\mathbf{v}_{\setminus j}^{\mathrm{D}}\right)^{\top}, \left(-\mathbf{v}_{\setminus j}^{\mathrm{N}}\right)^{\top}\right)}\\
&= \frac{\mathbb{E}\left[\varphi^{\alpha_j}(X_j - w)\, f_{\setminus j|j;\boldsymbol{\theta}_{\setminus j|j}}\left(\left(-\mathbf{v}_{\setminus j}^{\mathrm{D}}\right)^{\top}, \left(-\mathbf{v}_{\setminus j}^{\mathrm{N}}\right)^{\top} \,\middle|\, X_j\right)\right]}{f_{\setminus j;\boldsymbol{\theta}_{\setminus j}}\left(\left(-\mathbf{v}_{\setminus j}^{\mathrm{D}}\right)^{\top}, \left(-\mathbf{v}_{\setminus j}^{\mathrm{N}}\right)^{\top}\right)},
\end{aligned}
$$

with

$$
\begin{aligned}
f_{\setminus j;\boldsymbol{\theta}_{\setminus j}}\left(\left(-\mathbf{v}_{\setminus j}^{\mathrm{D}}\right)^{\top}, \left(-\mathbf{v}_{\setminus j}^{\mathrm{N}}\right)^{\top}\right) &= \int_{\mathbb{R}} f_{\boldsymbol{\theta}}\left(x_j, \left(-\mathbf{v}_{\setminus j}^{\mathrm{D}}\right)^{\top}, \left(-\mathbf{v}_{\setminus j}^{\mathrm{N}}\right)^{\top}\right) \mathrm{d}x_j\\
&= \int_{\mathbb{R}} f_{\setminus j|j;\boldsymbol{\theta}_{\setminus j|j}}\left(\left(-\mathbf{v}_{\setminus j}^{\mathrm{D}}\right)^{\top}, \left(-\mathbf{v}_{\setminus j}^{\mathrm{N}}\right)^{\top} \,\middle|\, x_j\right) f_{j;\boldsymbol{\theta}_j}(x_j)\,\mathrm{d}x_j\\
&= \mathbb{E}\left[f_{\setminus j|j;\boldsymbol{\theta}_{\setminus j|j}}\left(\left(-\mathbf{v}_{\setminus j}^{\mathrm{D}}\right)^{\top}, \left(-\mathbf{v}_{\setminus j}^{\mathrm{N}}\right)^{\top} \,\middle|\, X_j\right)\right].
\end{aligned}
$$

Therefore, by adopting Kabaila's (1999) method, we estimate $\mathrm{MCoAL}_{j|\setminus j}^{\alpha_j}\left(w;\boldsymbol{\theta}_{j|\setminus j}^{\boldsymbol{\alpha}_{\setminus j}^{\mathrm{D}},50\%}\right)$ by

$$
\mathrm{MCoAL}_{j|\setminus j}^{\alpha_j}\left(w;\hat{\boldsymbol{\theta}}_{j|\setminus j}^{\boldsymbol{\alpha}_{\setminus j}^{\mathrm{D}},50\%}\right) = \frac{\sum_{n\in\mathscr{N}} \varphi^{\alpha_i}(x_{j;n} - w)\, f_{\setminus j|j;\hat{\boldsymbol{\theta}}_{\setminus j|j}}\left(\left(-\hat{\mathbf{v}}_{\setminus j}^{\mathrm{D}}\right)^{\top}, \left(-\hat{\mathbf{v}}_{\setminus j}^{\mathrm{N}}\right)^{\top} \,\middle|\, x_{j;n}\right)}{\sum_{n\in\mathscr{N}} f_{\setminus j|j;\hat{\boldsymbol{\theta}}_{\setminus j|j}}\left(\left(-\hat{\mathbf{v}}_{\setminus j}^{\mathrm{D}}\right)^{\top}, \left(-\hat{\mathbf{v}}_{\setminus j}^{\mathrm{N}}\right)^{\top} \,\middle|\, x_{j;n}\right)}, \tag{62}
$$

where $\hat{\mathbf{v}}^{\mathrm{D}}_{\setminus j} = \left(\mathrm{VaR}^{\alpha_i}_i(\hat{\theta}_i)\right)_{i \in \mathscr{I}^{\mathrm{D}}_{\setminus j}}$ and $\hat{\mathbf{v}}^{\mathrm{N}}_{\setminus j} = \left(\mathrm{VaR}^{50\%}_k(\hat{\theta}_k)\right)_{k \in \mathscr{I}^{\mathrm{N}}_{\setminus j}}$. Similar to the VaR forecast, the backtesting performance of the MCoVaR forecast is assessed by evaluating this expected conditional asymmetric loss function at $-\mathrm{MCoVaR}^{\alpha_j}_{j|\setminus j}\left(\hat{\theta}^{\boldsymbol{\alpha}^{\mathrm{D}}_{\setminus j},50\%}_{j|\setminus j}\right)$, i.e.,

$$\mathrm{MCoAL}^{\alpha_j}_{j|\setminus j}\left[-\mathrm{MCoVaR}^{\alpha_j}_{j|\setminus j}\left(\hat{\theta}^{\boldsymbol{\alpha}^{\mathrm{D}}_{\setminus j},50\%}_{j|\setminus j}\right); \hat{\theta}^{\boldsymbol{\alpha}^{\mathrm{D}}_{\setminus j},50\%}_{j|\setminus j}\right].$$

This approach complements the CoVaR backtesting technique of Girardi and Ergün (2013) that extends the VaR backtesting methods of Kupiec (1995) and Christoffersen (1998).

5. Empirical Results

In this section, we employ the multivariate risk models and (Δ)MCoVaR formulas described in Sections 2 and 3 to investigate joint systemic risk transmissions across crypto and non-crypto markets. More specifically, we compute $(\Delta)\mathrm{MCoVaR}^{\alpha_j|\boldsymbol{\alpha}^{\mathrm{D}}_{\setminus j},50\%}_{j|\setminus j}$ for the following four cases:

- **Case 1:** if the targeted asset j is a crypto asset, the conditioning set $\mathscr{I}^{\mathrm{D}}_{\setminus j}$ consists of all the remaining crypto assets being jointly in distress, and the conditioning set $\mathscr{I}^{\mathrm{N}}_{\setminus j}$ contains all the non-crypto assets being jointly in normal states;
- **Case 2:** if the targeted asset j is a crypto asset, the conditioning set $\mathscr{I}^{\mathrm{D}}_{\setminus j}$ consists of all the non-crypto assets being jointly in distress, and the conditioning set $\mathscr{I}^{\mathrm{N}}_{\setminus j}$ contains all the remaining crypto assets being jointly in normal states;
- **Case 3:** if the targeted asset j is a non-crypto asset, the conditioning set $\mathscr{I}^{\mathrm{D}}_{\setminus j}$ consists of all the crypto assets being jointly in distress, and the conditioning set $\mathscr{I}^{\mathrm{N}}_{\setminus j}$ contains all the remaining non-crypto assets being jointly in normal states;
- **Case 4:** if the targeted asset j is a non-crypto asset, the conditioning set $\mathscr{I}^{\mathrm{D}}_{\setminus j}$ consists of all the remaining non-crypto assets being jointly in distress, and the conditioning set $\mathscr{I}^{\mathrm{N}}_{\setminus j}$ contains all the crypto assets being jointly in normal states.

This means that Case 1 (Case 4) allows us to investigate joint systemic risk transmissions within the crypto (non-crypto) markets. Meanwhile, Case 2 (Case 3) allows us to assess systemic risk jointly transmitted from the non-crypto (crypto) markets towards the crypto (non-crypto) markets. These mechanisms of systemic risk transmissions are summarized in Table 2.

Table 2. Four cases of systemic risk transmission mechanisms.

Case	j	$\mathscr{I}^{\mathrm{D}}_{\setminus j}$	$\mathscr{I}^{\mathrm{N}}_{\setminus j}$	Transmission Direction
1	C	Cs	NCs	C ← Cs
2	C	NCs	Cs	C ← NCs
3	NC	Cs	NCs	NC ← Cs
4	NC	NCs	Cs	NC ← NCs

C and NC stand for crypto and non-crypto assets, respectively.

5.1. Data

We selected five prominent cryptocurrencies, namely, Bitcoin (BTC, $i = 1$), Ethereum (ETH, $i = 2$), Ripple (XRP, $i = 3$), Litecoin (LTC, $i = 4$), and Monero (XMR, $i = 5$). They are the most liquid and long-standing cryptocurrencies (Moreno et al. 2022). The first four cryptocurrencies ($i = 1, 2, 3, 4$) were used by previous studies (i.e., Akhtaruzzaman et al. 2022; Borri 2019; Xu et al. 2021) that dealt with systemic risk transmissions within crypto markets. Therefore, the empirical results of this study could be compared with those revealed by such studies. The daily closing prices of these five cryptocurrencies were collected from CoinMarketCap.com (accessed on 14 November 2022), one of the cryptocurrency databases proven by Vidal-Tomás (2022) to be a correct database for empirically analyzing cryptocurrencies. CoinMarketCap.com showed us that, as of 23 February 2022, the global crypto market capitalization was USD 1716.90 billion, with Bitcoin (42.29%), Ethereum (18.40%), Ripple (2.02%), Litecoin (0.44%), and Monero (0.16%) comprising 63.31%. The corresponding 24-hour volume was USD 86.04 billion, with Bitcoin (25.39%), Ethereum (15.55%), Ripple (3.13%), Litecoin (0.86%), and Monero (0.12%) comprising 45.05%. As representations of non-crypto markets, we also included the S&P 500 composite index (SPX, $i = 6$), the S&P US Treasury Bond index (SPB, $i = 7$), the US dollar index (USD, $i = 8$), West Texas Intermediate crude oil (OIL, $i = 9$), and gold (GLD, $i = 10$) that may be impacted by the movements and bubble event in the crypto markets. Their daily closing (spot) price datasets were sourced from SPGlobal.com, SPGlobal.com, Investing.com, EIA.gov, and Nasdaq.com, respectively (accessed on 14 November 2022).

We considered the data period from 16 January 2018 to 23 February 2022,[13] which we split into a subperiod before COVID-19 and a subperiod during COVID-19, where 11 March 2020 was chosen as the starting point of the latter subperiod. The former subperiod is a quiet period over which no crisis or systemic event existed. Meanwhile, in addition to encompassing the global outbreak of the COVID-19 pandemic, the latter subperiod also covers the episode of the 2021 crypto bubble, as detected by Bazán-Palomino (2022) from the first week of November 2020 to the second week of May 2021. This bubble can be observed in Figure 1. Thus, our empirical analysis provides us with different mechanisms of systemic risk transmissions across crypto and non-crypto markets during a fully calm period and a stressful period. To provide a particular picture of the effect of the crypto bubble event on the systemic risk transmission mechanism, we also considered the 2021 bubble subperiod (2 November 2020–14 May 2021). The dataset $\{p_{i;n}\}$ of each asset i's prices over each subperiod was then transformed into the following return dataset: $\{x_{i;n}\}$, with $x_{i;n} = 100 \ln\left(\frac{p_{i;n}}{p_{i;n-1}}\right)$. Over the pre-COVID-19 (respectively, COVID-19) subperiod, it consisted of 532 (respectively, 487) observations. In particular, during the bubble subperiod, it contained 132 observations.

From Table 3, we observe that the crypto assets appeared to be much more volatile during the pre-COVID-19, COVID-19, and bubble periods compared to the non-crypto assets. All the asset returns tended to become more volatile, more skewed, and more heavy-tailed due to the COVID-19 pandemic. The highly volatile movement of the crypto-asset returns was more evident during the 2021 bubble period. This is in line with the finding of Bazán-Palomino (2022) that revealed an increase in the variance of crypto-portfolio returns in response to bubbles in the crypto market. The skewness of each asset return was significantly nonzero according to the D'Agostino test, and its excess kurtosis was significantly positive based on the Anscombe–Glynn test. Furthermore, the Jarque–Bera test result significantly confirmed that each asset return was not normally distributed. As depicted in Figure 2, all the crypto assets were strongly correlated with each other with positive Pearson's ρ and Kendall's τ, consistent with the findings of Borri (2019), Jiménez et al. (2020b), and Syuhada and Hakim (2020). They were also positively correlated with the S&P 500, oil, and gold, but the correlations were weak. Interestingly, they exhibited a negative correlation with the S&P US Treasury Bond and the US dollar. This is in line with evidence revealed by Choudhury et al. (2022) and Syuhada et al. (2022a) that these two non-crypto assets played roles as strong safe-havens. In addition, we detect from Figure 3 strong tail dependence among the crypto assets, suggesting a high possibility of the occurrence of their joint extreme events, which may cause greater financial instability (Jiménez et al. 2020a).

Table 3. Summary statistics of crypto- and non-crypto-asset returns.

	BTC	ETH	XRP	LTC	XMR	SPX	SPB	USD	OIL	GLD
Before COVID-19										
Mean	−0.07	−0.31	−0.32	−0.25	−0.33	0.01	0.03	0.01	−0.12	0.04
Variance	19.71	32.55	34.94	33.66	37.90	1.17	0.05	0.12	6.36	0.62
Skewness	−0.35 [a]	−0.48 [a]	0.38 [a]	0.40 [a]	−0.34 [a]	−1.13 [a]	−0.03	0.08	−2.50 [a]	−0.18
Excess Kurtosis	4.07 [b]	2.64 [b]	3.94 [b]	3.24 [b]	2.01 [b]	8.03 [b]	4.45 [b]	0.89 [b]	30.85 [b]	4.15 [b]
Jarque–Bera	391.04 [c]	181.39 [c]	369.32 [c]	255.06 [c]	103.44 [c]	1590.81 [c]	454.52 [c]	19.09 [c]	22,280.80 [c]	398.57 [c]
During COVID-19										
Mean	0.32	0.53	0.24	0.15	0.20	0.08	−0.01	−0.00	0.20	0.03
Variance	23.96	43.66	70.72	43.44	43.22	2.53	0.07	0.15	35.52	1.36
Skewness	−1.77 [a]	−1.23 [a]	0.36 [a]	−1.46 [a]	−2.01 [a]	−1.04 [a]	0.46 [a]	0.31 [a]	−2.68 [a]	−0.37 [a]
Excess Kurtosis	17.53 [b]	12.57 [b]	14.14 [b]	8.96 [b]	16.86 [b]	16.71 [b]	9.03 [b]	1.66 [b]	54.97 [b]	4.30 [b]
Jarque–Bera	6695.15 [c]	3435.93 [c]	4199.63 [c]	1858.86 [c]	6290.78 [c]	5937.76 [c]	1730.33 [c]	66.21 [c]	63,846.39 [c]	399.99 [c]
During Bubble										
Mean	0.99	1.79	1.34	1.36	0.92	0.18	−0.02	−0.03	0.46	−0.02
Variance	25.61	48.37	160.36	50.00	34.48	0.83	0.05	0.11	4.81	1.26
Skewness	−0.13	0.71 [a]	0.64 [a]	−0.62 [a]	−0.50 [a]	−0.30	0.14	0.13	−0.21	−1.00 [a]
Excess Kurtosis	1.60 [b]	3.77 [b]	7.10 [b]	1.27 [b]	2.62 [b]	0.50	2.07 [b]	−0.10	1.83 [b]	3.70 [b]
Jarque–Bera	17.11 [c]	101.20 [c]	324.21 [c]	19.33 [c]	49.52 [c]	3.90	28.02 [c]	0.43	22.64 [c]	109.28 [c]

[a] The skewness is significantly different from zero based on the D'Agostino test at the 5% level. [b] The excess kurtosis is significantly positive based on the Anscombe–Glynn test at the 5% level. [c] The Jarque–Bera test significantly rejects the null hypothesis of normality at the 5% level.

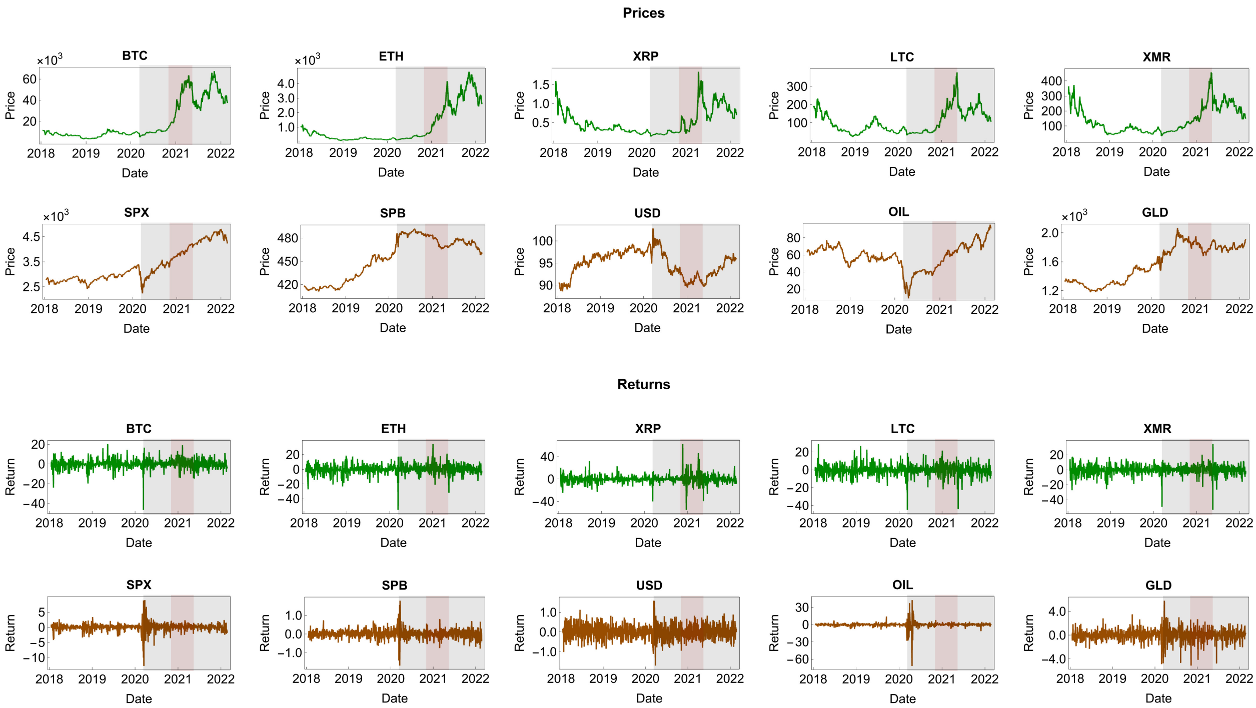

Figure 1. Daily prices and returns of crypto and non-crypto assets. The prices of the five crypto assets (i.e., BTC, ETH, XRP, LTC, and XMR) and the three indices (i.e., the SPX, SPB, and USD indices) are denominated in USD. Meanwhile, crude oil and gold are priced in USD per barrel and in USD per troy ounce, respectively. Green and brown represent the crypto and non-crypto assets, respectively. The shaded gray region shows the COVID-19 pandemic period (11 March 2020–23 February 2022), and the shaded red region indicates the 2021 crypto bubble period (2 November 2020–14 May 2021).

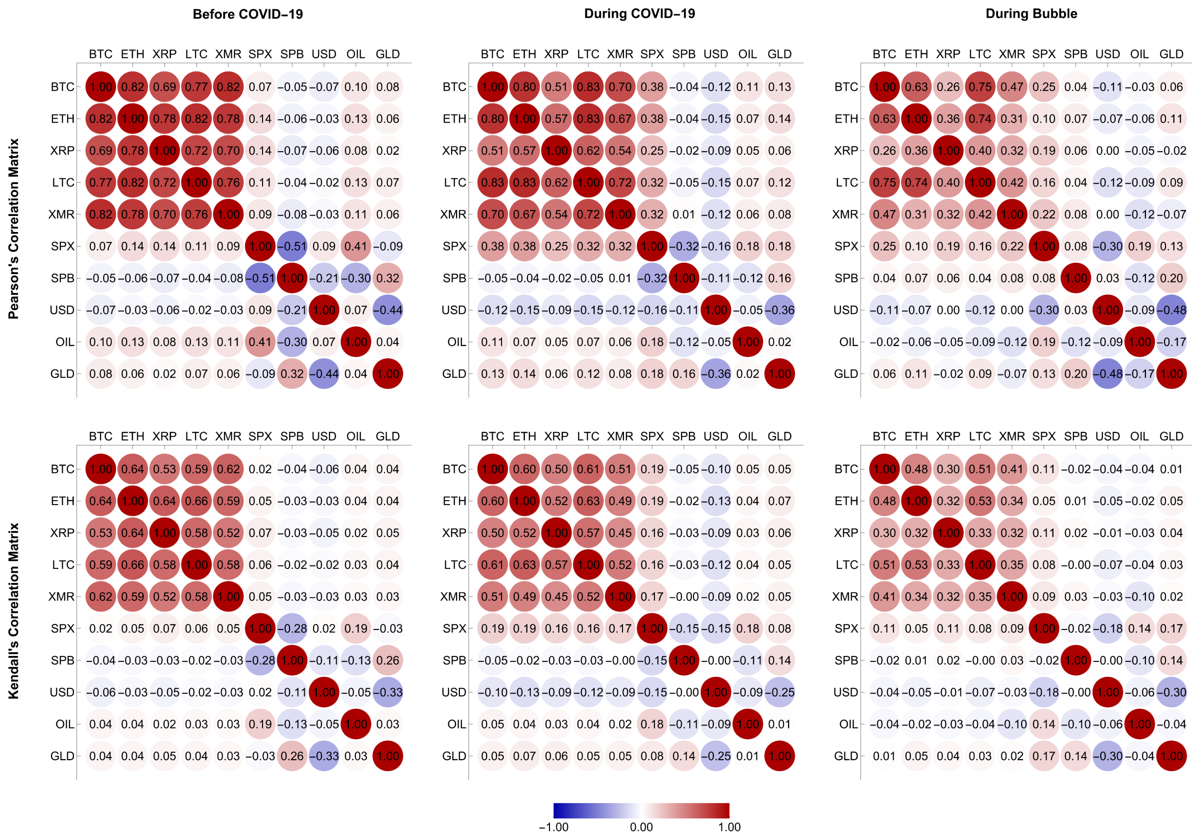

Figure 2. Empirical Pearson's and Kendall's correlation matrices of crypto- and non-crypto-asset returns.

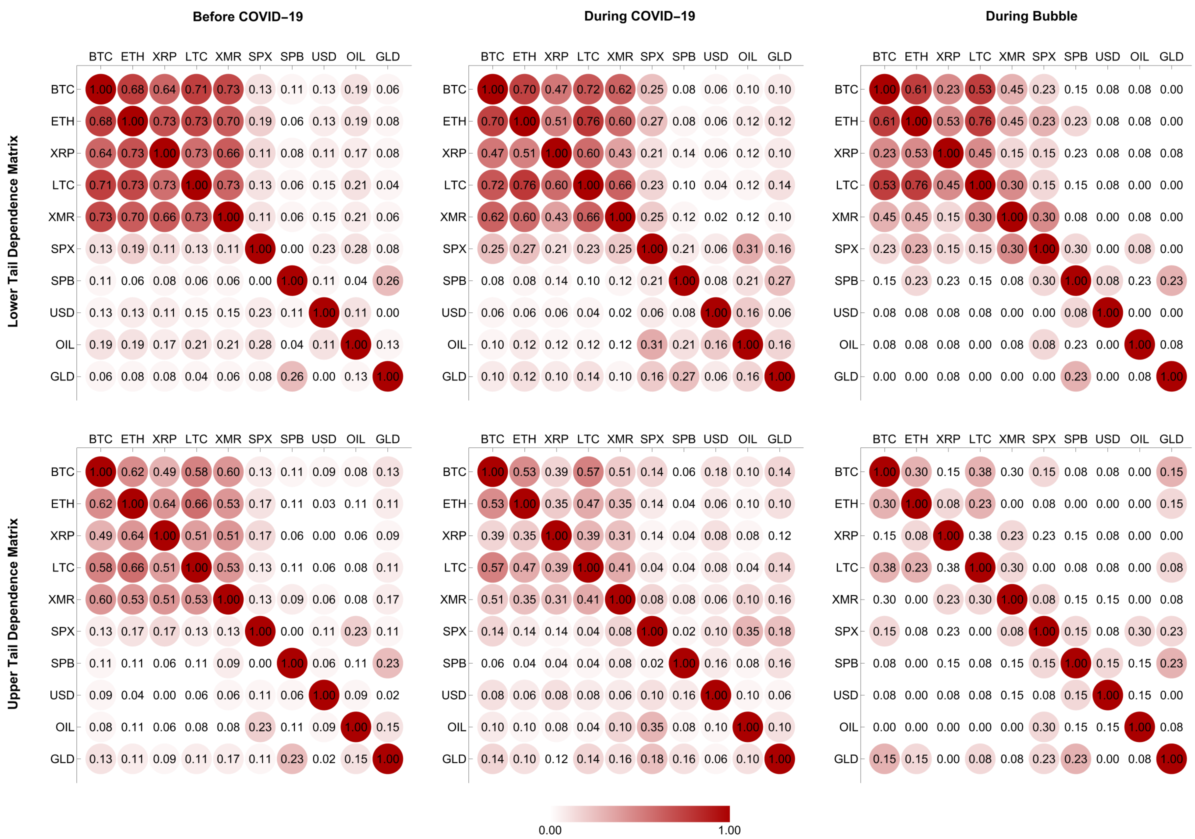

Figure 3. Empirical lower and upper tail dependence matrices of crypto- and non-crypto-asset returns.

5.2. Conditional Coverage and Backtesting Performances of MCoVaR Forecasts

We first computed the VaR forecast for each asset at the 5% (1%) level of significance or at the 95% (99%) level of confidence by assuming it to be in isolation. The resulting root-mean-square error (RMSE) of its estimated coverage probability (CP) is tabulated in Table 4, and the corresponding expected asymmetric loss function (AL) is provided in Table 5. If the VaR forecast has an estimated CP with the lowest RMSE, we say that it shows the best coverage performance. Meanwhile, if the VaR forecast produces the lowest expected AL, we say that it exhibits the best backtesting performance.

Table 4. RMSE of the estimated coverage probability $\mathrm{CP}_i^{\alpha_i}$ of the $\mathrm{VaR}_i^{\alpha_i}$ forecast.

	i									
	BTC	**ETH**	**XRP**	**LTC**	**XMR**	**SPX**	**SPB**	**USD**	**OIL**	**GLD**
$\alpha_i = 5\%$										
Before COVID-19										
N	1.13%	1.10%	1.00%	0.82%	0.96%	1.42%	0.92%	0.72%	2.53%	1.22%
T	**0.82%**	**0.81%**	**0.73%**	**0.60%**	**0.70%**	**1.03%**	**0.69%**	**0.52%**	1.87%	**0.91%**
SU	1.06%	1.00%	1.03%	0.88%	0.93%	1.12%	0.99%	0.71%	**1.61%**	1.15%
During COVID-19										
N	1.86%	1.73%	1.56%	1.65%	2.22%	1.77%	1.32%	0.77%	3.11%	1.11%
T	**1.26%**	**1.15%**	**1.04%**	**1.09%**	1.49%	**1.20%**	**0.91%**	**0.50%**	**2.13%**	**0.75%**
SU	1.28%	1.30%	1.47%	1.23%	**1.46%**	1.49%	1.31%	0.86%	2.62%	1.02%
During Bubble										
N	1.99%	2.10%	2.75%	2.02%	2.15%	1.73%	1.86%	1.48%	1.83%	2.66%
T	**1.67%**	**1.74%**	**2.32%**	**1.69%**	**1.80%**	**1.46%**	**1.57%**	**1.25%**	**1.54%**	2.25%
SU	1.89%	1.99%	3.28%	1.82%	1.94%	1.65%	1.91%	1.56%	1.90%	**2.17%**
$\alpha_i = 1\%$										
Before COVID-19										
N	0.41%	0.39%	0.37%	0.30%	0.33%	0.54%	0.34%	0.24%	1.04%	0.44%
T	**0.25%**	**0.24%**	**0.22%**	**0.19%**	**0.20%**	**0.32%**	**0.20%**	**0.15%**	**0.61%**	**0.26%**
SU	0.44%	0.38%	0.43%	0.36%	0.40%	0.50%	0.74%	0.26%	1.03%	0.74%
During COVID-19										
N	0.71%	0.67%	0.64%	0.62%	0.90%	0.72%	0.50%	0.28%	1.49%	0.42%
T	**0.36%**	**0.34%**	**0.32%**	**0.32%**	**0.45%**	**0.36%**	**0.26%**	**0.15%**	**0.72%**	**0.21%**
SU	0.96%	0.76%	0.71%	0.60%	0.72%	0.72%	0.75%	0.54%	2.12%	0.36%
During Bubble										
N	0.79%	0.95%	1.35%	0.81%	0.86%	0.65%	0.76%	0.53%	0.67%	1.17%
T	**0.60%**	**0.72%**	**1.00%**	**0.61%**	**0.65%**	**0.48%**	**0.57%**	**0.39%**	**0.50%**	**0.87%**
SU	0.98%	1.12%	2.97%	0.85%	1.00%	0.78%	1.01%	0.60%	1.11%	1.16%

Each RMSE value was computed based on Equation (58). For each asset *i* over each period, the lowest RMSE is presented in boldface.

We observe from Table 4 that the VaR we forecasted at the 5% and 1% significance levels using the normal model exhibited the worst coverage performance because it had an estimated CP with the highest RMSE for most assets. This is in line with evidence previously revealed from Table 3 that each asset return significantly deviated from the normality assumption. The most accurate VaR forecast was obtained if the Student's *t* model was taken into consideration. Meanwhile, the VaR forecast derived using Johnson's SU model was less accurate than that determined using Student's *t* model but was better than that computed using the normal model in the majority of cases. Similar results were also derived from Table 5, although this table shows the normal and Johnson's SU models to be slightly better in terms of the expected asymmetric loss function minimization. These results are consistent with the findings of previous studies conducted by, e.g., Venkataraman and Rao (2016), Troster et al. (2019), Castillo-Brais et al. (2022), and Hakim et al. (2022). Overall, the RMSE of the estimated CP and the expected AL of each VaR forecast tended to increase as the COVID-19 pandemic and the 2021 crypto bubble progressed. This evidence was more apparently detected in crypto assets where an increase in the former was approximately two times. This evidence might be caused by the increased variance and kurtosis of each asset return in response to the pandemic.

Table 5. Expected asymmetric loss function $AL_i^{\alpha_i}$ evaluated at the $-VaR_i^{\alpha_i}$ forecast.

	i									
	BTC	**ETH**	**XRP**	**LTC**	**XMR**	**SPX**	**SPB**	**USD**	**OIL**	**GLD**
$\alpha_i = 5\%$										
Before COVID-19										
N	37.58%	48.55%	49.50%	48.87%	52.00%	9.55%	1.87%	2.89%	21.66%	6.61%
T	**35.68%**	**45.99%**	46.95%	46.34%	**49.27%**	**9.04%**	**1.78%**	2.74%	**20.58%**	**6.27%**
SU	37.92%	49.19%	**45.50%**	**44.24%**	51.72%	10.48%	1.81%	**2.70%**	25.71%	6.51%
During COVID-19										
N	41.18%	55.89%	69.54%	56.62%	56.36%	13.51%	2.28%	3.19%	49.51%	10.09%
T	**37.47%**	**50.97%**	**63.75%**	**51.59%**	**51.52%**	**12.39%**	2.08%	2.93%	**45.50%**	**9.26%**
SU	43.83%	58.24%	65.02%	61.08%	63.66%	14.01%	**2.02%**	**2.83%**	57.97%	9.83%
During Bubble										
N	42.21%	57.39%	101.53%	61.90%	49.12%	7.63%	1.79%	2.79%	18.50%	9.67%
T	**41.21%**	56.45%	99.82%	**60.54%**	**48.28%**	**7.45%**	1.75%	2.74%	**18.14%**	**9.46%**
SU	42.33%	**52.02%**	**99.03%**	68.33%	52.73%	7.85%	**1.72%**	**2.67%**	18.94%	11.07%
$\alpha_i = 1\%$										
Before COVID-19										
N	**10.44%**	**13.50%**	**13.74%**	**13.54%**	**14.40%**	**2.62%**	**0.52%**	0.80%	**6.01%**	**1.83%**
T	11.68%	15.04%	15.39%	15.13%	16.13%	2.92%	0.58%	0.89%	6.71%	2.05%
SU	12.83%	16.12%	14.65%	13.91%	16.59%	3.74%	0.61%	**0.79%**	10.38%	2.19%
During COVID-19										
N	**11.49%**	**15.53%**	**19.50%**	**15.66%**	**15.65%**	**3.77%**	**0.63%**	0.89%	**13.92%**	**2.77%**
T	13.00%	17.62%	22.30%	17.70%	17.72%	4.28%	0.72%	1.02%	15.92%	3.15%
SU	17.05%	21.93%	24.01%	22.21%	24.43%	5.39%	0.71%	**0.85%**	25.01%	3.31%
During Bubble										
N	**11.85%**	16.02%	**28.93%**	**17.04%**	**13.87%**	**2.13%**	**0.50%**	0.78%	**5.13%**	**2.66%**
T	12.72%	17.33%	31.22%	18.21%	14.89%	2.28%	0.53%	0.84%	5.54%	2.87%
SU	13.35%	**15.96%**	33.91%	21.02%	17.36%	2.34%	0.54%	**0.74%**	6.00%	3.73%

Each expected AL was computed based on Equation (60). For each asset *i* over each period, the lowest expected AL is presented in boldface.

For each of the four cases mentioned in Table 2, we computed MCoVaR forecasts at the 5% and 1% significance levels and then assessed their accuracy by evaluating the RMSE of their estimated conditional coverage probability (MCoCP) and the corresponding expected conditional asymmetric loss function (MCoAL). The assessment results are presented in Tables 6 and 7 and summarized in Table 8. Similar to the accuracy assessment of the VaR forecast, the resulting MCoVaR forecast is said to exhibit the best conditional coverage performance if its estimated MCoCP has the smallest RMSE, and it is said to have the best backtesting performance if it produces the lowest expected MCoAL.

Table 6. RMSE of the estimated conditional coverage probability $\mathrm{MCoCP}_{j|\backslash j}^{\alpha_j|\boldsymbol{\alpha}_{\backslash j}^{\mathrm{D}},50\%}$ of the $\mathrm{MCoVaR}_{j|\backslash j}^{\alpha_j|\boldsymbol{\alpha}_{\backslash j}^{\mathrm{D}},50\%}$ forecast.

$j = \mathrm{C}$		Case 1 (C ← Cs)			Case 2 (C ← NCs)			$j = \mathrm{NC}$		Case 3 (NC ← Cs)			Case 4 (NC ← NCs)		
		Before COVID-19	**During COVID-19**	**During Bubble**	**Before COVID-19**	**During COVID-19**	**During Bubble**			**Before COVID-19**	**During COVID-19**	**During Bubble**	**Before COVID-19**	**During COVID-19**	**During Bubble**
$\alpha_j = 5\%$ and $\alpha_i = 5\%$, $i \in \mathscr{I}_{\backslash j}^{\mathrm{D}}$															
BTC	N	3.26%	4.82%	5.25%	2.26%	4.28%	7.13%	SPX	N	1.74%	3.31%	**3.89%**	3.74%	3.52%	6.44%
	T	3.40%	5.10%	**5.23%**	**1.64%**	2.70%	**5.14%**		T	4.93%	4.54%	4.33%	2.64%	3.09%	**4.55%**
	SU	3.78%	6.96%	6.47%	2.30%	3.23%	7.78%		SU	1.69%	3.00%	4.08%	3.29%	3.86%	6.74%
	N–T	**1.34%**	**2.94%**	5.87%	2.80%	3.22%	8.39%		N–T	**1.35%**	**1.24%**	4.02%	2.42%	3.08%	6.56%
	T–N	4.11%	7.28%	7.75%	2.23%	3.44%	6.93%		T–N	1.98%	2.89%	4.36%	2.37%	2.94%	5.53%
	T–T	1.82%	3.32%	6.74%	2.05%	**2.34%**	6.34%		T–T	1.53%	1.47%	4.15%	**2.00%**	**2.32%**	5.32%
	T–SU	4.73%	9.93%	9.14%	2.24%	2.39%	6.79%		T–SU	1.58%	2.51%	4.15%	2.10%	2.75%	5.49%
ETH	N	3.35%	4.60%	6.72%	3.73%	2.53%	6.53%	SPB	N	1.29%	1.95%	**3.65%**	3.37%	3.87%	7.23%
	T	3.62%	4.77%	6.82%	**2.45%**	**1.70%**	**4.48%**		T	4.51%	2.45%	3.98%	3.50%	3.24%	4.84%
	SU	3.43%	5.48%	10.51%	4.08%	2.38%	6.85%		SU	1.13%	2.28%	3.72%	3.73%	4.99%	8.44%
	N–T	**1.65%**	**2.67%**	**5.60%**	4.06%	3.06%	8.28%		N–T	1.17%	**1.32%**	4.69%	2.58%	2.73%	5.48%
	T–N	4.87%	6.80%	9.12%	3.32%	2.93%	6.62%		T–N	1.36%	1.85%	5.10%	2.21%	2.38%	4.84%
	T–T	2.06%	3.16%	6.19%	3.08%	2.19%	6.12%		T–T	1.31%	1.47%	4.88%	**2.11%**	**2.18%**	**4.29%**
	T–SU	5.31%	7.90%	10.61%	3.60%	2.24%	6.51%		T–SU	**1.12%**	1.71%	4.77%	2.21%	2.53%	5.07%
XRP	N	2.52%	3.04%	5.42%	2.57%	2.97%	6.20%	USD	N	**1.21%**	1.82%	**3.73%**	3.26%	3.09%	**4.00%**
	T	2.66%	3.08%	5.63%	**1.85%**	**2.22%**	**4.60%**		T	4.20%	2.37%	4.13%	2.87%	3.70%	6.30%
	SU	3.13%	3.98%	9.52%	2.79%	4.01%	7.08%		SU	1.28%	1.81%	3.96%	3.43%	3.78%	4.45%
	N–T	**1.29%**	**1.16%**	**3.25%**	2.92%	3.39%	7.02%		N–T	1.31%	**1.24%**	3.79%	2.27%	2.34%	4.56%
	T–N	3.51%	5.28%	7.96%	2.28%	2.98%	6.54%		T–N	1.41%	1.42%	3.88%	2.08%	2.12%	4.18%
	T–T	1.69%	1.59%	3.44%	2.15%	2.51%	5.10%		T–T	1.44%	1.34%	3.92%	**1.96%**	**2.01%**	4.00%
	T–SU	4.27%	6.11%	13.73%	2.25%	3.02%	7.63%		T–SU	1.51%	1.32%	3.87%	2.04%	2.14%	4.12%

Table 6. *Cont.*

$j = \mathrm{C}$		Case 1 (C ← Cs)			Case 2 (C ← NCs)			$j = \mathrm{NC}$		Case 3 (NC ← Cs)			Case 4 (NC ← NCs)		
		Before COVID-19	**During COVID-19**	**During Bubble**	**Before COVID-19**	**During COVID-19**	**During Bubble**			**Before COVID-19**	**During COVID-19**	**During Bubble**	**Before COVID-19**	**During COVID-19**	**During Bubble**
LTC	N	2.25%	5.82%	6.41%	2.75%	2.46%	5.51%	OIL	N	3.30%	3.20%	3.24%	8.07%	5.80%	5.08%
	T	2.25%	5.84%	6.31%	**1.82%**	**1.75%**	**3.81%**		T	6.17%	3.24%	3.60%	4.37%	3.62%	**4.17%**
	SU	2.93%	5.92%	7.75%	2.85%	5.86%	6.50%		SU	1.80%	2.89%	3.21%	7.08%	6.41%	5.51%
	N–T	**1.20%**	**2.70%**	**5.14%**	3.07%	3.00%	7.36%		N–T	**1.34%**	**1.44%**	**3.10%**	2.86%	2.52%	6.33%
	T–N	2.85%	7.56%	6.97%	2.31%	2.57%	5.56%		T–N	3.07%	3.30%	3.39%	3.84%	3.76%	5.35%
	T–T	1.48%	3.32%	5.83%	2.37%	2.12%	5.24%		T–T	1.39%	1.73%	3.24%	**2.33%**	**1.98%**	5.04%
	T–SU	3.91%	7.69%	7.89%	2.49%	2.70%	5.18%		T–SU	1.65%	2.14%	3.16%	3.26%	3.81%	5.22%
XMR	N	2.42%	5.68%	4.35%	3.22%	3.03%	8.81%	GLD	N	2.18%	1.64%	3.36%	2.70%	4.88%	**4.34%**
	T	2.58%	6.17%	4.59%	**2.07%**	**2.06%**	**6.31%**		T	4.91%	2.14%	3.50%	**1.84%**	3.01%	4.66%
	SU	3.18%	4.68%	4.88%	3.30%	4.04%	10.34%		SU	1.93%	1.77%	2.90%	2.70%	5.67%	5.43%
	N–T	**1.36%**	**2.84%**	**3.98%**	3.75%	3.06%	10.65%		N–T	**1.52%**	**1.34%**	**2.88%**	2.34%	2.85%	5.51%
	T–N	3.00%	7.05%	6.15%	2.84%	3.38%	8.70%		T–N	2.03%	1.73%	3.75%	2.43%	2.57%	4.80%
	T–T	1.65%	3.37%	4.47%	2.67%	2.40%	7.97%		T–T	1.66%	1.52%	2.94%	2.03%	**2.28%**	4.46%
	T–SU	3.89%	5.79%	6.72%	2.88%	2.72%	8.84%		T–SU	1.58%	1.61%	2.93%	2.50%	2.62%	4.63%
$\alpha_j = 1\%$ and $\alpha_i = 1\%$, $i \in \mathscr{I}^{\mathrm{D}}_{\setminus j}$															
BTC	N	1.58%	2.54%	3.11%	0.89%	2.23%	5.16%	SPX	N	0.70%	1.69%	**2.10%**	1.92%	1.78%	4.93%
	T	1.55%	**2.21%**	**2.81%**	**0.52%**	0.93%	**2.49%**		T	3.18%	2.36%	2.39%	0.82%	1.11%	**1.97%**
	SU	2.62%	10.65%	7.41%	0.90%	1.51%	5.56%		SU	0.70%	1.70%	2.75%	1.77%	1.96%	5.45%
	N–T	**0.58%**	2.91%	6.82%	1.06%	1.44%	6.59%		N–T	0.46%	0.50%	2.46%	1.05%	1.43%	4.44%
	T–N	2.22%	4.72%	5.29%	0.73%	1.28%	3.51%		T–N	0.74%	1.38%	2.34%	0.82%	1.13%	2.62%
	T–T	0.59%	3.83%	8.23%	0.60%	**0.83%**	3.10%		T–T	**0.44%**	**0.50%**	2.25%	**0.64%**	**0.67%**	2.59%
	T–SU	4.41%	19.07%	11.05%	1.10%	1.77%	3.58%		T–SU	0.67%	1.52%	2.58%	0.94%	1.43%	3.09%
ETH	N	1.65%	2.36%	4.48%	2.03%	1.14%	5.00%	SPB	N	0.52%	0.83%	**1.93%**	1.68%	2.08%	5.10%
	T	1.56%	**2.02%**	**3.99%**	**0.84%**	**0.62%**	**2.17%**		T	2.93%	1.11%	2.15%	1.20%	1.00%	2.28%
	SU	2.11%	5.80%	12.76%	2.28%	0.85%	5.20%		SU	0.56%	1.49%	2.28%	1.90%	3.07%	7.19%
	N–T	0.79%	2.36%	6.12%	2.03%	1.33%	6.23%		N–T	0.44%	0.54%	3.05%	1.19%	1.30%	3.68%
	T–N	2.84%	4.33%	7.27%	1.22%	1.06%	3.23%		T–N	0.48%	0.71%	3.09%	0.75%	0.90%	**2.18%**
	T–T	**0.78%**	3.07%	7.22%	1.09%	0.74%	2.72%		T–T	**0.41%**	**0.51%**	2.78%	**0.67%**	**0.78%**	2.35%
	T–SU	4.30%	11.27%	14.49%	2.16%	1.45%	3.37%		T–SU	0.54%	1.03%	3.12%	1.48%	1.67%	3.43%

Table 6. *Cont.*

$j = \mathrm{C}$		Case 1 (C ← Cs)			Case 2 (C ← NCs)			$j = \mathrm{NC}$		Case 3 (NC ← Cs)			Case 4 (NC ← NCs)		
		Before COVID-19	**During COVID-19**	**During Bubble**	**Before COVID-19**	**During COVID-19**	**During Bubble**			**Before COVID-19**	**During COVID-19**	**During Bubble**	**Before COVID-19**	**During COVID-19**	**During Bubble**
XRP	N	1.15%	1.50%	3.44%	1.21%	1.41%	4.28%	USD	N	0.46%	0.78%	1.96%	1.74%	1.48%	2.31%
	T	1.15%	1.48%	3.60%	**0.63%**	0.90%	**2.37%**		T	2.78%	1.04%	1.90%	1.08%	1.49%	3.75%
	SU	1.90%	2.37%	12.32%	1.33%	2.40%	6.38%		SU	0.50%	0.90%	2.14%	1.83%	1.94%	2.66%
	N–T	**0.64%**	**0.56%**	**2.42%**	1.33%	1.56%	5.07%		N–T	0.48%	0.51%	2.03%	1.05%	1.08%	2.58%
	T–N	1.77%	3.31%	5.84%	0.80%	1.16%	3.68%		T–N	0.48%	0.51%	1.77%	0.74%	0.74%	1.77%
	T–T	0.77%	0.68%	2.60%	0.67%	**0.81%**	2.46%		T–T	**0.45%**	**0.46%**	**1.69%**	**0.68%**	**0.64%**	**1.61%**
	T–SU	3.35%	4.98%	21.19%	1.19%	1.93%	8.69%		T–SU	0.48%	0.55%	1.79%	0.92%	1.08%	1.86%
LTC	N	1.04%	3.35%	3.93%	1.31%	1.09%	3.43%	OIL	N	1.55%	1.62%	1.57%	5.41%	3.69%	3.11%
	T	0.97%	2.71%	**3.55%**	**0.69%**	**0.58%**	**1.50%**		T	4.16%	1.82%	1.57%	1.35%	1.36%	**1.90%**
	SU	1.80%	6.48%	8.98%	1.40%	3.09%	4.42%		SU	1.27%	2.16%	1.63%	6.23%	4.88%	3.61%
	N–T	**0.76%**	**2.29%**	5.96%	1.37%	1.41%	5.13%		N–T	0.61%	0.49%	1.56%	1.59%	1.17%	4.26%
	T–N	1.42%	4.96%	4.37%	0.78%	0.90%	2.57%		T–N	1.31%	1.51%	1.51%	1.67%	1.80%	2.36%
	T–T	0.78%	3.07%	6.86%	0.78%	0.67%	2.28%		T–T	**0.58%**	**0.45%**	**1.30%**	**1.30%**	**0.59%**	2.22%
	T–SU	2.81%	10.26%	8.88%	1.29%	1.32%	2.30%		T–SU	1.15%	1.95%	1.50%	2.67%	3.87%	2.98%
XMR	N	1.05%	3.21%	**2.51%**	1.65%	1.52%	7.57%	GLD	N	0.88%	0.66%	1.58%	1.22%	2.95%	2.76%
	T	1.05%	2.73%	2.53%	**0.64%**	**0.81%**	**3.19%**		T	3.19%	0.94%	1.74%	**0.54%**	0.88%	2.38%
	SU	2.37%	4.20%	4.43%	1.75%	2.49%	9.65%		SU	1.12%	0.78%	1.49%	1.57%	3.66%	3.68%
	N–T	**0.80%**	**2.48%**	3.47%	1.95%	1.63%	9.67%		N–T	0.58%	0.48%	1.30%	1.03%	1.45%	3.38%
	T–N	1.42%	4.47%	3.77%	0.96%	1.48%	5.00%		T–N	0.76%	0.65%	1.65%	0.92%	1.00%	2.01%
	T–T	0.88%	3.38%	3.93%	0.81%	1.06%	4.02%		T–T	**0.55%**	**0.45%**	**1.18%**	0.85%	**0.73%**	**1.75%**
	T–SU	3.42%	6.13%	7.60%	1.44%	1.66%	5.26%		T–SU	0.87%	0.62%	1.55%	1.91%	1.39%	2.21%

C and NC stand for crypto and non-crypto assets, respectively. Each RMSE value was computed based on Equation (59). For each targeted asset j and each case over each period, the lowest RMSE is presented in boldface.

Table 7. Expected conditional asymmetric loss function $\mathrm{MCoAL}_{j|\setminus j}^{\alpha_j|\boldsymbol{\alpha}_{\setminus j}^{\mathrm{D}},50\%}$ evaluated at the $-\mathrm{MCoVaR}_{j|\setminus j}^{\alpha_j|\boldsymbol{\alpha}_{\setminus j}^{\mathrm{D}},50\%}$ forecast.

$j = \mathrm{C}$		Case 1 (C ← Cs)			Case 2 (C ← NCs)			$j = \mathrm{NC}$		Case 3 (NC ← Cs)			Case 4 (NC ← NCs)		
		Before COVID-19	**During COVID-19**	**During Bubble**	**Before COVID-19**	**During COVID-19**	**During Bubble**			**Before COVID-19**	**During COVID-19**	**During Bubble**	**Before COVID-19**	**During COVID-19**	**During Bubble**
$\alpha_j = 5\%$ and $\alpha_i = 5\%$, $i \in \mathscr{I}_{\setminus j}^{\mathrm{D}}$															
BTC	N	27.31%	35.38%	62.62%	18.56%	23.87%	28.95%	SPX	N	9.55%	17.70%	11.20%	8.24%	11.18%	**8.89%**
	T	**18.06%**	**22.21%**	**39.16%**	28.68%	33.11%	45.36%		T	**6.70%**	**10.11%**	**7.99%**	11.89%	14.59%	12.29%
	SU	42.14%	41.23%	57.19%	15.59%	20.47%	28.04%		SU	10.17%	22.22%	10.90%	**8.17%**	**10.22%**	9.23%
	N–T	43.65%	42.49%	42.04%	**12.54%**	**18.90%**	**27.24%**		N–T	11.65%	22.61%	10.32%	9.60%	13.43%	10.50%
	T–N	22.31%	27.89%	51.47%	20.46%	26.69%	33.12%		T–N	9.09%	14.22%	8.65%	11.27%	14.95%	12.06%
	T–T	27.56%	32.47%	54.39%	19.08%	27.87%	36.85%		T–T	7.91%	12.00%	8.07%	13.92%	18.15%	12.33%
	T–SU	26.45%	37.89%	55.23%	20.95%	29.84%	36.43%		T–SU	9.05%	13.46%	8.50%	13.61%	18.58%	11.93%
ETH	N	36.00%	41.02%	64.98%	25.65%	31.96%	45.56%	SPB	N	1.69%	2.51%	2.33%	1.66%	2.19%	3.15%
	T	**24.38%**	30.03%	38.41%	36.66%	44.93%	60.42%		T	**1.34%**	**1.83%**	1.89%	2.07%	2.73%	3.09%
	SU	50.34%	67.05%	64.11%	22.66%	27.26%	40.50%		SU	1.67%	2.62%	2.35%	**1.65%**	**2.15%**	2.76%
	N–T	50.91%	61.73%	66.48%	**14.96%**	**25.67%**	**39.39%**		N–T	1.72%	2.63%	2.27%	1.71%	2.48%	**2.48%**
	T–N	25.81%	**29.61%**	41.23%	24.83%	35.21%	48.50%		T–N	1.56%	2.25%	1.96%	1.90%	2.72%	2.89%
	T–T	32.96%	35.84%	53.89%	22.24%	36.34%	53.14%		T–T	1.45%	1.98%	**1.88%**	2.10%	3.09%	2.79%
	T–SU	30.29%	44.65%	**37.71%**	25.55%	38.33%	50.02%		T–SU	1.49%	1.98%	1.89%	2.08%	3.06%	2.83%
XRP	N	43.32%	98.81%	197.73%	30.58%	60.02%	108.40%	USD	N	3.15%	3.43%	2.67%	3.06%	3.93%	2.93%
	T	**29.76%**	46.38%	**101.04%**	48.81%	82.47%	186.28%		T	**2.50%**	2.94%	**2.50%**	3.89%	4.23%	3.12%
	SU	52.54%	157.57%	202.63%	26.86%	53.52%	109.91%		SU	3.18%	3.44%	2.63%	3.02%	3.64%	**2.88%**
	N–T	50.74%	134.95%	217.40%	**21.42%**	**36.55%**	**104.65%**		N–T	3.09%	3.39%	2.83%	**2.91%**	**3.61%**	3.14%
	T–N	31.14%	**45.13%**	116.49%	32.35%	55.69%	122.50%		T–N	2.78%	3.09%	2.66%	3.14%	3.70%	3.23%
	T–T	37.19%	49.08%	134.84%	33.53%	57.86%	147.66%		T–T	2.61%	2.91%	2.56%	3.32%	3.82%	3.29%
	T–SU	33.91%	50.79%	132.49%	33.54%	59.18%	147.06%		T–SU	2.64%	**2.89%**	2.58%	3.26%	3.77%	3.26%

Table 7. *Cont.*

$j = \mathrm{C}$		Case 1 (C ← Cs)			Case 2 (C ← NCs)			$j = \mathrm{NC}$		Case 3 (NC ← Cs)			Case 4 (NC ← NCs)		
		Before COVID-19	**During COVID-19**	**During Bubble**	**Before COVID-19**	**During COVID-19**	**During Bubble**			**Before COVID-19**	**During COVID-19**	**During Bubble**	**Before COVID-19**	**During COVID-19**	**During Bubble**
LTC	N	33.87%	37.91%	69.47%	29.80%	26.65%	37.87%	OIL	N	23.03%	61.19%	19.74%	**29.59%**	61.22%	**19.48%**
	T	**30.74%**	**25.40%**	**46.05%**	44.53%	39.34%	54.59%		T	**16.69%**	38.73%	**17.61%**	32.64%	73.56%	27.12%
	SU	36.29%	58.43%	51.70%	26.02%	22.11%	**35.78%**		SU	24.39%	68.83%	20.35%	41.17%	71.34%	19.71%
	N–T	39.46%	62.73%	78.73%	**22.50%**	**21.68%**	38.96%		N–T	26.66%	49.34%	21.06%	30.96%	**54.53%**	21.91%
	T–N	32.05%	29.10%	56.09%	31.62%	30.88%	47.68%		T–N	21.27%	43.99%	18.51%	31.93%	65.34%	25.12%
	T–T	35.29%	37.35%	60.40%	33.70%	30.61%	52.29%		T–T	19.27%	**27.17%**	17.84%	41.06%	78.61%	27.31%
	T–SU	35.17%	43.63%	64.91%	32.60%	33.16%	53.50%		T–SU	20.73%	36.58%	18.34%	43.49%	88.83%	26.97%
XMR	N	38.00%	56.22%	109.22%	**29.07%**	41.64%	44.70%	GLD	N	6.89%	11.37%	8.94%	7.01%	11.91%	**8.04%**
	T	**28.25%**	**38.02%**	**58.34%**	44.98%	59.48%	79.00%		T	**5.03%**	**8.66%**	**8.10%**	8.96%	15.01%	9.79%
	SU	60.06%	118.40%	86.95%	26.91%	38.47%	45.59%		SU	7.08%	12.16%	9.31%	7.41%	13.40%	8.08%
	N–T	64.91%	110.63%	86.82%	25.76%	**36.71%**	**38.96%**		N–T	6.56%	12.73%	10.19%	**6.85%**	**11.85%**	9.29%
	T–N	29.37%	46.00%	74.55%	35.75%	47.55%	47.78%		T–N	5.75%	10.05%	8.86%	7.49%	12.66%	10.07%
	T–T	36.73%	48.59%	76.23%	39.00%	53.47%	56.23%		T–T	5.21%	9.19%	8.49%	8.50%	15.10%	11.46%
	T–SU	36.59%	60.78%	71.84%	39.82%	57.14%	56.46%		T–SU	5.42%	9.59%	9.09%	8.34%	14.76%	11.59%
$\alpha_j = 1\%$ and $\alpha_i = 1\%$, $i \in \mathscr{I}^{\mathrm{D}}_{\setminus j}$															
BTC	N	9.91%	3.98%	4.44%	4.99%	6.42%	8.02%	SPX	N	**2.74%**	7.54%	2.82%	**2.24%**	3.01%	2.76%
	T	**5.23%**	5.80%	6.26%	14.81%	13.34%	14.14%		T	2.96%	**4.52%**	**2.05%**	5.35%	8.37%	3.32%
	SU	12.30%	52.24%	11.87%	4.29%	6.31%	8.71%		SU	3.27%	12.47%	2.32%	2.51%	**3.00%**	2.71%
	N–T	20.22%	74.31%	17.70%	**3.37%**	**5.35%**	**7.57%**		N–T	4.04%	11.65%	2.65%	3.16%	4.67%	2.51%
	T–N	7.26%	**3.30%**	**3.48%**	7.07%	9.44%	13.29%		T–N	2.88%	5.57%	3.07%	6.02%	8.88%	**2.18%**
	T–T	13.00%	12.87%	10.48%	9.96%	14.47%	17.71%		T–T	3.58%	7.03%	2.74%	6.85%	15.28%	2.93%
	T–SU	10.58%	21.00%	9.12%	9.38%	14.59%	16.98%		T–SU	3.49%	7.00%	2.47%	6.81%	14.99%	3.11%
ETH	N	9.41%	10.24%	8.79%	6.86%	8.48%	11.78%	SPB	N	0.47%	0.73%	0.68%	0.44%	0.62%	0.75%
	T	**6.55%**	**9.94%**	12.13%	19.38%	21.85%	21.51%		T	0.51%	0.74%	0.73%	0.86%	1.38%	0.94%
	SU	13.56%	69.27%	16.70%	6.62%	7.74%	**11.16%**		SU	0.49%	0.91%	0.69%	**0.43%**	**0.58%**	0.74%
	N–T	21.74%	73.10%	42.33%	**4.21%**	**7.05%**	11.31%		N–T	0.50%	0.85%	0.65%	0.48%	0.75%	**0.67%**
	T–N	8.16%	12.91%	**7.23%**	8.31%	12.07%	15.10%		T–N	**0.46%**	**0.67%**	**0.63%**	0.65%	1.96%	1.08%
	T–T	11.20%	20.13%	24.71%	11.90%	18.13%	21.37%		T–T	0.49%	0.77%	0.65%	1.07%	1.86%	1.06%
	T–SU	10.10%	22.10%	12.19%	11.46%	19.12%	19.06%		T–SU	0.49%	0.75%	0.64%	1.03%	1.89%	0.86%

Table 7. *Cont.*

$j = \mathrm{C}$		Case 1 (C ← Cs)			Case 2 (C ← NCs)			$j = \mathrm{NC}$		Case 3 (NC ← Cs)			Case 4 (NC ← NCs)		
		Before COVID-19	**During COVID-19**	**During Bubble**	**Before COVID-19**	**During COVID-19**	**During Bubble**			**Before COVID-19**	**During COVID-19**	**During Bubble**	**Before COVID-19**	**During COVID-19**	**During Bubble**
XRP	N	26.67%	162.34%	253.69%	8.13%	16.18%	**36.97%**	USD	N	0.82%	0.90%	0.71%	0.82%	1.15%	0.73%
	T	11.06%	28.36%	72.89%	22.58%	62.31%	51.68%		T	0.86%	1.06%	0.83%	1.34%	**1.67%**	1.02%
	SU	15.26%	40.88%	43.06%	7.26%	16.32%	46.27%		SU	0.83%	0.92%	**0.70%**	0.80%	0.97%	**0.72%**
	N–T	27.86%	57.63%	103.03%	**6.03%**	**11.67%**	48.23%		N–T	0.81%	0.90%	0.76%	**0.77%**	0.97%	0.80%
	T–N	**8.02%**	**26.93%**	123.92%	11.46%	18.42%	187.87%		T–N	**0.77%**	**0.87%**	0.77%	1.05%	1.31%	0.91%
	T–T	14.91%	41.83%	58.79%	16.88%	44.22%	77.43%		T–T	0.79%	0.91%	0.78%	1.16%	1.40%	0.99%
	T–SU	12.40%	35.10%	**35.44%**	15.26%	41.37%	49.88%		T–SU	0.79%	0.90%	0.77%	1.13%	1.35%	0.96%
LTC	N	12.49%	**4.76%**	5.16%	7.95%	7.03%	9.82%	OIL	N	6.70%	23.31%	**5.49%**	**12.81%**	**23.34%**	**5.29%**
	T	8.57%	7.67%	8.34%	17.29%	20.39%	25.83%		T	6.55%	21.44%	7.16%	19.88%	39.20%	10.52%
	SU	13.04%	23.98%	19.27%	7.20%	5.90%	**9.48%**		SU	9.02%	33.45%	5.87%	29.67%	35.16%	5.44%
	N–T	24.80%	28.33%	20.72%	**6.55%**	**5.60%**	10.54%		N–T	9.85%	21.97%	6.26%	13.82%	26.50%	6.81%
	T–N	**4.71%**	14.10%	**5.07%**	11.45%	10.27%	16.48%		T–N	**6.53%**	**14.18%**	5.99%	23.81%	101.26%	12.65%
	T–T	13.45%	23.64%	12.43%	14.80%	15.29%	23.59%		T–T	7.57%	16.71%	6.69%	56.09%	116.15%	8.52%
	T–SU	9.44%	37.71%	13.56%	14.66%	16.12%	22.32%		T–SU	8.49%	21.69%	6.60%	41.07%	112.13%	8.52%
XMR	N	17.42%	42.76%	82.97%	7.76%	11.39%	12.44%	GLD	N	1.87%	3.27%	**2.37%**	**1.90%**	**3.65%**	**2.17%**
	T	**9.53%**	**13.36%**	27.95%	22.77%	30.31%	35.27%		T	1.91%	3.89%	3.13%	5.07%	4.94%	4.55%
	SU	14.74%	38.56%	21.96%	7.48%	12.27%	14.03%		SU	2.03%	3.77%	2.72%	2.21%	4.60%	2.17%
	N–T	23.65%	48.67%	25.60%	**7.39%**	**11.14%**	**11.50%**		N–T	1.93%	4.07%	3.23%	2.02%	3.66%	2.66%
	T–N	9.90%	19.41%	40.51%	12.86%	17.12%	24.75%		T–N	**1.70%**	**3.09%**	2.68%	2.78%	9.40%	4.49%
	T–T	12.70%	37.64%	**15.68%**	19.42%	43.62%	27.02%		T–T	1.83%	3.82%	3.45%	5.04%	5.19%	6.22%
	T–SU	12.01%	59.91%	15.78%	17.89%	45.05%	25.80%		T–SU	1.83%	3.77%	3.44%	5.03%	5.17%	5.69%

C and NC stand for crypto and non-crypto assets, respectively. Each expected MCoAL was computed based on Equation (62). For each targeted asset j and each case over each period, the lowest expected MCoAL is presented in boldface.

Table 8. Number of $\mathrm{MCoVaR}_{j|\backslash j}^{\alpha_j|\boldsymbol{\alpha}_{\backslash j}^{\mathrm{D}},50\%}$ models with the best accuracy.

Model	Lowest RMSE of Estimated MCoCP			Lowest Expected MCoAL		
	Before COVID-19	During COVID-19	During Bubble	Before COVID-19	During COVID-19	During Bubble
$\alpha_j = 5\%$ and $\alpha_i = 5\%$, $i \in \mathscr{I}_{\backslash j}^{\mathrm{D}}$						
N	1	0	5	2	0	3
T	6	4	8	10	6	8
SU	0	0	0	2	2	2
N–T	8	10	6	6	8	5
T–N	0	0	0	0	2	0
T–T	4	6	1	0	1	1
T–SU	1	0	0	0	1	1
$\alpha_j = 1\%$ and $\alpha_i = 1\%$, $i \in \mathscr{I}_{\backslash j}^{\mathrm{D}}$						
N	0	0	3	4	3	5
T	6	5	10	3	4	1
SU	0	0	0	1	2	3
N–T	4	3	1	6	5	4
T–N	0	0	1	6	6	5
T–T	10	12	5	0	0	1
T–SU	0	0	0	0	0	1

This table summarizes Tables 6 and 7 by counting the number of multivariate models resulting in the $\mathrm{MCoVaR}_{j|\backslash j}^{\alpha_j|\boldsymbol{\alpha}_{\backslash j}^{\mathrm{D}},50\%}$ forecast, whose estimated conditional coverage probability $\mathrm{MCoCP}_{j|\backslash j}^{\alpha_j|\boldsymbol{\alpha}_{\backslash j}^{\mathrm{D}},50\%}$ possesses the lowest RMSE, and whose expected $\mathrm{MCoAL}_{j|\backslash j}^{\alpha_j|\boldsymbol{\alpha}_{\backslash j}^{\mathrm{D}},50\%}$ has the lowest value.

We found that the three classical models (i.e., the normal, Student's t, and Johnson's SU models) competed in accurately forecasting the MCoVaR for the crypto and non-crypto assets under study. However, the classical Student's t model tended to perform best in many cases with the smallest RMSE values. This best MCoVaR forecasting performance is consistent with its ability to produce the most accurate individual VaR forecast before COVID-19, during COVID-19, and during the 2021 crypto bubble, as previously detected from Table 4.

Compared to the aforementioned classical models, copula-based models tended to perform better in producing an accurate MCoVaR forecast. More specifically, among the resulting 20 MCoVaR forecasts for the four cases, we found 13 (16) MCoVaR forecasts to possess an estimated MCoCP with the lowest RMSE when formulated at the 5% significance level using the latter models before (during) COVID-19. At the 1% level of significance, 14 (15) copula-based MCoVaR forecasts exhibited an estimated MCoCP with the lowest RMSE before (during) COVID-19. A notable exception when examining the conditional coverage performance of the MCoVaR forecast was that only 7 out of 20 copula-based MCoVaR forecasts had an estimated MCoCP with the smallest RMSE during the 2021 bubble episode. This evidence demonstrates the importance of considering copulas for enhancing the conditional coverage performance of the MCoVaR forecast. In more detail, the models determined based on the normal and Student's t copulas with Student's t margins (i.e., the N–T and T–T models) performed competitively in forecasting MCoVaR with the best conditional coverage performance over the pre-COVID-19 and COVID-19 periods. This suggests that, in addition to copulas, the non-normality of their margins is also of significance for better forecasting MCoVaR. These results are in line with what Karimalis and Nomikos (2018) and Bianchi et al. (2023) concluded from their studies on forecasting CoVaR based on copulas with non-normal margins.

When utilizing the expected MCoAL to assess the MCoVaR backtesting performance, we found slightly different assessment results. More specifically, among the resulting 20 MCoVaR forecasts for the four cases, we had 12 copula-based MCoVaR forecasts at the 5% significance level with the lowest expected MCoAL during COVID-19. At the 1% level of significance, 12 (11) copula-based MCoVaR forecasts possessed the lowest expected MCoAL before (during) COVID-19, and 11 copula-based MCoVaR forecasts exhibited the lowest expected MCoAL during the 2021 bubble. These were mainly produced by the N–T and T–N models.

5.3. Quantifying Joint Transmissions of Systemic Risk Using ΔMCoVaR Forecasts

Our next aim was to find the ΔMCoVaR for each targeted (crypto/non-crypto) asset by calculating the difference between (1) its MCoVaR when the conditioning crypto/non-crypto assets were jointly in distress and (2) its MCoVaR when all the conditioning assets were jointly in their median or normal states. If this ΔMCoVaR is significantly positive, we say that the distressed conditioning assets significantly serve as joint transmitters of systemic risk and that the targeted asset significantly acts as a systemic risk receiver. The positivity of the ΔMCoVaR forecast was examined by testing

$\mathbf{H_0}$: $\Delta\mathrm{MCoVaR}_{j|\backslash j}^{\alpha_j|\boldsymbol{\alpha}_{\backslash j}^{\mathrm{D}},50\%} \leq 0 \textit{ or } \mathrm{MCoVaR}_{j|\backslash j}^{\alpha_j|\boldsymbol{\alpha}_{\backslash j}^{\mathrm{D}},50\%} \leq \mathrm{MCoVaR}_{j|\backslash j}^{\alpha_j|50\%,50\%}$

$\mathbf{H_1}$: $\Delta\mathrm{MCoVaR}_{j|\backslash j}^{\alpha_j|\boldsymbol{\alpha}_{\backslash j}^{\mathrm{D}},50\%} > 0 \textit{ or } \mathrm{MCoVaR}_{j|\backslash j}^{\alpha_j|\boldsymbol{\alpha}_{\backslash j}^{\mathrm{D}},50\%} > \mathrm{MCoVaR}_{j|\backslash j}^{\alpha_j|50\%,50\%}$

using the two-sample Kolmogorov–Smirnov test proposed by Abadie (2002) and Bernal et al. (2014).

We provide in Table 9 the resulting ΔMCoVaR forecasts at the 5% and 1% levels of significance for the four cases stated in Table 2. We observed that non-normal models appeared to produce ΔMCoVaR forecasts with a relatively higher magnitude. As the COVID-19 pandemic and the 2021 crypto bubble progressed, the ΔMCoVaR forecasts determined under any model setting tended to increase in value. This suggests a higher tendency of joint systemic risk transmissions across the crypto and non-crypto markets due to the pandemic and crypto bubble. This is in line with the finding of Akhtaruzzaman et al. (2022) that provided evidence of pandemic-driven contagion channels across crypto assets only by utilizing the so-called systemic risk contagion index built based on ΔCoVaR. However, this is contrary to Bazán-Palomino's (2022) empirical result that highlighted weak interdependence and contagion among Bitcoin, Ethereum, and Ripple during the bubble period.

When regarding each crypto asset as the targeted asset, we found that it received systemic risk contributions from the other crypto assets being much larger than those from the non-crypto assets before and during COVID-19 and during the 2021 crypto bubble (see the "Case 1" and "Case 2" columns of Table 9). This result confirmed the evidence pointed out by Yi et al. (2018) and Borri (2019) that the crypto assets were significantly subject to volatility and tail risk spillovers within the crypto markets. This evidence might result from strongly positive dependence among the crypto assets and weak dependence between the crypto and non-crypto assets (see Figure 2). In particular, Ripple and Bitcoin were the largest and smallest receivers, respectively, in the mechanism of joint systemic risk transmissions within the crypto markets over the pre-COVID-19, COVID-19, and 2021 bubble periods. Bitcoin's significant role as the smallest systemic risk receiver indicates that this most prominent crypto asset was less systemically vulnerable. This finding is consistent with what Akhtaruzzaman et al. (2022) uncovered using their proposed systemic risk contagion index. More specifically, among the 17 selected cryptocurrencies, they found Bitcoin to rank second to last for being systemically vulnerable and having low potential to cause systemic disruption. Our finding is, however, contrary to the empirical result of Xu et al. (2021) that showed Bitcoin to be the largest systemic risk receiver. Their reason is that, among the 23 sampled crypto assets whose systemic risk spillover mechanism was studied through a tail-event driven network approach, Bitcoin exhibited the largest systemic risk receiver index. Their conclusion might come from the fact that Bitcoin possessed the largest market capitalization, and the proposed systemic risk receiver index was proportional to the crypto market capitalizations.

Table 9. $\Delta\text{MCoVaR}_{j|\backslash j}^{\alpha_j|\boldsymbol{\alpha}^{\mathrm{D}}_{\backslash j},50\%}$ forecasts.

$j = \mathrm{C}$		Case 1 (C ← Cs)			Case 2 (C ← NCs)			$j = \mathrm{NC}$		Case 3 (NC ← Cs)			Case 4 (NC ← NCs)		
		Before COVID-19	**During COVID-19**	**During Bubble**	**Before COVID-19**	**During COVID-19**	**During Bubble**			**Before COVID-19**	**During COVID-19**	**During Bubble**	**Before COVID-19**	**During COVID-19**	**During Bubble**
$\alpha_j = 5\%$ and $\alpha_i = 5\%$, $i \in \mathscr{I}^{\mathrm{D}}_{\backslash j}$															
BTC	N	6.85 *	7.12 *	6.90 *	−0.72	1.26 *	1.13 *	SPX	N	0.11 *	1.02 *	0.52 *	−0.24	−0.45	0.10 *
	T	7.24 *	7.66 *	7.90 *	2.26 *	4.63 *	4.63 *		T	0.41 *	1.51 *	0.79 *	0.75 *	1.12 *	0.92 *
	SU	9.72 *	12.34 *	8.85 *	−0.71	1.46 *	1.23 *		SU	0.15 *	1.80 *	0.65 *	−0.27	−0.54	0.14 *
	N–T	9.09 *	10.52 *	10.17 *	−0.83	0.32 *	0.00		N–T	0.10 *	0.98 *	0.37 *	−0.15	−0.11	0.40 *
	T–N	6.76 *	7.44 *	7.45 *	−0.15	1.58 *	1.40 *		T–N	0.18 *	0.85 *	0.41 *	0.24 *	0.44 *	0.66 *
	T–T	7.53 *	8.56 *	9.02 *	0.48 *	2.37 *	2.30 *		T–T	0.24 *	0.98 *	0.50 *	0.54 *	0.95 *	0.93 *
	T–SU	8.52 *	11.48 *	9.19 *	0.45 *	2.84 *	2.17 *		T–SU	0.30 *	1.31 *	0.53 *	0.63 *	1.23 *	0.96 *
ETH	N	9.25 *	9.86 *	9.66 *	1.03 *	0.89 *	1.02 *	SPB	N	−0.01	0.05 *	0.03 *	−0.13	−0.16	0.17 *
	T	9.66 *	10.61 *	11.16 *	4.47 *	5.60 *	6.18 *		T	0.06 *	0.17 *	0.11 *	0.06 *	0.12 *	0.39 *
	SU	12.92 *	16.50 *	10.71 *	1.08 *	0.91 *	1.00 *		SU	−0.01	0.08 *	0.04 *	−0.13	−0.17	0.24 *
	N–T	12.07 *	13.57 *	16.00 *	0.30 *	0.33 *	0.41 *		N–T	−0.02	0.01 *	0.01 *	−0.03	−0.04	0.08 *
	T–N	9.31 *	9.96 *	10.32 *	1.55 *	1.97 *	2.36 *		T–N	0.00	0.04 *	0.03 *	0.04 *	0.07 *	0.14 *
	T–T	10.29 *	11.32 *	13.39 *	1.87 *	3.02 *	3.46 *		T–T	0.02 *	0.07 *	0.05 *	0.10 *	0.18 *	0.23 *
	T–SU	11.68 *	14.31 *	10.50 *	2.22 *	3.44 *	2.83 *		T–SU	0.01 *	0.07 *	0.05 *	0.09 *	0.17 *	0.21 *
XRP	N	8.29 *	9.22 *	10.10 *	−0.99	0.72 *	3.35 *	USD	N	−0.02	−0.04	−0.01	−0.23	−0.36	−0.39
	T	9.03 *	11.29 *	13.50 *	3.87 *	9.92 *	15.88 *		T	0.08 *	0.13 *	0.10 *	0.09 *	0.03 *	−0.21
	SU	10.27 *	15.48 *	13.92 *	−0.87	0.80 *	3.87 *		SU	−0.02	−0.04	−0.01	−0.23	−0.35	−0.39
	N–T	11.77 *	17.32 *	24.22 *	−0.28	0.71 *	5.32 *		N–T	−0.02	−0.07	−0.02	−0.28	−0.35	−0.32
	T–N	8.55 *	11.67 *	14.04 *	1.19 *	3.38 *	8.88 *		T–N	0.01	−0.03	0.02 *	−0.19	−0.25	−0.25
	T–T	9.73 *	12.86 *	18.74 *	1.91 *	4.48 *	13.18 *		T–T	0.04 *	0.02 *	0.05 *	−0.10	−0.13	−0.20
	T–SU	9.18 *	14.29 *	17.18 *	1.86 *	5.18 *	11.97 *		T–SU	0.03 *	0.02	0.04 *	−0.12	−0.13	−0.21

Table 9. *Cont.*

$j = \mathrm{C}$		Case 1 (C ← Cs)			Case 2 (C ← NCs)			$j = \mathrm{NC}$		Case 3 (NC ← Cs)			Case 4 (NC ← NCs)		
		Before COVID-19	**During COVID-19**	**During Bubble**	**Before COVID-19**	**During COVID-19**	**During Bubble**			**Before COVID-19**	**During COVID-19**	**During Bubble**	**Before COVID-19**	**During COVID-19**	**During Bubble**
LTC	N	8.82 *	11.17 *	11.73 *	1.00 *	−1.31	−1.71	OIL	N	0.28 *	0.25	−0.72	1.54 *	0.26	−1.00
	T	9.41 *	11.66 *	12.97 *	5.11 *	3.06 *	2.74 *		T	1.05 *	3.09 *	0.06	4.43 *	7.86 *	0.92 *
	SU	10.21 *	19.85 *	17.18 *	0.89 *	−1.42	−1.91		SU	0.49 *	0.41	−0.84	3.74 *	0.72 *	−1.21
	N–T	12.10 *	14.94 *	13.96 *	0.90 *	−0.84	−1.11		N–T	0.07 *	−0.31	−0.67	0.68 *	0.04	−0.35
	T–N	8.91 *	10.69 *	10.66 *	2.46 *	0.32 *	0.72 *		T–N	0.28 *	0.25	−0.35	1.53 *	2.30 *	0.45 *
	T–T	10.24 *	12.19 *	12.57 *	3.07 *	1.41 *	1.95 *		T–T	0.48 *	0.61 *	−0.15	2.89 *	3.47 *	1.06 *
	T–SU	9.29 *	16.12 *	14.59 *	2.91 *	1.69 *	1.93 *		T–SU	0.62 *	1.21 *	−0.22	3.95 *	6.91 *	0.98 *
XMR	N	9.43 *	8.85 *	5.53 *	−0.16	0.94 *	−0.86	GLD	N	0.06 *	0.01	−0.15	0.12 *	0.12 *	−0.88
	T	10.03 *	10.10 *	7.08 *	4.22 *	6.99 *	4.72 *		T	0.29 *	0.52 *	0.20 *	0.94 *	1.48 *	−0.16
	SU	12.88 *	18.81 *	8.89 *	−0.17	1.30 *	−1.24		SU	0.07 *	−0.02	−0.21	0.21 *	0.29 *	−1.04
	N–T	12.62 *	13.51 *	10.74 *	0.41 *	0.94 *	−0.67		N–T	0.08 *	0.07 *	−0.05	0.17 *	−0.09	−0.26
	T–N	9.16 *	8.84 *	7.22 *	2.11 *	3.00 *	1.30 *		T–N	0.13 *	0.17 *	0.07 *	0.42 *	0.33 *	0.07 *
	T–T	10.69 *	10.64 *	9.31 *	3.02 *	4.68 *	2.66 *		T–T	0.18 *	0.30 *	0.16 *	0.69 *	0.78 *	0.29 *
	T–SU	11.43 *	14.91 *	10.42 *	3.22 *	6.20 *	2.67 *		T–SU	0.19 *	0.34 *	0.18 *	0.69 *	0.86 *	0.31 *
$\alpha_j = 1\%$ and $\alpha_i = 1\%$, $i \in \mathscr{I}^{\mathrm{D}}_{\setminus j}$															
BTC	N	9.69 *	10.06 *	9.75 *	−1.02	1.78 *	1.60 *	SPX	N	0.16 *	1.44 *	0.73 *	−0.34	−0.64	0.14 *
	T	13.40 *	15.51 *	14.02 *	7.42 *	12.63 *	11.36 *		T	1.21 *	3.67 *	1.67 *	2.53 *	4.05 *	2.42 *
	SU	20.87 *	30.80 *	16.89 *	−1.12	2.72 *	2.01 *		SU	0.30 *	4.61 *	1.07 *	−0.53	−1.12	0.22 *
	N–T	28.51 *	31.63 *	23.59 *	−1.31	0.54 *	0.00		N–T	0.25 *	3.10 *	0.62 *	−0.34	−0.27	0.68 *
	T–N	9.45 *	10.40 *	10.44 *	1.06 *	3.66 *	3.62 *		T–N	0.36 *	1.34 *	0.67 *	0.77 *	1.22 *	1.22 *
	T–T	19.38 *	20.76 *	18.45 *	2.91 *	8.11 *	7.36 *		T–T	0.87 *	3.27 *	1.03 *	3.00 *	5.46 *	2.15 *
	T–SU	16.73 *	26.64 *	16.83 *	2.96 *	10.58 *	6.68 *		T–SU	1.00 *	3.83 *	1.06 *	2.94 *	5.77 *	2.13 *
ETH	N	13.09 *	13.94 *	13.66 *	1.46 *	1.26 *	1.45 *	SPB	N	−0.01	0.07 *	0.04 *	−0.18	−0.23	0.24 *
	T	17.70 *	21.47 *	19.92 *	11.80 *	16.02 *	15.73 *		T	0.20 *	0.50 *	0.28 *	0.34 *	0.60 *	0.88 *
	SU	25.74 *	40.64 *	22.12 *	1.73 *	1.62 *	1.65 *		SU	−0.01	0.17 *	0.07 *	−0.22	−0.32	0.51 *
	N–T	34.61 *	38.36 *	48.01 *	0.47 *	0.55 *	0.73		N–T	−0.03	0.03 *	0.02 *	−0.06	−0.08	0.18 *
	T–N	12.99 *	13.96 *	14.45 *	3.58 *	4.65 *	5.57 *		T–N	0.03 *	0.09 *	0.07 *	0.14 *	0.21 *	0.27 *
	T–T	24.61 *	26.48 *	33.43 *	5.77 *	10.09 *	12.28 *		T–T	0.09 *	0.27 *	0.19 *	0.42 *	0.82 *	0.80 *
	T–SU	21.33 *	32.09 *	20.17 *	6.24 *	12.39 *	8.31 *		T–SU	0.08 *	0.26 *	0.15 *	0.40 *	0.75 *	0.59 *

Table 9. *Cont.*

$j = \mathrm{C}$		**Case 1 (C ← Cs)**			**Case 2 (C ← NCs)**			$j = \mathrm{NC}$		**Case 3 (NC ← Cs)**			**Case 4 (NC ← NCs)**		
		Before COVID-19	**During COVID-19**	**During Bubble**	**Before COVID-19**	**During COVID-19**	**During Bubble**			**Before COVID-19**	**During COVID-19**	**During Bubble**	**Before COVID-19**	**During COVID-19**	**During Bubble**
XRP	N	11.72 *	13.04 *	14.28 *	−1.41	1.02 *	4.74 *	USD	N	−0.03	−0.06	−0.01	−0.33	−0.51	−0.55
	T	17.15 *	24.92 *	26.59 *	12.41 *	29.38 *	39.61 *		T	0.32 *	0.53 *	0.31 *	0.57 *	0.57 *	−0.10
	SU	21.85 *	42.04 *	33.46 *	−1.39	1.61 *	8.25 *		SU	−0.04	−0.07	−0.01	−0.36	−0.55	−0.55
	N–T	35.84 *	69.49 *	102.16 *	−0.48	1.43 *	14.67 *		N–T	−0.03	−0.12	−0.02	−0.43	−0.55	−0.46
	T–N	11.96 *	16.38 *	20.06 *	3.54 *	7.55 *	16.84 *		T–N	0.05 *	0.01 *	0.07 *	−0.14	−0.21	−0.26
	T–T	24.54 *	38.98 *	64.95 *	7.51 *	19.82 *	70.83 *		T–T	0.14 *	0.18 *	0.15 *	0.07 *	0.09 *	−0.12
	T–SU	17.53 *	33.49 *	40.01 *	6.23 *	19.19 *	39.81 *		T–SU	0.12 *	0.15 *	0.12 *	0.02	0.06	−0.15
LTC	N	12.48 *	15.79 *	16.58 *	1.41 *	−1.85	−2.41	OIL	N	0.39 *	0.36	−1.02	2.18 *	0.36	−1.41
	T	17.55 *	23.04 *	22.41 *	13.68 *	10.86 *	9.48 *		T	3.10 *	10.31 *	1.24 *	11.10 *	23.87 *	3.78 *
	SU	20.62 *	46.49 *	31.20 *	1.41 *	−2.28	−2.94		SU	1.20 *	1.13	−1.49	10.47 *	2.02 *	−2.10
	N–T	33.36 *	44.56 *	30.14 *	1.51 *	−1.32	−1.74		N–T	0.19 *	−0.98	−1.31	1.89 *	0.13 *	−0.70
	T–N	12.43 *	14.91 *	14.91 *	5.12 *	2.21 *	3.31 *		T–N	0.69 *	1.20 *	−0.14	3.17 *	5.64 *	1.48 *
	T–T	23.64 *	29.00 *	24.20 *	9.41 *	5.96 *	7.41 *		T–T	2.05 *	3.88 *	0.54 *	15.46 *	26.78 *	4.71 *
	T–SU	17.01 *	33.68 *	25.25 *	7.60 *	7.62 *	7.60 *		T–SU	2.75 *	7.16 *	0.35 *	18.43 *	36.61 *	3.81 *
XMR	N	13.34 *	12.51 *	7.82 *	−0.23	1.33 *	−1.22	GLD	N	0.08 *	0.01	−0.21	0.16 *	0.17 *	−1.25
	T	18.68 *	21.28 *	13.56 *	12.44 *	20.21 *	13.93 *		T	0.89 *	1.80 *	0.84 *	2.61 *	4.41 *	0.65 *
	SU	25.11 *	49.38 *	18.80 *	−0.28	2.59 *	−2.22		SU	0.13 *	−0.05	−0.38	0.41 *	0.61 *	−1.76
	N–T	33.42 *	43.30 *	28.71 *	0.69 *	1.81 *	−1.21		N–T	0.16 *	0.16 *	−0.10	0.36 *	−0.21	−0.53
	T–N	12.78 *	12.42 *	10.24 *	4.89 *	6.46 *	4.09 *		T–N	0.26 *	0.39 *	0.25 *	0.87 *	0.91 *	0.48 *
	T–T	23.82 *	27.11 *	21.78 *	9.80 *	17.64 *	10.84 *		T–T	0.56 *	1.16 *	0.71 *	2.56 *	3.77 *	1.69 *
	T–SU	20.69 *	35.20 *	21.14 *	9.28 *	23.37 *	10.33 *		T–SU	0.55 *	1.17 *	0.74 *	2.27 *	3.24 *	1.64 *

C and NC stand for crypto and non-crypto assets, respectively. The asterisk * indicates that the $\Delta\mathrm{MCoVaR}_{j|\backslash j}^{\alpha_j|\boldsymbol{\alpha}^{D}_{\backslash j},50\%}$ forecast is significantly positive based on the two-sample Kolmogorov–Smirnov test at the 5% level.

Furthermore, Ripple and Bitcoin were negatively impacted by systemic risk jointly transmitted from the non-crypto assets amid the pre-COVID-19 period. This indicates that the Ripple and Bitcoin markets became less risky when global non-crypto markets moved from normal situations to stressful circumstances during such a period. Meanwhile, Litecoin was found to be the largest receiver of systemic risk jointly transmitted from the non-crypto assets. As the pandemic and bubble progressed, joint transmissions of systemic risk from the non-crypto assets negatively impacted Litecoin and positively affected the remaining crypto assets. This was a notable exception where the systemic impacts of the non-crypto markets on the Litecoin market substantially declined due to the COVID-19 pandemic and crypto bubble. A similar exception was Monero, which received decreased systemic impacts from the non-crypto markets during the bubble period.

Conversely, when each non-crypto asset was treated as the targeted asset, the joint systemic risk contributions of the crypto assets to the non-crypto asset were not found to be as large as the joint systemic risk contributions of the crypto assets to the other within the crypto markets. In particular, the joint transmissions of systemic risk from the crypto assets tended to have a small positive impact on the S&P 500, oil, and gold and a small negative effect on the S&P US Treasury Bond and the US dollar. This is in line with evidence previously shown from Figure 2 that the crypto assets exhibited a weakly positive correlation with the former three non-crypto assets and a weakly negative correlation with the latter two non-crypto assets. This is also consistent with the finding of Jang et al. (2019) that documented interdependence between Bitcoin and other global assets, including the S&P 500 and gold. Meanwhile, joint transmissions of systemic risk within the non-crypto markets had a tendency to negatively impact the S&P 500, the S&P US Treasury Bond, and the US dollar and positively influence the two commodities before and during COVID-19. Overall, compared to the systemic impacts of the non-crypto markets, the systemic impacts of the crypto markets on the former three non-crypto assets appeared to be larger, and the systemic impacts of the crypto markets on the latter two non-crypto assets seemed to be smaller. Among the five non-crypto assets examined in this study, oil was found to be the largest receiver of systemic risk jointly transmitted from the crypto assets and from the remaining non-crypto assets. Interestingly, the systemic impacts of the crypto and non-crypto markets on the US dollar significantly decreased as a result of the COVID-19 pandemic and the 2021 crypto bubble.

6. Conclusions

This study proposed to analytically formulate the MCoVaR systemic risk measure for a targeted asset by considering that a set of conditioning assets were jointly in distress and that a set of the remaining conditioning assets were jointly in their median or normal situations. The formulation was carried out by modeling their returns through an approach based on multivariate copulas, which enabled us to study their margins and dependence structure separately. Classical multivariate risk models, including multivariate normal and Student's t benchmark models and a multivariate Johnson's SU model, were also considered. These methodological frameworks were applied to investigate joint systemic risk transmissions across crypto and non-crypto markets over periods before and during the global outbreak of the COVID-19 pandemic, which covers the 2021 crypto bubble.

By examining the RMSE of the estimated conditional coverage probability (MCoCP) and the expected conditional asymmetric loss function (MCoAL) of the resulting MCoVaR forecast, the copula-based models with non-normal margins outperformed the aforementioned three classical models in accurately forecasting MCoVaR. This suggests the importance and significance of combining copulas with asymmetric and leptokurtic margins for formulating an accurate MCoVaR forecast and thus complements previous studies, e.g., Cao (2013), Bernardi and Petrella (2015), Bernardi et al. (2017), Torri et al. (2021), Chen et al. (2022), and Hakim et al. (2022), that relied on classical models. The so-called multivariate Archimedean copulas and vine copulas may also be taken into consideration to capture asymmetric tail dependence among multiple asset returns. However, their conditional copula function $C_{j|\setminus j;\vartheta_{j|\setminus j}}$ for high dimensions has a very complex expression and thus no explicit inverse $C^{-1}_{j|\setminus j;\vartheta_{j|\setminus j}}$. Furthermore, ARMA-GARCH specifications may also be considered to capture the stylized facts of dynamic crypto- and non-crypto-asset returns and volatilities. Nonetheless, the use of these models leads us to require a greater effort for computing the expected value of our proposed MCoAL by accounting for a conditioning information set and cross-sectional dependence. Thus, these alternative models were not employed in this study, but they may become an interesting direction for future research. In addition, further statistical tests of our proposed (MCo)AL may be carried out through the Diebold–Mariano (DM) test for pairwise comparisons and the model confidence set (MCS) procedure for equal predictive ability (EPA), as in Bernardi and Catania (2016), Le (2020), and Jiménez et al. (2022).

By computing the corresponding ΔMCoVaR forecast, we found non-normally distributed classical models and copulas with non-normal margins to produce this forecast with a higher value, considerably more evident during the COVID-19 pandemic and the 2021 crypto bubble. This indicates the rising tendency of crypto and non-crypto markets to jointly transmit systemic risk due to the pandemic and bubble. Furthermore, we highlighted that joint transmissions of systemic risk from the crypto markets highly impacted each crypto asset and oil. In addition to oil, the S&P 500 and gold also received a positive systemic impact from the crypto markets, although this impact was not as large as what each crypto asset received. This result supported evidence of the crypto markets as potential sources of global financial instability triggering systemic risk, particularly during the ongoing COVID-19 pandemic and the recent 2021 bubble episode. The improvement in the conditional coverage performance of the copula-based MCoVaR forecast may lead to an enhancement in managing systemic risk in global financial markets in the presence of crypto markets. In contrast, the systemic impact received by the S&P US Treasury Bond and the US dollar was negative, in line with their strong safe-haven properties. In future research, it is necessary to include another class of crypto assets, namely, stablecoins, well known to exhibit stable volatility (as their name suggests) and strong safe-haven characteristics. It is important to examine whether these stable crypto assets also play roles as potential sources of systemic risk (as traditional crypto assets do).

Author Contributions: Conceptualization, A.H. and K.S.; methodology, A.H. and K.S.; software, A.H.; validation, A.H. and K.S.; formal analysis, A.H.; resources, K.S.; data curation, A.H.; writing—original draft preparation, A.H.; writing—review and editing, A.H. and K.S.; supervision, K.S.; project administration, K.S.; funding acquisition, K.S. All authors have read and agreed to the published version of the manuscript.

Funding: This work was funded by the Institut Teknologi Bandung (ITB)/Kemendikbudristek, Indonesia, under the grant of PDKN 2022.

Institutional Review Board Statement: Not applicable.

Informed Consent Statement: Not applicable.

Data Availability Statement: The data analyzed in this study are publicly available at CoinMarketCap.com, SPGlobal.com, Investing.com, EIA.gov, and Nasdaq.com (accessed on 14 November 2022).

Acknowledgments: This work is part of the dissertation research of the first author (A.H.). He would like to thank the German Academic Exchange Service (*Deutscher Akademischer Austauschdienst* [DAAD]) for providing the In-Country/In-Region Scholarship Program that supported his doctoral study at the Institut Teknologi Bandung (ITB), Indonesia. All the authors are also grateful to the academic editor and anonymous reviewers for their careful reading and valuable comments that led to significant improvement of this paper.

Conflicts of Interest: The authors declare no conflict of interest. The funders had no role in the design of the study; in the collection, analyses, or interpretation of data; in the writing of the manuscript; or in the decision to publish the results.

Notes

1 It is well known that VaR is elicitable because there exists a loss or scoring function, particularly an asymmetric piecewise-linear loss function, minimized by VaR; see Gneiting (2011). This fact makes the VaR forecast easy to backtest using some backtesting procedures, such as unconditional coverage and independence tests (Christoffersen 1998; Kupiec 1995), coverage probabilities (Hakim et al. 2022; Kabaila and Syuhada 2008), or expected asymmetric loss functions (Bernardi and Catania 2016; González-Rivera et al. 2004; Jiménez et al. 2022; Le 2020; Syuhada et al. 2021). Since the MCoVaR systemic risk measure is basically the VaR risk measure of a targeted entity's risk conditional on other entities' risks, it is also an elicitable risk measure. This motivated us to rely on MCoVaR (instead of other systemic risk measures, such as MCoES, MES, and SRISK) for systemic risk quantification and propose backtesting techniques for the MCoVaR forecast evaluation.

2 We denote the probability functions that correspond to the distribution functions $G_{(\mathbf{0},\mathbf{P},\boldsymbol{\omega})}$, $F_{(\boldsymbol{\mu},\boldsymbol{\Sigma},\boldsymbol{\omega})}$, $G_{i;\omega_i}$, and $F_{i;(\mu_i,\sigma_i^2,\omega_i)}$ as follows: $g_{(\mathbf{0},\mathbf{P},\boldsymbol{\omega})}$, $f_{(\boldsymbol{\mu},\boldsymbol{\Sigma},\boldsymbol{\omega})}$, $g_{i;\omega_i}$, and $f_{i;(\mu_i,\sigma_i^2,\omega_i)}$, respectively.

3 Embrechts et al. (2003b) stated that if the joint distribution function of X_i and X_j is exchangeable, i.e., $F_{ij;\boldsymbol{\theta}_{ij}} = F_{ji;\boldsymbol{\theta}_{ji}}$, then $\lambda^{\mathrm{L}}_{ij;\boldsymbol{\theta}_{ij}} = 2\lim_{u\to 0+} \mathbb{P}\left(\left\{X_j < F^{-1}_{j;\boldsymbol{\theta}_j}(u)\right\} \,\middle|\, \left\{X_i = F^{-1}_{i;\boldsymbol{\theta}_i}(u)\right\}\right)$ and $\lambda^{\mathrm{U}}_{ij;\boldsymbol{\theta}_{ij}} = 2\lim_{u\to 1-} \mathbb{P}\left(\left\{X_j > F^{-1}_{j;\boldsymbol{\theta}_j}(u)\right\} \,\middle|\, \left\{X_i = F^{-1}_{i;\boldsymbol{\theta}_i}(u)\right\}\right)$.

4 In Ding's (2016) original study assuming $\mathbf{X}$ to admit an I-variate Student's t distribution, with a covariance matrix $\frac{\nu}{\nu-2}\boldsymbol{\Sigma}$, the conditional distribution of $\mathbf{X}_2 \mid \{\mathbf{X}_1 = \mathbf{x}_1\}$ is an $(I-K)$-variate Student's t distribution, with a covariance matrix $\frac{\nu+(\mathbf{x}_1-\boldsymbol{\mu}_1)^\top\boldsymbol{\Sigma}_{11}^{-1}(\mathbf{x}_1-\boldsymbol{\mu}_1)}{\nu+K}\left(\boldsymbol{\Sigma}_{22}-\boldsymbol{\Sigma}_{21}\,\boldsymbol{\Sigma}_{11}^{-1}\,\boldsymbol{\Sigma}_{12}\right)$.

5 According to Remark 1, the resulting coefficient $2T_{\nu+1}\left(-\sqrt{\frac{1-\rho_{ij}}{1+\rho_{ij}}(\nu-1)}\right)$ of the lower and upper tail dependence of our proposed Student's t model is different from the coefficient $2T_{\nu+1}\left(-\sqrt{\frac{1-\rho_{ij}}{1+\rho_{ij}}(\nu+1)}\right)$ of the lower and upper tail dependence of Student's t model discussed in Demarta and McNeil (2005).

6 The corresponding function $c_{\boldsymbol{\vartheta}}(\mathbf{u}) = \frac{\partial^I}{\partial u_1\cdots\partial u_I}C_{\boldsymbol{\vartheta}}(\mathbf{u})$ is called the copula density.

7 Student's t copula constructed in this study using our proposed standardized Student's t distribution $\mathcal{T}_I(\mathbf{0},\mathbf{P},\nu)$, with Pearson's correlation matrix $\mathbf{P}$, is different from the one discussed in Demarta and McNeil (2005).

8 According to Remark 1 as well as Notes 5 and 7, the coefficient $2T_{\nu+1}\left(-\sqrt{\frac{1-\rho_{ij}}{1+\rho_{ij}}(\nu-1)}\right)$ of the lower and upper tail dependence of our proposed Student's t copula is different from the coefficient $2T_{\nu+1}\left(-\sqrt{\frac{1-\rho_{ij}}{1+\rho_{ij}}(\nu+1)}\right)$ of the lower and upper tail dependence of Student's t copula discussed in Demarta and McNeil (2005).

9 If Student's t margins have common degrees of freedom $\nu_i = \nu$ that equal the degrees of freedom of Student's t copula, then their joint distribution is $\mathcal{T}_I(\boldsymbol{\mu},\boldsymbol{\Sigma},\nu)$, as discussed in Section 2.1.

10 In their original works, Bernardi and Petrella (2015) and Bernardi et al. (2017) considered the same significance level $\alpha_i = \alpha$ for the VaR of each distressed asset $i \in \mathscr{I}^{\mathrm{D}}_{\setminus j}$. In this study, we generalize their (Δ)MCoVaR definition by allowing the conditioning assets in $\mathscr{I}^{\mathrm{D}}_{\setminus j}$ to be distressed at different levels.

11 The notation $\mathbb{I}_A$ denotes the indicator function of any set A, with a value of $\mathbb{I}_A(a) = 1$ if $a \in A$ and zero otherwise.

12 Our asymmetric loss function is different from the one proposed by previous studies, e.g., González-Rivera et al. (2004) and Bernardi and Catania (2016), i.e., $\frac{1}{N}\sum_{n\in\mathscr{N}}\varphi^{\alpha_i}(x_{i;n}-w)$, with $\varphi^{\alpha_i}(x_{i;n}-w) = \left(\alpha_i - \mathbb{I}_{(-\infty,0]}(x_{i;n}-w)\right)(x_{i;n}-w)$.

13 A period before 16 January 2018 encompasses the 2017 crypto bubble, as documented by Bazán-Palomino (2022) from the first week of March 2017 to the second week of January 2018. Meanwhile, during a period spanning from 24 February 2022 up to present, the geopolitical conflict between Russia and Ukraine occurred and impacted global financial markets. However, these two periods are out of the scope of this study.

References

Abadie, Alberto. 2002. Bootstrap Tests for Distributional Treatment Effects in Instrumental Variable Models. *Journal of the American Statistical Association* 97: 284–92. [CrossRef]

Adrian, Tobias, and Markus K. Brunnermeier. 2016. CoVaR. *American Economic Review* 106: 1705–41. [CrossRef]

Agosto, Arianna, and Alessia Cafferata. 2020. Financial Bubbles: A Study of Co-explosivity in the Cryptocurrency Market. *Risks* 8: 34. [CrossRef]

Akhtaruzzaman, Md, Sabri Boubaker, Duc K. Nguyen, and Molla R. Rahman. 2022. Systemic Risk-Sharing Framework of Cryptocurrencies in the COVID–19 Crisis. *Finance Research Letters* 47: 102787. [CrossRef] [PubMed]

Almeida, Dora, Andreia Dionísio, Isabel Vieira, and Paulo Ferreira. 2022. Uncertainty and Risk in the Cryptocurrency Market. *Journal of Risk and Financial Management* 15: 532. [CrossRef]

Baur, Dirk G., and Thomas Dimpfl. 2021. The Volatility of Bitcoin and Its Role as a Medium of Exchange and a Store of Value. *Empirical Economics* 61: 2663–83. [CrossRef]

Baur, Dirk G., KiHoon Hong, and Adrian D. Lee. 2018. Bitcoin: Medium of Exchange or Speculative Assets? *Journal of International Financial Markets, Institutions & Money* 54: 177–89.

Bazán-Palomino, Walter. 2022. Interdependence, Contagion and Speculative Bubbles in Cryptocurrency Markets. *Finance Research Letters* 49: 103132. [CrossRef]

Bernal, Oscar, Jean-Yves Gnabo, and Grégory Guilmin. 2014. Assessing the Contribution of Banks, Insurance and Other Financial Services to Systemic Risk. *Journal of Banking & Finance* 47: 270–87.

Bernard, Carole, and Claudia Czado. 2015. Conditional Quantiles and Tail Dependence. *Journal of Multivariate Analysis* 138: 104–26. [CrossRef]

Bernardi, Mauro, and Lea Petrella. 2015. Interconnected Risk Contributions: A Heavy-Tail Approach to Analyze U.S. Financial Sectors. *Journal of Risk and Financial Management* 8: 198–226. [CrossRef]

Bernardi, Mauro, and Leopoldo Catania. 2016. Comparison of Value-at-Risk Models Using the MCS Approach. *Computational Statistics* 31: 579–608. [CrossRef]

Bernardi, Mauro, Antonello Maruotti, and Lea Petrella. 2017. Multiple Risk Measures for Multivariate Dynamic Heavy-Tailed Models. *Journal of Empirical Finance* 43: 1–32. [CrossRef]

Bernardi, Mauro, Fabrizio Durante, and Piotr Jaworski. 2016. CoVaR of Families of Copulas. *Statistics & Probability Letters* 120: 8–17.

Bianchi, Michele L., Giovanni De Luca, and Giorgia Rivieccio. 2023. Non-Gaussian Models for CoVaR Estimation. *International Journal of Forecasting* 39: 391–404. [CrossRef]

Bonaccolto, Giovanni, Nicola Borri, and Andrea Consiglio. 2023. Breakup and Default Risks in the Great Lockdown. *Journal of Banking & Finance* 147: 106308.

Borri, Nicola. 2019. Conditional Tail-Risk in Cryptocurrency Markets. *Journal of Empirical Finance* 50: 1–19. [CrossRef]

Caferra, Rocco, and David Vidal-Tomás. 2021. Who Raised from the Abyss? A Comparison between Cryptocurrency and Stock Market Dynamics during the COVID-19 Pandemic. *Finance Research Letters* 43: 101954. [CrossRef]

Cao, Zhili. 2013. Systemic Risk Measures, Banking Supervision and Financial Stability. Ph.D. thesis, Université de Toulouse 1 Capitole, Toulouse, France.

Castillo-Brais, Brenda, Ángel León, and Juan Mora. 2022. Estimating Value-at-Risk and Expected Shortfall: Do Polynomial Expansions Outperform Parametric Densities? *Mathematics* 10: 4329. [CrossRef]

Catania, Leopoldo, and Stefano Grassi. 2022. Forecasting Cryptocurrency Volatility. *International Journal of Forecasting* 38: 878–94. [CrossRef]

Chan, Joshua C. C., and Dirk P. Kroese. 2010. Efficient Estimation of Large Portfolio Loss Probabilities in *t*-Copula Models. *European Journal of Operational Research* 205: 361–67. [CrossRef]

Cheah, Eng-Tuck, and John Fry. 2015. Speculative Bubbles in Bitcoin Markets? An Empirical Investigation into the Fundamental Value of Bitcoin. *Economics Letters* 130: 32–36. [CrossRef]

Chen, Yan, Dongxu Mo, and Zezhou Xu. 2022. A Study of Interconnections and Contagion among Chinese Financial Institutions Using a ΔCoVaR Network. *Finance Research Letters* 45: 102395. [CrossRef]

Cherubini, Umberto, and Elisa Luciano. 2001. Value-at-risk Trade-off and Capital Allocation with Copulas. *Economic Notes: Review of Banking, Finance and Monetary Economics* 30: 235–56. [CrossRef]

Choi, Pilsun, and Kiseok Nam. 2008. Asymmetric and Leptokurtic Distribution for Heteroscedastic Asset Returns: The S_U-Normal Distribution. *Journal of Empirical Finance* 15: 41–63. [CrossRef]

Choi, Pilsun, Insik Min, and Keehwan Park. 2012. S_U-$\Delta CoVaR$. *Economics Letters* 115: 218–20. [CrossRef]

Choudhury, Tonmoy, Harald Kinateder, and Biwesh Neupane. 2022. Gold, Bonds, and Epidemics: A Safe Haven Study. *Finance Research Letters* 48: 102978. [CrossRef] [PubMed]

Christoffersen, Peter F. 1998. Evaluating Interval Forecasts. *International Economic Review* 39: 841–62. [CrossRef]

Chu, Jeffrey, Saralees Nadarajah, and Stephen Chan. 2015. Statistical Analysis of the Exchange Rate of Bitcoin. *PLoS ONE* 10: e0133678. [CrossRef]

Corbet, Shaen, Charles Larkin, and Brian Lucey. 2020. The Contagion Effects of the COVID-19 Pandemic: Evidence from Gold and Cryptocurrencies. *Finance Research Letters* 35: 101554. [CrossRef]

Corbet, Shaen, Brian Lucey, and Larisa Yarovaya. 2018. Datestamping the Bitcoin and Ethereum Bubbles. *Finance Research Letters* 26: 81–88. [CrossRef]

Demarta, Stefano, and Alexander J. McNeil. 2005. The *t* Copula and Related Copulas. *International Statistical Review* 73: 111–29. [CrossRef]

Ding, Peng. 2016. On the Conditional Distribution of the Multivariate *t* Distribution. *The American Statistician* 70: 293–95. [CrossRef]

Embrechts, Paul, and Andrea Höing. 2006. Extreme VaR Scenarios in Higher Dimensions. *Extremes* 9: 177–92. [CrossRef]

Embrechts, Paul, Andrea Höing, and Alessandro Juri. 2003a. Using Copulae to Bound the Value-at-Risk for Functions of Dependent Risks. *Finance and Stochastics* 7: 145–67. [CrossRef]

Embrechts, Paul, Filip Lindskog, and Alexander McNeil. 2003b. Modelling dependence with copulas and applications to risk management. In *Handbook of Heavy Tailed Distributions in Finance*. Edited by Svetlozar T. Rachev. Amsterdam: Elsevier Science B.V., pp. 329–84.

Girardi, Giulio, and A. Tolga Ergün. 2013. Systemic Risk Measurement: Multivariate GARCH Estimation of CoVaR. *Journal of Banking & Finance* 37: 3169–80.

Gneiting, Tilmann. 2011. Making and Evaluating Point Forecasts. *Journal of the American Statistical Association* 106: 746–62. [CrossRef]
González-Rivera, Gloria, Tae-Hwy Lee, and Santosh Mishra. 2004. Forecasting Volatility: A Reality Check Based on Option Pricing, Utility Function, Value-at-Risk, and Predictive Likelihood. *International Journal of Forecasting* 20: 629–45. [CrossRef]
Gurrola, Pedro. 2008. Capturing Fat-Tail Risk in Exchange Rate Returns Using SU Curves: A Comparison with the Normal Mixture and Skewed Student Distributions. *The Journal of Risk* 10: 73–100. [CrossRef]
Hakim, Arief, A. N. M. Salman, Yeva Ashari, and Khreshna Syuhada. 2022. Modifying (M)CoVaR and Constructing Tail Risk Networks through Analytic Higher-Order Moments: Evidence from the Global Forex Markets. *PLoS ONE* 17: e0277756. [CrossRef]
Hakwa, Brice, Manfred Jäger-Ambrożewicz, and Barbara Rüdiger. 2015. Analysing Systemic Risk Contribution Using a Closed Formula for Conditional Value at Risk through Copula. *Communications on Stochastic Analysis* 9: 131–58. [CrossRef]
Haykir, Ozkan, and Ibrahim Yagli. 2022. Speculative Bubbles and Herding in Cryptocurrencies. *Financial Innovation* 8: 78. [CrossRef]
Jang, Sung M., Eojin Yi, Chang Kim, and Kwangwon Ahn. 2019. Information Flow between Bitcoin and Other Investment Assets. *Entropy* 21: 1116. [CrossRef]
Jaworski, Piotr. 2017. On Conditional Value at Risk (CoVaR) for Tail-Dependent Copulas. *Dependence Modeling* 5: 1–19. [CrossRef]
Jiménez, Inés, Andrés Mora-Valencia, and Javier Perote. 2020a. Risk Quantification and Validation for Bitcoin. *Operations Research Letters* 48: 534–41. [CrossRef]
Jiménez, Inés, Andrés Mora-Valencia, and Javier Perote. 2022. Semi-Nonparametric Risk Assessment with Cryptocurrencies. *Research in International Business and Finance* 59: 101567. [CrossRef]
Jiménez, Inés, Andrés Mora-Valencia, Trino-Manuel Ñíguez, and Javier Perote. 2020b. Portfolio Risk Assessment under Dynamic (Equi)Correlation and Semi-Nonparametric Estimation: An Application to Cryptocurrencies. *Mathematics* 8: 2110. [CrossRef]
Johnson, N. L. 1949. Systems of Frequency Curves Generated by Method of Translation. *Biometrika* 36: 149–76. [CrossRef]
Kabaila, Paul. 1999. An Efficient Simulation Method for the Computation of a Class of Conditional Expectations. *Australian & New Zealand Journal of Statistics* 41: 331–36.
Kabaila, Paul, and Syuhada, Khreshna. 2008. Improved Prediction Limits for AR(p) and ARCH(p) Processes. *Journal of Time Series Analysis* 29: 213–23. [CrossRef]
Karimalis, Emmanouil N., and Nikos K. Nomikos. 2018. Measuring Systemic Risk in the European Banking Sector: A Copula *CoVaR* Approach. *The European Journal of Finance* 24: 944–75. [CrossRef]
Koenker, Roger, and Gilbert Bassett. 1978. Regression Quantiles. *Econometrica* 46: 33–50. [CrossRef]
Kuan, Chung-Ming, Jin-Huei Yeh, and Yu-Chin Hsu. 2009. Assessing Value at Risk with CARE, the Conditional Autoregressive Expectile Models. *Journal of Econometrics* 8: 87–107. [CrossRef]
Kupiec, Paul H. 1995. Techniques for Verifying the Accuracy of Risk Measurement Models. *The Journal of Derivatives* 3: 73–84. [CrossRef]
Le, Trung H. 2020. Forecasting Value at Risk and Expected Shortfall with Mixed Data Sampling. *International Journal of Forecasting* 36: 1362–79. [CrossRef]
Li, Jianping, Xiaoqian Zhu, Cheng-Few Lee, Dengsheng Wu, Jichuang Feng, and Yong Shi. 2015. On the Aggregation of Credit, Market and Operational Risks. *Review of Quantitative Finance and Accounting* 44: 161–89. [CrossRef]
Li, Yanshuang, Xintian Zhuang, Jian Wang, and Zibing Dong. 2021. Analysis of the Impact of COVID-19 Pandemic on G20 Stock Markets. *The North American Journal of Economics and Finance* 58: 101530. [CrossRef]
Mainik, Georg, and Eric Schaanning. 2014. On Dependence Consistency of CoVaR and Some Other Systemic Risk Measures. *Statistics & Risk Modeling* 31: 49–77.
McNeil, Alexander J., and Johanna Nešlehová. 2009. Multivariate Archimedean Copulas, d-Monotone Functions and ℓ_1-Norm Symmetric Distributions. *The Annals of Statistics* 37: 3059–97. [CrossRef] [PubMed]
McNeil, Alexander J., Rüdiger Frey, and Paul Embrechts. 2015. *Quantitative Risk Management: Concepts, Techniques and Tools*, rev. ed. Princeton: Princeton University Press.
Moreno, David, Marcos Antoli, and David Quintana. 2022. Benefits of Investing in Cryptocurrencies When Liquidity Is a Factor. *Research in International Business and Finance* 63: 101751. [CrossRef]
Nadarajah, Saralees, and Samuel Kotz. 2005. Mathematical Properties of the Multivariate t Distribution. *Acta Applicandae Mathematicae* 89: 53–84. [CrossRef]
Núñez, José A., Mario I. Contreras-Valdez, and Carlos A. Franco-Ruiz. 2019. Statistical Analysis of Bitcoin during Explosive Behavior Periods. *PLoS ONE* 14: e0213919. [CrossRef] [PubMed]
Patra, Saswat. 2021. Revisiting Value-at-Risk and Expected Shortfall in Oil Markets under Structural Breaks: The Role of Fat-Tailed Distributions. *Energy Economics* 101: 105452. [CrossRef]
Rehman, Mobeen U., Paraskevi Katsiampa, Rami Zeitun, and Xuan V. Vo. 2022. Conditional Dependence Structure and Risk Spillovers between Bitcoin and Fiat Currencies. *Emerging Markets Review*, *in press*. [CrossRef]
Rosenberg, Joshua V., and Til Schuermann. 2006. A General Approach to Integrated Risk Management with Skewed, Fat-Tailed Risks. *Journal of Financial Economics* 79: 569–614. [CrossRef]
Sharif, Arshian, Chaker Aloui, and Larisa Yarovaya. 2020. COVID-19 Pandemic, Oil Prices, Stock Market, Geopolitical Risk and Policy Uncertainty Nexus in the US Economy: Fresh Evidence from the Wavelet-Based Approach. *International Review of Financial Analysis* 70: 101496. [CrossRef]
Sklar, Abe. 1959. Fonctions de Répartition à n Dimensions et Leurs Marges. *Publications de l'Institut de Statistique de l'Université de Paris* 8: 229–31.

Som, Ankit, and Parthajit Kayal. 2022. A Multicountry Comparison of Cryptocurrency *vs* Gold: Portfolio Optimization through Generalized Simulated Annealing. *Blockchain: Research and Applications* 3: 100075. [CrossRef]

Syuhada, Khreshna, and Arief Hakim. 2020. Modeling Risk Dependence and Portfolio VaR Forecast through Vine Copula for Cryptocurrencies. *PLoS ONE* 15: e0242102. [CrossRef]

Syuhada, Khreshna, Arief Hakim, and Risti Nur'aini. 2021. The Expected-Based Value-at-Risk and Expected Shortfall Using Quantile and Expectile with Application to Electricity Market Data. *Communications in Statistics: Simulation and Computation*, *in press*. [CrossRef]

Syuhada, Khreshna, Arief Hakim, Djoko Suprijanto, Intan Muchtadi-Alamsyah, and Lukman Arbi. 2022a. Is Tether a Safe Haven of Safe Haven amid COVID-19? An Assessment against Bitcoin and Oil Using Improved Measures of Risk. *Resources Policy* 79: 103111. [CrossRef]

Syuhada, Khreshna, Djoko Suprijanto, and Arief Hakim. 2022b. Comparing Gold's and Bitcoin's Safe-Haven Roles against Energy Commodities during the COVID-19 Outbreak: A Vine Copula Approach. *Finance Research Letters* 46: 102471. [CrossRef] [PubMed]

Tong, Y. L. 1990. *The Multivariate Normal Distribution*. New York: Springer.

Torri, Gabriele, Rosella Giacometti, and Tomáš Tichý. 2021. Network Tail Risk Estimation in the European Banking System. *Journal of Economic Dynamics & Control* 127: 104125.

Troster, Victor, Aviral K. Tiwari, Muhammad Shahbaz, and Demian N. Macedo. 2019. Bitcoin Returns and Risk: A General GARCH and GAS Analysis. *Finance Research Letters* 30: 187–93. [CrossRef]

van Dorp, Johan R., and Michael C. Jones. 2020. The Johnson System of Frequency Curves—Historical, Graphical, and Limiting Perspectives. *The American Statistician* 74: 37–52. [CrossRef]

Venkataraman, Sree V., and S. V. D. Nageswara Rao. 2016. Estimation of Dynamic VaR Using $\mathrm{JS_U}$ and PIV Distributions. *Risk Management* 18: 111–34.

Vidal-Tomás, David. 2022. Which Cryptocurrency Data Sources Should Scholars Use? *International Review of Financial Analysis* 81: 102061. [CrossRef]

Wang, Gang-Jin, Chi Xie, Danyan Wen, and Longfeng Zhao. 2019. When Bitcoin Meets Economic Policy Uncertainty (EPU): Measuring Risk Spillover Effect from EPU to Bitcoin. *Finance Research Letters* 31: 489–97. [CrossRef]

Wang, Gang-Jin, Xin-yu Ma, and Hao-yu Wu. 2020. Are Stablecoins Truly Diversifiers, Hedges, or Safe Havens against Traditional Cryptocurrencies as Their Name Suggests? *Research in International Business and Finance* 54: 101225. [CrossRef]

Xu, Qiuhua, Yixuan Zhang, and Ziyang Zhang. 2021. Tail-Risk Spillovers in Cryptocurrency Markets. *Finance Research Letters* 38: 101453. [CrossRef]

Yi, Shuyue, Zishuang Xu, and Gang-Jin Wang. 2018. Volatility Connectedness in the Cryptocurrency Market: Is Bitcoin a Dominant Cryptocurrency? *International Review of Financial Analysis* 60: 98–114. [CrossRef]

Yu, Jiang, Yue Shang, and Xiafei Li. 2021. Dependence and Risk Spillover among Hedging Assets: Evidence from Bitcoin, Gold, and USD. *Discrete Dynamics in Nature and Society* 2021: 2010705. [CrossRef]